Soils and Rocks Volume 38, N. 2 2015

ISSN 1980-9743

Soils and Rocks

Soils and Rocks

An International Journal of Geotechnical and Geoenvironmental Engineering

Volume 38, N. 2
May-August 2015

Soils and Rocks is an International Journal of Geotechnical and Geoenvironmental Engineering published by

ABMS - Brazilian Association for Soil Mechanics and Geotechnical Engineering
Av. Queiroz Filho, 1700 – Torre A Sky, Sala 106 – Vila Hamburguesa
05319-000, São Paulo, SP
Brazil

SPG – Portuguese Geotechnical Society
LNEC, Avenida do Brasil, 101
1700-066 Lisboa
Portugal

Issue Date: *August 2015*

Issue: *400 copies and 800 online-distributed copies*

Manuscript Submission: *For review criteria and manuscript submission information, see Instructions for Authors at the end.*

SOILS and ROCKS

An International Journal of Geotechnical and Geoenvironmental Engineering

Editor Waldemar Coelho Hachich - University of São Paulo, Brazil

Co-editor Manuel Matos Fernandes - University of Porto, Portugal

“Ad hoc” Reviewers (2014-2015)

Soils and Rocks publishes papers in English in the broad fields of Geotechnical Engineering, Engineering Geology and Geo-environmental Engineering. The Journal is published in April, August and December. Subscription price is US$ 90.00 per year. The journal, with the name “Solos e Rochas”, was first published in 1978 by the Graduate School of Engineering, Federal University of Rio de Janeiro (COPPE-UFRJ). In 1980 it became the official magazine of the Brazilian Association for Soil Mechanics and Geotechnical Engineering (ABMS), acquiring the national character that had been the intention of its founders. In 1986 it also became the official Journal of the Brazilian Association for Engineering Geology and the Environment (ABGE) and in 1999 became the Latin American Geotechnical Journal, following the support of Latin-American representatives gathered for the Pan-American Conference of Guadalajara (1996). In 2007 the journal acquired the status of an international journal under the name of Soils and Rocks, published by the Brazilian Association for Soil Mechanics and Geotechnical Engineering (ABMS), Brazilian Association for Engineering Geology and the Environment (ABGE) and Portuguese Geotechnical Society (SPG). In 2010, ABGE decided to publish its own journal and left the partnership.

Soils and Rocks

1978,	1 (1, 2)
1979,	1 (3), 2 (1,2)
1980-1983,	3-6 (1, 2, 3)
1984,	7 (single number)
1985-1987,	8-10 (1, 2, 3)
1988-1990,	11-13 (single number)
1991-1992,	14-15 (1, 2)
1993,	16 (1, 2, 3, 4)
1994-2010,	17-33 (1, 2, 3)
2011,	34 (1, 2, 3, 4)
2012-2014,	35-37 (1, 2, 3)
2015,	**38 (1, 2,**

ISSN 1980-9743 CDU 624.131.1

ISSN 1980-9743

SOILS and ROCKS

An International Journal of Geotechnical and Geoenvironmental Engineering

Publication of

ABMS - Brazilian Association for Soil Mechanics and Geotechnical Engineering

SPG - Portuguese Geotechnical Society

Volume 38, N. 2, May-August 2015

Table of Contents

Manuel Rocha Lecture

Manuel Rocha (1913-1981) was honoured by the Portuguese Geotechnical Society with the establishment of the Lecture Series bearing his name in 1984.

Having completed the Civil Engineering Degree at the Technical University of Lisbon (1938) he did post-graduate training at MIT. He was the driving force behind the creation of the research team in Civil Engineering that would lead to the foundation of the National Laboratory for Civil Engineering (LNEC), in Lisbon. He was Head of LNEC from 1954 to 1974 and led it to the cutting edge of research in Civil Engineering.

His research work had great impact in the area of concrete dams and rock mechanics. He was the 1st President of the International Society for Rock Mechanics and organized its 1st Congress in Lisbon (1966). He did consultancy work in numerous countries. He was Honorary President of the Portuguese Geotechnical Society, having promoted with great commitment the cooperation between Portugal and Brazil in the area of Civil Engineering, and member of the National Academy of Sciences of the USA. Recognized as a brilliant researcher, scientist and professor, with a sharp, discerning intellect allied to a prodigious capacity for work and management, he was truly a man of many talents.

The 2014 Manuel Rocha Lecturer was **ANTÓNIO SILVA CARDOSO**, born in Mozambique in 1955, Professor of Geotechnical Engineering in the Faculty of Engineering of University of Porto. He was Vice-Chancellor and member of the Board of the University of Porto. He has participated in research projects and collaborated on the orientation of doctoral and master dissertations. He was director of the journal Geotecnia (in Portuguese and Spanish). He is author or co-author of over 150 publications in books, journals and proceedings of national and international technical and scientific meetings. He has exercised the engineering profession in more than 50 projects, either in Portugal or in other countries.

Soils and Rocks
v. 38, n. 2

Emerging Trends in Geotechnical Engineering

A.S. Cardoso

Abstract. . Geotechnical engineering is one of the first technical and scientific fields to intervene in any infrastructure or urban development project and, in many cases, it is the most important. In the course of time many methodological, analytical, numerical and technological innovations have been discovered and used both in field and in laboratory investigations in the analysis, design and construction of geotechnical structures. The fields in which geotechnical engineering plays an important role and where these innovations have been introduced are very wide and spread out by very different scales. The world globalization, the unsustainable use of resources, the climate changes caused by human activities, the increase of natural disasters, the recognized lack of infrastructure to meet people's needs and also to protect against the consequences of climate changes, decisively condition the evolution of engineering and obviously also of geotechnical engineering. These factors require the problems and their solutions to be addressed in a global, integrated and multidisciplinary way. This lecture outlines a perspective on the future of geotechnics, starting by characterizing various conditioning factors and society's needs. The developed prospect is naturally fragmented and incomplete, and it could not be otherwise, as it is a personal perspective conditioned by the interests and limitations of the author.
Keywords: future development of geotechnics, social, economic and environmental conditioning factors, geotechnical issues.

1. Introduction

In recent years the future development of geotechnics has sparked the interest of many institutions and individuals (ASCE, 2007; IITG / IGS, 2012; NRC, 2006; Brandl, 2011; Breedeveld, 2012; Chowdhury & Flentje, 2007; Clough, 2006; Francisca, 2011; Hajra, 2012; Long, 2006; Matos Fernandes, 2010; Nelson, 2013; Reddy, 2011; Shackelford, 2005; Simpson & Tatsuoka, 2008), adopting very different perspectives: specific or global, local, regional or worldwide, more or less related to economic and social environment, etc.

Geotechnical engineering is one of the first technical and scientific fields to intervene in any infrastructure or urban development project and, in many cases, it is the most important. In the course of time many methodological, analytical, numerical and technological innovations have been discovered and used both in field and in laboratory investigations in the analysis, design and construction of geotechnical structures.

The globalization of economic organization (production and trade) and of information circulation, the unsustainable use of resources, the environmental changes caused by human activities, the increase of natural disasters, in particular those caused by hydraulic reasons, the recognized lack of infrastructure to meet people's needs and also to protect against the consequences of climate changes, decisively condition the evolution of engineering and obviously also of geotechnical engineering. These factors require problems and their solutions to be addressed in a global, integrated and multidisciplinary way.

This text outlines a view over the future development of geotechnical engineering, starting with the analysis of some conditioning factors: social, economic and environmental factors are considered in Chapter 2; geotechnical conditioning factors are discussed in Chapter 3. In Chapter 4 a brief characterization of world's infrastructure needs is outlined, using data produced mainly by international organizations. Chapters 5 and 6 state the future trends of geotechnical engineering, from a generic point of view.

2. General Conditioning Factors

2.1.Scope

This chapter addresses various factors that influence the development of geotechnical engineering, both for societal and for technological reasons. The point of view presented here is partial and the argumentation is limited, as it couldn't be otherwise. It's aim is basically to present some of the major trends of the social evolution of the world (population growth and urbanization, concern with environment's evolution, increasing social scrutiny) and some general conditioning factors of that evolution: some natural (climate change and natural disasters) and others technological. We should bear in mind that it is in the proper use of technology that rests the possibility of finding the appropriate responses to current difficulties, which must be conditioned and limited by the relevant social factors, including the need to ensure its sustainability.

2.2. Climate change and increasing natural disasters

Although the understanding of Earth's climate continues to lack certainty, there is already a powerful and credible body of evidence, obtained from multiple different registration and research processes, proving that climate is changing and that these changes are largely caused by hu-

António Silva Cardoso, Full Professor, Faculty of Engineering, University of Porto, 4200-465 Porto, Portugal. e-mail: scardoso@fe.up.pt.

man activities (NRC, 2010). Scientific evidence also shows that climate changes entail significant risks for many natural and human systems. Different studies have come to similar conclusions, which are shared by many national and international organizations (USGCRP, 2009; IPCC, 2007; etc.) and have acquired a high degree of trust:

- Earth is warming. Detailed observations of surface temperature (both in oceans and on land) show that the Earth's average surface temperature during the first decade of this century was 0.8 °C higher than in the first decade of the twentieth century, registering a more pronounced warming in the past 3 decades.
- In recent decades most warming can be attributed to human activities that release carbon dioxide (CO_2) and other greenhouse gases (GHGs) into the atmosphere. The burning of fossil fuels - coal, oil and natural gas - for energy production is the main cause of climate change, but agriculture, deforestation and some industrial activities also significantly contribute to that. Figure 1 shows the evolution of global CO_2 emissions since 1860.
- Other climate changes are closely associated with global warming, such as increasing frequency of intense rainfall, reduction of snow and ice cover at the poles, more frequent and intense heat waves, sea level rise and ocean acidification. Individually and collectively, these changes jeopardize a broad spectrum of environmental and human systems, including water resources, coastal environment, ecosystems, agriculture, fisheries, human health, etc.
- Current CO_2 concentration in the atmosphere is about 380 ppm. Studies suggest that 550 ppm can be a threshold which triggers severe weather effects (IPCC, 2000). It is estimated that in 2050 CO_2 concentration will achieve 550 ppm, unless decisive actions are carried out by the international community.
- The magnitude of climate changes and the severity of their impacts depend decisively upon the actions undertaken by human societies in response to the risks. But we should bear in mind that, despite the international agreement to stabilize the concentration of GHGs at levels that prevent dangerous human interference with the climate system (UNFCCC, 1992, 2009), global CO_2 and other GHGs emissions continue to increase.

The frequency of natural disasters appears to have been increasing during the last decades, as can be seen in Fig. 2. The sharp increase in the number of events is partly explained by the increase of number and detail of observation and recording, since there is no reason why seismic activity shouldn't register a pattern of constant incidence. In any case, it is clear that catastrophic events of hydrological character have experienced continued growth. In addition to a solid body of research on the causes and consequences of climate change, there is a growing and more diverse body of knowledge on policies, methodologies and technologies that can be used to limit / control future climate change (Fragaszy *et al.*, 2011).

As for the implementation of these measures, *i.e.*, the steps that must be taken, we are still moving at a snail's pace, but are improving. In fact, a key issue before the implementation of the necessary actions, i.e. the recognition that the climate changes should be considered in decisions and actions that are taken in a wide range of sectors, has undoubtedly grow.

2.3. Population and cities growth

Based in documents of the United Nations and World Bank (UN, 2010; WDR, 2009; WB / UN, 2010), crucial aspects of population and cities growth are described and it is argued that past and predicted evolutions favor increased vulnerability to natural phenomena.

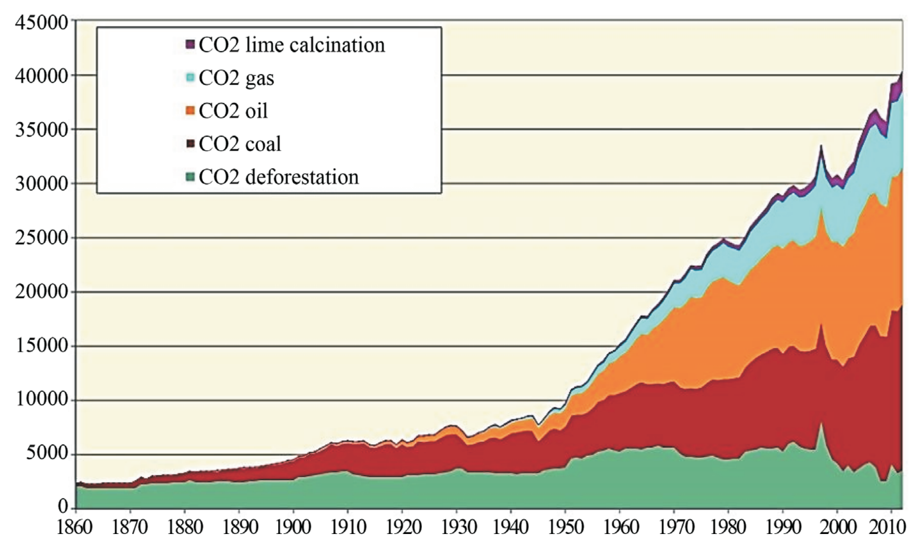

Figure 1 - Evolution of global CO_2 emissions since 1860, in millions of tons. (Source: http://www.manicore.com/anglais/documentation_a/greenhouse/evolution.html).

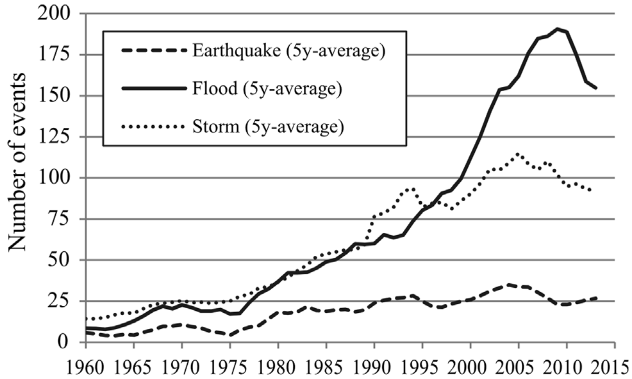

Figure 2 - Number (average of 5 years) of events recorded each year from 1910 to 2009 (Source: EM-DAT - OFDA / CRED International Disasters Database).

Cities occupy only 1.5 percent of the world's land area but produce half of GDP. The prosperity of cities comes from the high productivity provided by the division of labor, a result of people and goods agglomeration, and from the low cost acquisition of information and technology (know-how) (WB / UN, 2010). On the other hand, the prosperity of cities is an economic magnet, attracting people and investments.

Historically, production has grown by about 1-2 percentage points more than the population, explaining why per capita income has increased almost everywhere. Much of the growth occurred in the cities, where per capita income is higher. This is not new: it is well known that cities concentrate prosperity (WDR, 2009).

Population of cities has also continuously grown. Current world population is around 7.3 billion, a little more than half living in cities. In 2050 population is expected to have reached 9.5 billion, when, according to UN estimates, world's urban population will increase to 70 per cent. Figure 3 summarizes the trends of the last few decades and points to the current forecast for the next decades. In 2050 compared to 1950, *i.e.* in 100 years, the world, rural and urban populations are expected to increase 3.6, 1.6 and 8.6 times, respectively. Europe is the continent with less variations: only 30% of population growth as a result of the doubling of urban population accompanied by a rural population decrease to less than half. Africa is the continent experiencing the most dramatic change: the total population increases by about 9 times, rural population increases about 4 times and urban population about 37 times.

Due to the strong and continuous urbanization increase, in many cities roads capacity, water supply and sewage treatment systems are sold out or on the way to become exhausted. Services did not maintain adequate levels largely because cities have not invested enough in infrastructure. Congestion, pollution and frustration can eventually choke the continuous growth of such cities.

Urban concentration increases the risks of its inhabitants to natural hazards. It is estimated that in 2050 the number of people exposed to tropical cyclones and earthquakes in large cities is more than double, ascending from 310 million in 2000 to 680 million in 2050 in the case of tropical cyclones, and from 370 to 870 million in the case of earthquakes (WB / UN, 2010).

The reasons for increased vulnerability of societies to natural disasters can be summed up as follows (WEF, 2011): a) population growth: between 1950 and 2010 the world population grew from 2.5 to 6.9 billion, thereby increasing the number of people living in vulnerable areas; b) location: population growth occurred in areas more vulnerable to natural disasters, as coastal areas and river banks; c) urbanization: the lack of proper urban planning and the lack of quality of the projects and constructions exacerbate the effects of natural disasters; d) economic value: economic development led to more valuable infrastructures, and

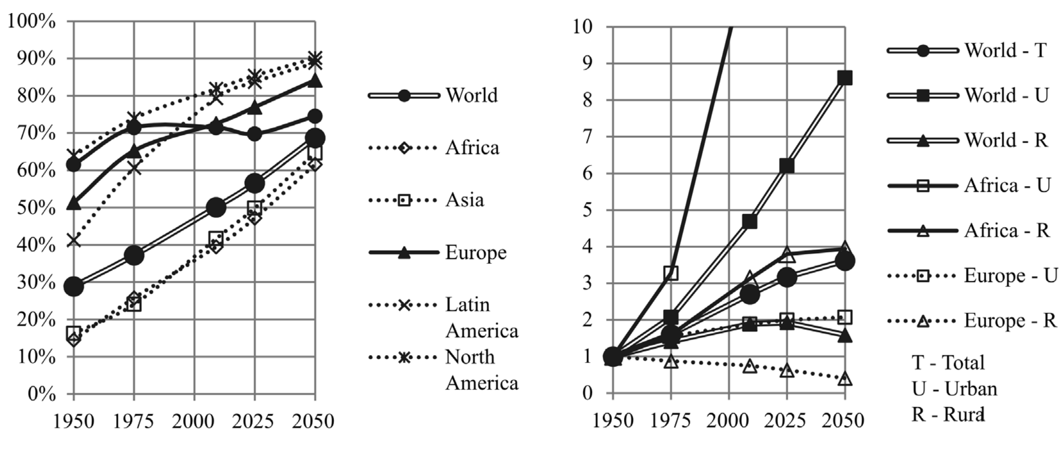

a) b)

Figure 3 - a) Urban population percentage in each continent; b) Change in the total, urban and rural population compared to 1950, in the World, Europe and Africa.

therefore increased the risk of economic losses; e) climate change.

2.4. Social scrutiny

2.4.1. Preamble

Hansford (2011) refers to the existing infrastructure needs all over the world and emphasizes the role of engineers in finding and implementing solutions to meet these needs. Nevertheless, in his opinion, the current economic environment has unprecedented conditioning factors, which "(...) led to massive cuts in public sector spending and inevitable scrutiny of infrastructure investment plans; scrutiny to levels that our industry has never seen before (...)". Probably the growing social scrutiny of the construction sector is due to the concern about the uncontrolled costs and execution times, particularly of the public works, and to the perception of corruption in the sector.

2.4.2. Costs and timing of the works: discrepancy between forecasts and reality

Lambe (1973) pointed out that "(...) predicting is a key step in the process of creating and maintaining a construction facility, *i.e.* the practice of civil engineering (...)". Decisions to proceed with more or less important investments are based in forecasts of costs and other impacts, such as environmental, level of infrastructure usage (traffic, etc.), direct and indirect economic benefits, etc. Inaccuracies in the estimation of cost, demand and other impacts of projects are much more common and widespread than one might think (Cardoso, 2013). Flyvbjerg (2006, 2014) has been building an important database of works carried out around the world, whose data confirms that either the underestimation of costs as the optimistic estimation of usage levels of the built infrastructures are common. Flyvbjerg (2006) also concluded that there has been no improvement of forecasts quality over time. The cost-benefit ratios are often wrong, not just in a small degree, which implies that the viability estimates are misleading in many cases. So, the information on which investment decisions in new projects are based can be highly inaccurate and biased, leading to high-risk projects.

Sidebar 1 describes the Boston case as an example of well-known international projects (other are *e.g.* the Channel Tunnel or the "Calle 30" project in Madrid) where the predictions failed at a very high degree. There are several distinct reasons for these, in some cases, major differences, from economic, political and social causes (inflation, labor problems, etc.) to technical reasons (shortcomings of the primary studies, deficiencies of the designs, unforeseen situations, especially due to geotechnical reasons, etc). Flyvbjerg and others (2005, 2006) have deeply studied the subject (Cardoso, 2013, gave a brief summary of these studies); they consider that, more than by technical reasons, forecasts' inaccuracies are explained by two main reasons: 1) psychological reasons - generally forecasts present an optimistic bias, *i.e.* most people have a cognitive predisposition that leads them to judge future events at a more positive light than what would be rationally justified by actual experience; 2) political reasons - the inaccuracies are explained in terms of false strategic statements; according to these explanations, when making the estimation of project results, analysts and managers deliberately and strategically overestimate the benefits and underestimate the costs in order to increase the likelihood of their projects to be approved and funded, rather than those of their competitors. Optimistic behavior and strategic misrepresentation, both involve deception, but as the later implies an intention the first not; optimistic tendency lies in self-deception. Anyway, the inaccuracies of the estimates entail additional costs and revenue losses due to delays in the operation of built infrastructure. Moreover, the extension of the construction period is also quite common, a fact that can eventually lead to additional costs and / or result losses.

Direct and/or indirect costs that are regarded as excessive and not sufficiently justified (Long, 2006) and especially the lack of control of these costs become increasingly

Sidebar 1. Boston Central Artery

The construction of the Central Artery / Tunnel Project (Big Dig Boston) included especially underground works: i) the existing Central Artery (Interstate 93), a motorway with six lanes through the city center, has been replaced by an underground highway (5.6 km) and by two bridges with 14 lanes for crossing the Charles River; ii) Interstate 90 was extended, through a tunnel under Boston Harbor, to the airport. The project started in 1982 and the construction in 1991; it was expected to end in 1998 with a cost of US$ 2,800 million (1982 costs). In fact, the work was completed in 2006 - that is, took twice the prescribed construction time - with a cost of US$ 14,600 million (2006 prices, *i.e.* US$ 8,080 million in 1982 prices), which means almost three times the estimated cost.

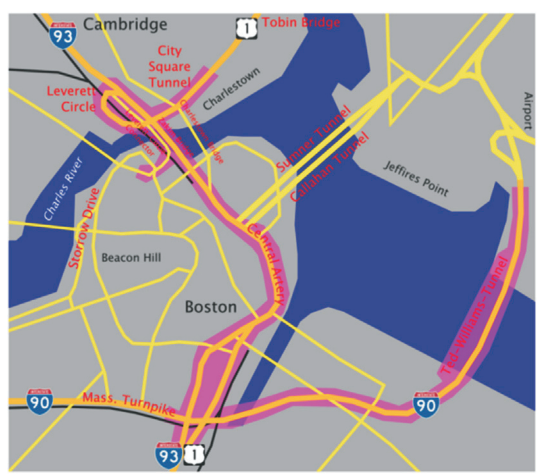

less socially acceptable, diverging in relation to estimates that had supported the decision to move forward. It is clear that the awareness of the economic, social and political importance of these issues has been increasing and that, since the second half of the previous decade, states, especially the European States and the USA, have been adopting measures to control this problem (Flyvbjerg, 2014).

2.4.3. Perception of corruption in the construction sector

At a summit meeting (ASCE, 2007) organized to discuss the future of civil engineering, the participants discussed the issues and trends that affect the sector and identified, among others, "(...) occurrence of corruption in the global engineering and construction industry (...)". This problem has been addressed in reports and studies conducted by international agencies (*e.g.*, Kenny, 2009, WB/UN, 2010, and Hardoon & Heinrich, 2011).

Very recently there were two international surveys on corruption. The first was prepared by Transparency International (Hardoon & Heinrich, 2011) in order to assign, for the fifth time, the Bribe Payers Index, see Table 1. The index ranks 28 of the world's largest economies (distributed across all regions of the world and representing almost 80 per cent of all products, services and investments circulating in the world) according to the perceived likelihood of companies from these countries to pay bribes abroad. It is based on the views of business executives as captured by Transparency International's 2011 Bribe Payers Survey. The Bribe Payers Survey also captures perceptions of bribery across business sectors, see Table 1. Public works contracts and construction sector detain the worst values, detached from the rest.

The second survey on corruption in construction industry, from the Chartered Institute of Building (CIOB, 2013), involved 701 construction professionals, about 60% of whom were directors, senior managers and consultants and about 30% were middle and base managers; almost all worked in organizations / companies with over 200 employees. The main findings were: a) 49% of respondents believe that corruption is widespread in the British construction industry, 2% less than in the first survey published in 2006; b) 42.5% of the participants suggest that corruption can occur at any stage of a building development, while 35% consider it more likely during the pre-qualification and tender phases; c) virtually everybody considers important or very important (more than 3/4) to face the problem of corruption.

2.4.4. Challenge for engineers

Many projects similar to the ones criticized and questioned because they didn't not fulfill what was expected when released, will be needed in our cities. The question is whether we will be able to do them if we don't succeed in significantly reduce costs, risks and construction time, not to mention our ability to manage them properly, meaning to fight against corruption. Long (2006) opines that if we do not find better ways - more reliable, with lower costs and shorter periods of social disturbance - to solve the traditional problems, especially in the cities, the social, economic and environmental constraints will make the solutions increasingly more inaccessible. In the same line of reasoning Hansford (2011) states that "(...) the imperative today is to deliver more for less (...)".

2.5. Computers performance and computing costs

The powerful evolution of informatics and computers decisively affected all human activities and also the evolution of geotechnics. Much of the progress made in under-

Table 1 - Adapted from Hardoon & Heinrich (2011).

Bribe Payers Index 2011		Perceptions of foreign bribery by sector	
Country / Territory	Score	Sector	Score
Netherlands, Switzerland, Belgium, Germany, Japan, Australia, Canada	8.5-8.8	Agriculture, Light manufacturing, Civilian aerospace, Information technology	7.0-7.1
Singapore, United Kingdom, United States, France, Spain	8.0-8.3	Banking and finance, Forestry, Consumer services	6.8-6.9
S. Korea, Brazil, Hong Kong, Italy, Malaysia, S. Africa, Taiwan, India, Turkey	7.5-7.9	Telecommunications, Transport. and storage, Arms, defense and military, Fisheries	6.6-6.7
Saudi Arabia, Argentina, United Arab Emirates, Indonesia, Mexico	7.0-7.4	Heavy manufacturing, Pharmac. and healthcare, Power generation and transmission	6.4-6.5
China	6.5	Mining, Oil and gas, Real estate, property, legal and business services, Utilities	6.1-6.3
Russia	6.1	Public works contracts and construction	5.3
Average	7.8	Average	6.6

Note: [Countries / Territories] [Sectors] are scored on a scale of 0-10, where a maximum score of 10 corresponds with the view that companies [from that country] [in that sector] *never* bribe [abroad] and a 0 corresponds to the view that they *always* do.

standing the behavior of geomaterials would not have been possible without the use of numerical methods. The current capacity to analyze and predict the behavior of geotechnical structures, in operating conditions, in ultimate states or even in post-failure situations, is based on the development of methods of analysis with universal character (meaning that any geometric or boundary initial conditions may be considered). This analysis is obligatorily numeric and therefore dependent on the available computation capacity.

Figure 4 briefly tells the history of computer evolution, which can be summarized as follows: 1) the number of transistors (transistor count) of microprocessors has increased more than 30 times every 10 years; the increasing of GPUs (Graphics Processing Unit) transistors count has been even greater, about 100 times every 10 years; 2) the processing speed, measured in FLOPS (Floating-Point Operations Per Second), has grown about 600 times every 10 years; 3) the operation cost of supercomputers has decreased about 400 times every 10 years.

Since the 90s, the growing computer performance and the advances in the development of very powerful programs for geotechnical design provided the possibility to carry out advanced numerical analysis, including 3D calculations, at an ever lower cost. The development of "friendly" interfaces further facilitated the use of numerical analysis.

Nevertheless, we should bear in mind that to carry out complex calculations and achieve good results we undoubtedly need a good knowledge of numerical methods, but also of mechanics and other areas of physics (and possibly, chemistry) and, above all, of soil and / or rock mechanics. This is sometimes forgotten in practice. This issue is perhaps even more relevant in geotechnics than in any other area, given the complex and uncertain character of the properties of geomaterials and of the processes to evaluate them.

2.6. Complexity

The increasingly globalized world, where information on whatever occurs wherever it may be, is available almost immediately, is also characterized by a permanent growth in complexity. That is, procedures and actions are conditioned by increasingly diverse factors and growing interdependencies. Complexity also results from the fact that humans face increasingly difficult and global challenges that, years ago, were simply not considered.

Traditional methodologies for the study of systems' behavior based on independent component analysis can no longer be used when complexity level rises. The difficulty of a complex system is that often the parts interact with each other in time and space, making it non-linear. The best example of a non-linear system is a living organism, in which molecular processes occurring within the cells cannot be clearly separated from processes occurring at a macroscopic level; other examples of complex systems are the climate and the economy.

Geotechnics is genetically a complex discipline, since geotechnical engineering practice requires working with a very limited set of information on complex materials whose state can radically change over short distances and over time (Marr, 2006). Therefore, the collaboration of experts from different disciplinary sub-areas is often required.

Social and economic environment, that affect methods and options, also contribute to the complexity of geotechnics. The increasing number of factors - economic, social and environmental - that must be taken into account in all construction activities and the growing social concern

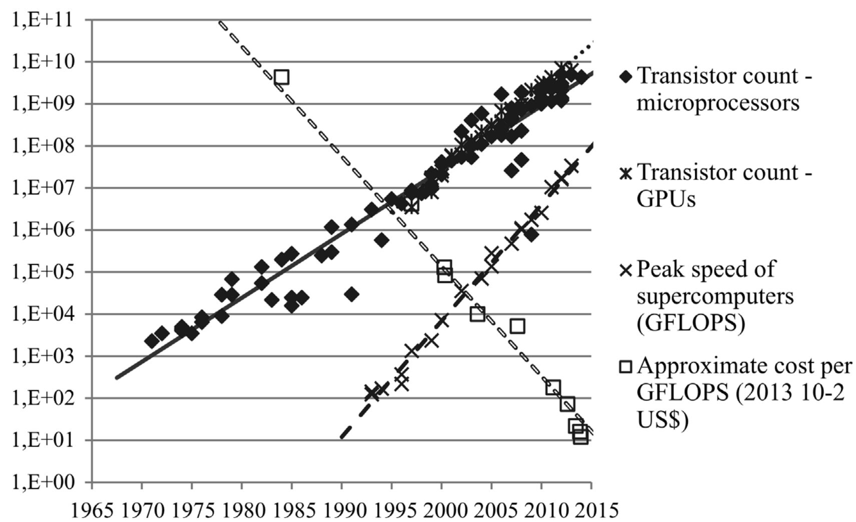

Figure 4 - Evolution of computers: number of transistors, processing speed of supercomputers and costs (Sources: http://en.wikipedia.org/wiki/History_of_ supercomputing; http://en.wikipedia.org/wiki/Transistor_count; http://en.wikipedia.org/wiki/FLOPS).

with the consequences of works (including the environmental ones) imply higher and higher complexity levels, making it essential to have a multidisciplinary approach.

The best strategy to survive and thrive under complex conditions is to develop adaptability to conditions that are perpetually changing (Rzevski & Skobelev, 2014). This type of strategy is not strange to geotechnical engineers; the Observational Method was conceived to enhance the adaptability to conditions that are complex and therefore not completely known in advance. Indeed, according to Nicholson *et al.* (1999), "(...) the Observational Method in ground engineering is a continuous, managed, integrated, process of design, construction control, monitoring and review that enables previously defined modifications to be incorporated during or after construction as appropriate. All these aspects have to be demonstrably robust. The objective is to achieve greater overall economy without compromising safety (...)".

Complex systems are characterized by the fact that they frequently change, being therefore necessary, when trying to study and manage them, to have methodologies able to react quickly and positively to changes permanently and in real time (Rzevski & Skobelev, 2014).

2.7. Conclusion

The acceleration of global population growth and of the intensive use of perishable resources happened relatively recently, and led to major imbalances. Indeed, the data collected by historical economists show that until around 1750 both the population and the means available for people to live had a very slow evolution over time, as shown in Fig. 5. That is, until the advent of the Industrial Revolution, population and income per capita remained almost stationary over hundreds of years, progressing very slowly, and the income did not show major differences between regions (see Fig. 5).

Since the Industrial Revolution (Industrial Revolution was the introduction of new manufacturing processes during the period from 1760 to sometime between 1820 and 1840 and began in Britain) it is observed that: 1) global population starts to grow exponentially; 2) GDP per capita begins to grow fast in certain regions of the world; 3) in other regions evolution is much slower or occurs after a certain interval relative to the first, so the differentiation between countries and regions of the world gradually increases.

The crucial factor for the sharp and rapid growth of GDP per capita was the technological progress (Clark, 2007). The Industrial Revolution consisted of the first appearance of fast economic growth fueled by a production efficiency made possible by advances in knowledge. The pace of that technological and cultural revolution is no longer related with the natural rhythms, with the biological adaptation and even less with the geological evolution.

Today's world still has enormous needs - briefly characterized in Chapter 4 - which are more acutely felt in less developed countries, but these insufficiencies need to be addressed using methodologies and processes different from those employed in previous periods, much more conditioned by factors of sustainability. In any case, if technology was what allowed the progress achieved since the Industrial Revolution, it will also be technology - now developed to ensure sustainability - to find solutions to current problems. Technologies and scientific knowledge are of inestimable value to the identification and solving of problems, to the development of robust and low-cost projects, to the efficient and safe execution of buildings, to guarantee long-term maintenance, to protect against natural hazards and to a continued respect for the environment (NRC, 2006).

3. Background. Geotechnical Issues

3.1. Subjects covered

The central objective of this chapter is to describe what are meant to be the current gaps in geotechnical knowledge and practice, despite the fact that many and no-

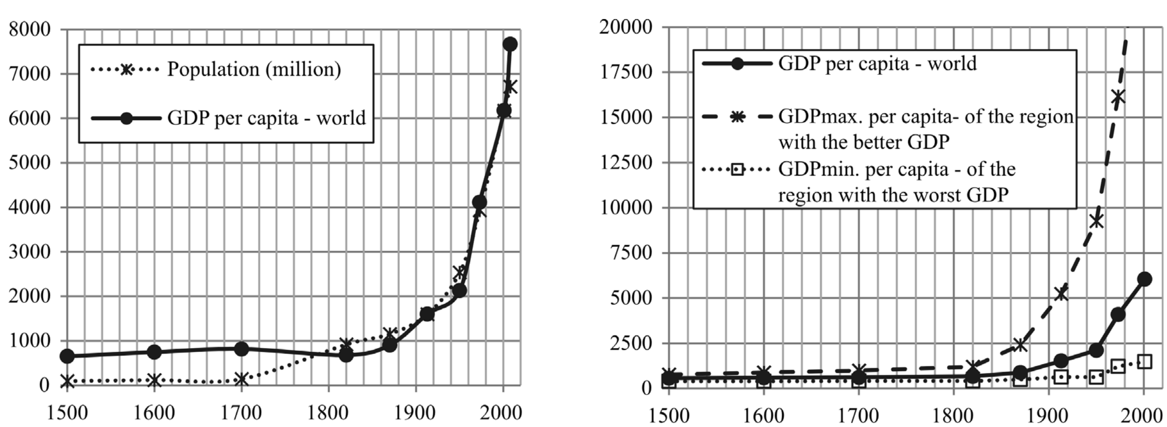

Figure 5 - E volution of population and GDP per capita worldwide (GDP: 1990 Int. GK$ - 1990 International Geary-Khamis dollars) (Source: Maddison, 2014).

table progress were already achieved. That description is done in the last section of the chapter.

In the next section it is noted that, although from the theoretical point of view many phenomena are well mastered and appropriate procedures are well known, in the practice, accidents continue to occur in various types of geotechnical structures, some with very serious consequences. Some examples of recent accidents are presented.

The following section presents two specific cases illustrating the difficulty geotechnical engineers experience while making quantitatively reliable forecasts. If qualitatively the behavior of geotechnical structures is or may be (there are powerful numerical tools to make this possible) well known, regarding to quantitative aspects, the ability to predict values that reasonably fit the real ones, for many types of geotechnical structures, is still rather poor, as shown by the examples presented.

3.2. State of the practice and state of the art. Accidents

3.2.1. Preamble

In many respects, geotechnics is a mature scientific field. In addition to an already well-developed understanding of the fundamental behavior of soils and rocks, technological advances enabled the finding of solutions to many important and complex problems (Long, 2006): 1) we know how to build proper foundations, safe dams, stable roads and tunnels; 2) we have a reasonable knowledge of groundwater behavior, how to extract oil resources and how to develop a geothermal field; 3) we understand quite well which factors lead to soil liquefaction during earthquakes or to the occurrence of landslides; 4) etc. The biggest problem that remains is that "(...) the state of the practice worldwide does not match the state of the art (...)" (Long, 2006). Even when the knowledge exists, reasons of economic and financial policy or ignorance lead, quite frequently to dangerous practices.

3.2.2. Examples of some collapses occurred recently

Figure 6 shows the collapse of a 13-floor building occurred in Shanghai on June 27, 2009. Part c) of the figure outlines the explanation provided for such spectacular and unusual collapse. Anyway observing parts a) and b) it is possible to conclude that the piles had no reinforcements or were insufficiently reinforced.

Figure 7 relates to the collapse of an anchored diaphragm wall that took place on March 3, 2009, in Cologne. The collapse of the wall caused the overthrow of the 7-storey building that housed one of the most important German historical archives, evacuated before the accident, and of two adjacent buildings, in one of which (n. 230) lived the two fatalities. The rupture occurred during the final phase of a 28 m deep excavation and has been due to the inflow of water and loose materials in the excavation, which caused differential settlements of building foundations and, subsequently, its collapse.

Figure 8 refers to a landslide occurred in March 2014 in Oso, USA. This landslide had dramatic consequences - caused 43 deaths, the deadliest in the history of the USA. Note the clear signs of slope instability, clearly visible in the photo taken before the accident.

The latter case (Fig. 9) refers to the tailing dam rupture at Mount Polley mine, explored by Imperial Metals. It is a copper and gold open pit, located in British Columbia, Canada. In August 4 2014 the dam suffered a large rupture, causing the release of 25 million m^3 of contaminated water and mine waste into the existing system of natural lakes nearby.

3.2.3. Causes of collapse

Delatte (2006) studied some well-documented cases of structural ruptures and concluded that there are aspects common to many of them, which are: 1) to reach knowledge and good practice limits at the time; 2) not paying enough attention to early signs of misbehavior; 3) supervision problems during construction; 4) lack of robustness and redundancy of the project; 5) maintenance and inspection problems.

Day (2009) studied several historical cases of collapse of geotechnical structures published in the specialized literature and concluded that the main causes of the failure or deficient behavior are those shown in Table 2; often inadequate behavior is due to a combination of two or more of these reasons. In any case, water and / or water pressure are the factors that most often contribute to the occurrence of bad behavior of geotechnical structures.

3.3. Prediction of geotechnical structures behavior

3.3.1.Preamble

Despite the very significant developments already achieved, given the difficulties involved, behavior predictability of geotechnical actual works remains relatively limited. Indeed, most of the benchmarking processes that have been carried out have led to relatively poor results. Two very different illustrative examples are presented below.

3.3.2. Piles constructed on residual soils

The International Event Prediction - Behaviour of Bored, CFA and Driven Piles in Residual Soils was organized in association with ISC'2 (2nd International Conference on Site Characterization), held at the Faculty of Engineering, University of Porto, in 2004, in order to estimate the load capacities of piles installed in granite residual soils using different methods. All details of the event as well as some later interpretations were collected in a volume published in 2008 (Viana da Fonseca & Santos, 2008).

The characterization of the experimental site was carefully done using field (SPT, DPSH, CPT, DMT, PMT,

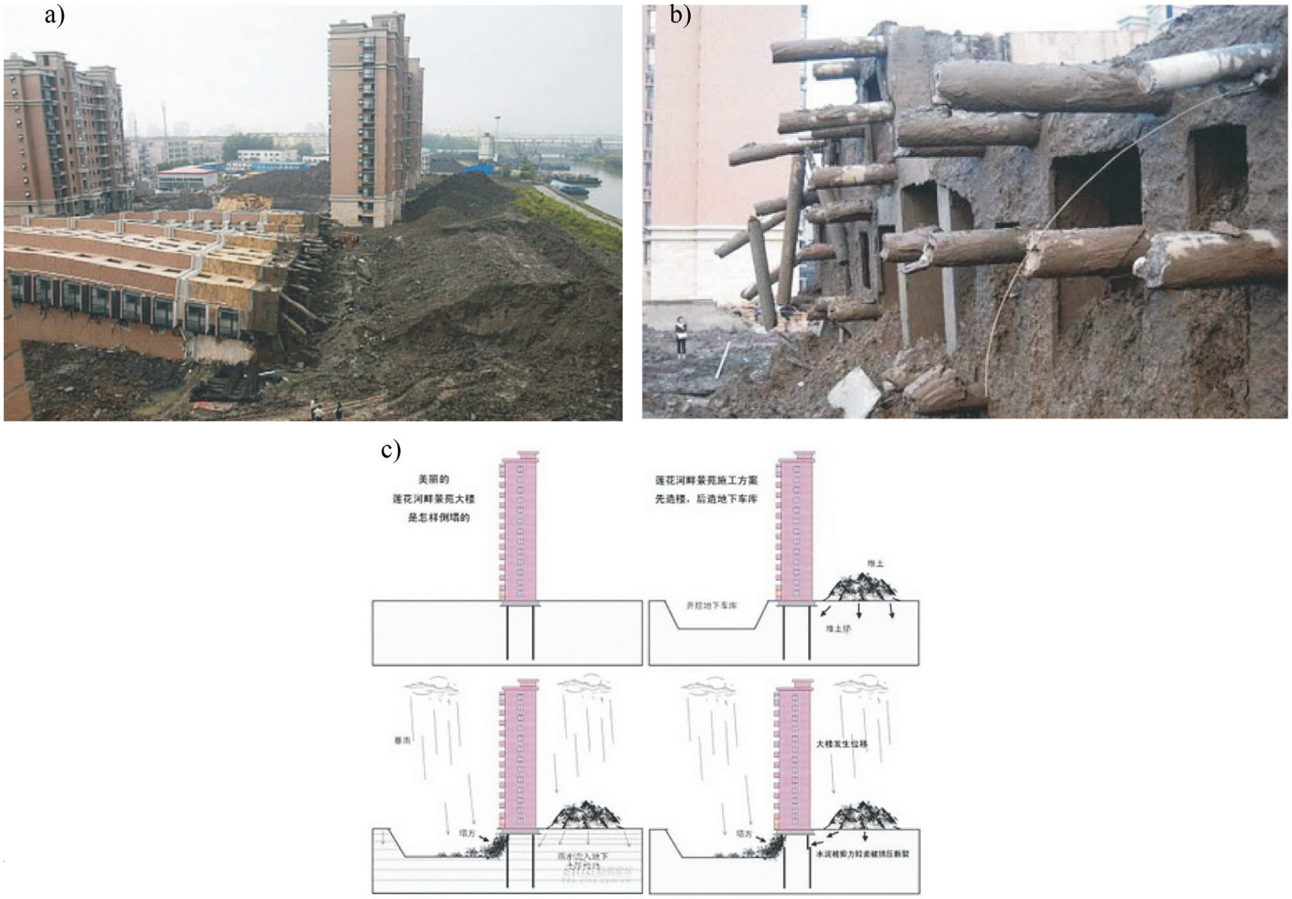

Figure 6 - Building collapse in Shanghai in June 2009.

SP, crosshole seismic testing) and laboratory tests (triaxial, resonant column and oedometric tests). 3 pairs of 6 m-long piles were installed: 1 pair of prefabricated driven piles (C1 and C2) with a 350 mm-side square section, 1 pair of bored piles (E0 and E9) with 600 mm diameter and 1 pair of continuous flight auger (CFA) piles (T1 and T2) with the same diameter. Piles C1, E9 and T1 were tested statically (vertical). In order to study the lateral resistance mobilization, the last two piles were instrumented with 6 gauges placed in their centers at 1.02 m intervals. A load cell was installed on the basis of pile E9.

32 international teams, nine of which were Portuguese, participated in the event. Table 3 shows the number of forecasts presented.

$R_Q = Q / Q_{SPLT}$ (s/b = 10%) is the ratio between the resistance estimated by the different participants, Q, and the resistance measured on the trial for a settlement equal to 10% of pile diameter, Q_{SPLT} (s/b = 10%). Predictions made for piles T1 and E9, in terms of their R_Q values, are gathered in Fig. 10. Figure 11 presents R_Q values for C1 pile resistance.

Concerning piles T1 and E9 the following may be concluded: a) pile resistance estimates are located mostly in the non-secure side, *i.e.* they are too optimistic; b) in both cases, total resistance estimates result from a "strange combination" of two completely wrong estimates; indeed, almost all methods very distinctly overestimate (mostly on pile E9 case) the tip resistance and, less unanimously and not so distinctly, underestimate (mostly on pile E9 case) lateral resistance; c) therefore, in general terms, the resistance mobilization mechanism was not adequately captured by the methodologies employed by the participants in the event. With regard to the driven pile it appears that most forecasts underestimate its resistance.

The general conclusion of the careful forecasting exercise briefly described is that the methods used - probably most of them developed for sedimentary soils - cannot capture the specific characteristics of residual soils. Indeed, one can argue that the general poor quality of the forecasts is due to the fact that soils are residual soils. Despite the careful characterization of the experimental site, the complexity of residual soils behavior, the ignorance that still exists of the characteristics of this behavior and the lack of experience in the application of methodologies mainly developed for sedimentary soils to residual soils without the necessary adjustments - which are only likely to become appropriate after obtaining sufficient experience - do not allow achieving further encouraging results.

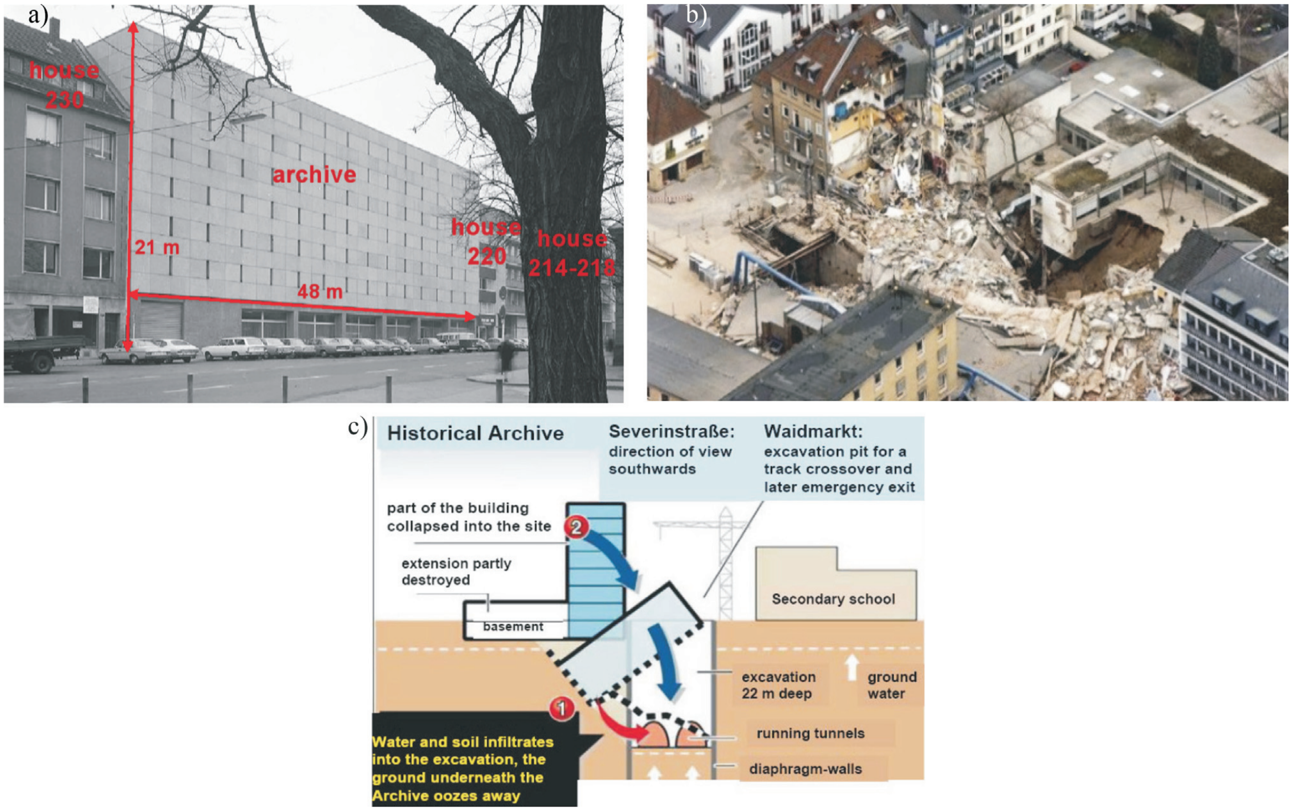

Figure 7 - a) The archive and adjacent buildings; b) Photograph after the collapse; c) Interpretation of the causes of the collapse (Haack, 2009).

Figure 8 - Landslide occurred in March 2014 in Oso, USA. The photo on the left was taken before the landslide and the one on the right after.

3.3.3. Excavation supported by a curtain anchored in sand

The second case (Schweiger, 2002) is a completely different situation and refers to the behavior in service of an anchored excavation in Berlin sandy soils, whose properties were relatively well-known by the teams who participated in the forecast. The forecast exercise tries to emulate, as far as possible, the methodologies commonly used in practical engineering projects of the same type. Thus, the exercise had the following characteristics (Fig. 12): a) as, in practice, geotechnical reports hardly provide all the data required by the numerical analyzes, only limited data on Berlin sands properties was provided, such as reference values of deformation and resistance parameters often used in the design of excavations in Berlin sands; b) some oedometric and triaxial tests results were supplied, however the participants had to evaluate the deformability values to be used in calculations, based on their experience; c)

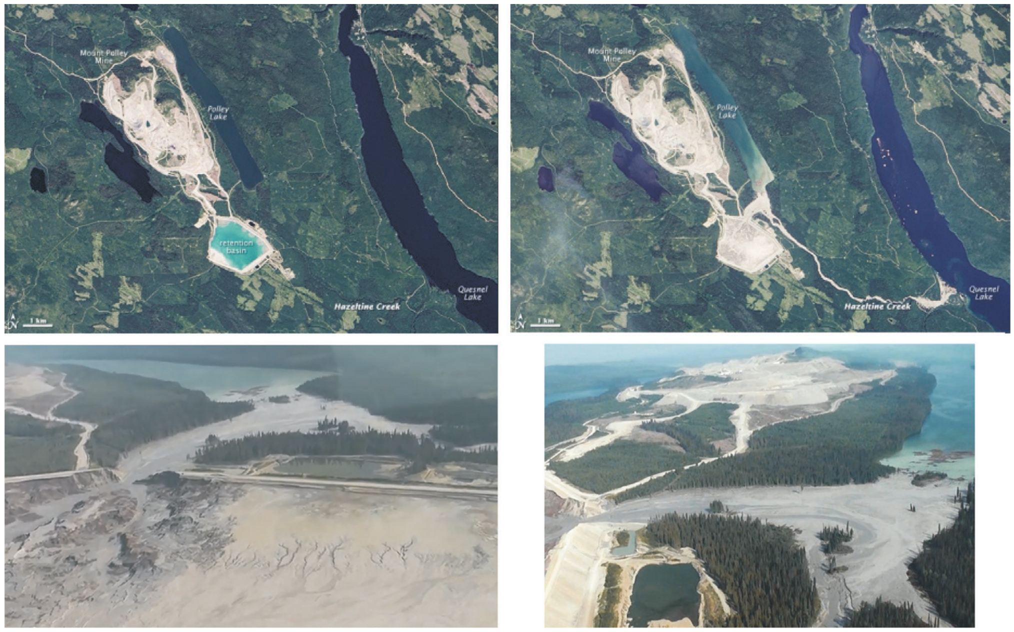

Figure 9 - The tailing dam rupture at Mount Polley mine (Canada), held in 4/8/2014.

Table 2 - Most common causes of geotechnical failures (Day, 2009).

Cause	Description
Inadequate geotechnical investigation	Budgetary or programme restraints can result in insufficient investiga-tion to adequately model the conditions on the site. Nevertheless, even the most comprehensive investigations may fail to reveal critical conditions that affect the geotechnical behavior of the profile.
Incorrect parameters	Many reasons, including: i) poor sampling and testing procedures; ii) selection of inappropriate parameters for particular design situation (*e.g.* mean values, lower characteristic values or upper characteristic values); iii) underestimation of the variability of soil properties.
Inappropriate analysis model	Failure to recognize the critical failure mechanism, *e.g.* drained v. undrained failure of slopes or foundations, internal v. external stability of reinforced fills.
Underestimation of actions	The inaccurate assessment of magnitude, distribution or combination of actions (forces or displacements), the disregard of particular load case or the change of the use of the structure over time.
Unexpected groundwater regimes or changes in moisture content	Shifts in ground water levels can increase structure loads and decrease soil shearing resistance. Seepage forces can also have an adverse effect on stability. Changes in the moisture content of partially saturated soils can cause softening, heave or collapse settlements.
Substandard workmanship or materials	Not following the required construction procedures (including sequence and timing), not meeting the specification requirements, the employment of inappropriate construction techniques, non-compliance of material properties with design assumptions.
Non consideration of abnormal events in design	Extreme meteorological events (including temperature, precipitation or wind), accidental impact, errors in construction or use of structure.

normal values (linear elastic) were proposed for the properties of the concrete reinforced wall ; d) the problem actually emulated a real work, horizontal displacements of the wall were measured; prestressing forces applied to the anchors and data on construction sequence were provided; e) it was assumed that the problem was plane strain, that the effect of wall construction could be neglected and that the hydraulic "cut off" installed at 33 m-depth (Fig. 12) was not a structural support; f) it was imposed any restriction on the constitutive model, the discretization, the type of elements, etc

Table 3 - Forecasts presented by the participants.

Methods		Bored pile (E9)	CFA pile (T1)	Precast driven pile (C1)
Analytical based on load capacity formulas using the basic parameters, c', ϕ', etc.		15	15	16
Empirical based on results of tests "in situ":	- SPT	19	11	18
	- CPT	35	18	54
	- PMT	8	8	6

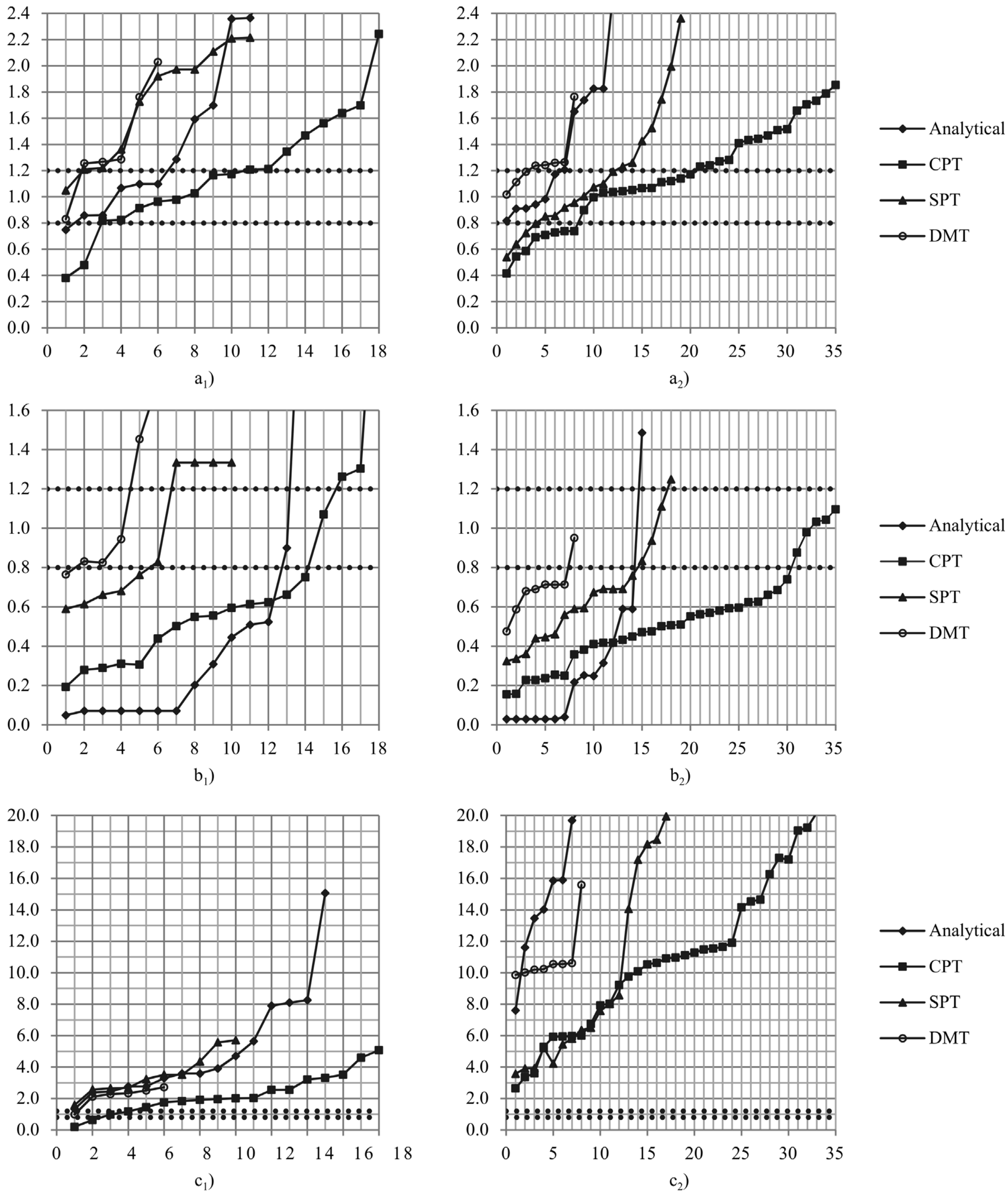

Figure 10 - R_Q values of: a) pile resistance; b) shaft resistance; c) base resistance; piles T1 (side 1, left) and E9 (side 2, right).

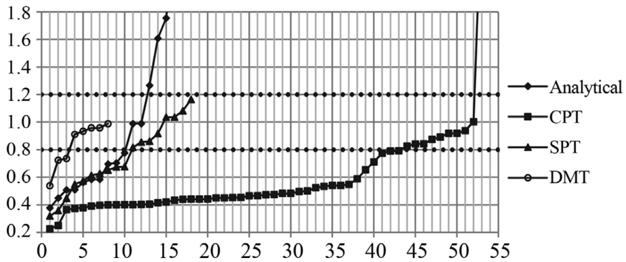

Figure 11 - R_Q values of all forecasts of pile C1 resistance.

.; the use of soil-wall interface elements and the calculation domain size shown in Fig. 12 were suggested.

Twenty wall behavior forecasts were presented by geotechnical engineers or teams from universities and consulting firms. A wide variety of computer programs and constitutive laws was used; most participants used perfect (8) and hardening (6) elastic-plastic models; hypoplastic formulations were still used (3 participants).

The various participants did not significantly differ in the values of the ground strength parameters admitted but differed in the dilatancy values, between 0 and 15 degrees. As expected, there was a wider range of options in regard to deformability, and most analysts adopted values based on their own experience.

The options relating to the interfaces, the elements type, the analyzed area size, the anchors modeling process, the constituent model implementation details and the resolution process of the nonlinear system were also several.

Parts a) and b) of Fig. 13 show the final displacements obtained in some of the twenty calculations: i) the estimated maximum wall horizontal displacement varies between 8 and 67 mm; ii) the foreseen maximum soil settlement varies between -16 (uplift) and 45 mm. Six of the twenty calculations were discharged because (Schweiger, 2002) they yielded much higher or unreasonable displacements.

There are two estimates (mostly B15 and B11) that very reasonably fit the measured wall horizontal displacements. Other calculation (B9) estimates displacements about 40% higher than the measured ones in the central area, but deviates too much at the top and at the bottom of the wall. The remaining calculations deviate too much from the measured values - the estimated horizontal displacements are higher (1.5 to 2.5 x) or much higher (up to 8 x) than the measured ones. On the other hand, some calculations predict much lower wall displacements (less than

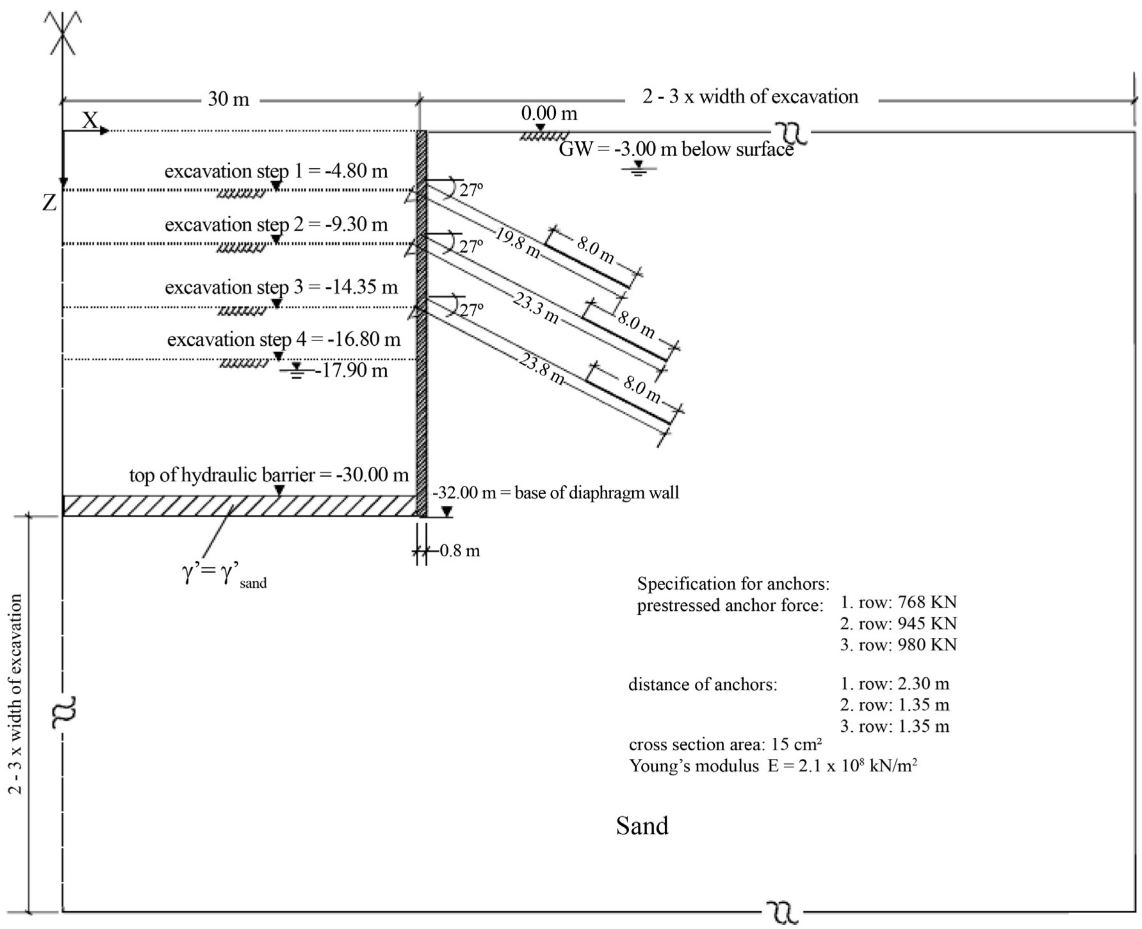

Figure 12 - Characteristics of the anchored excavation in Berlin sands (Schweiger, 2002).

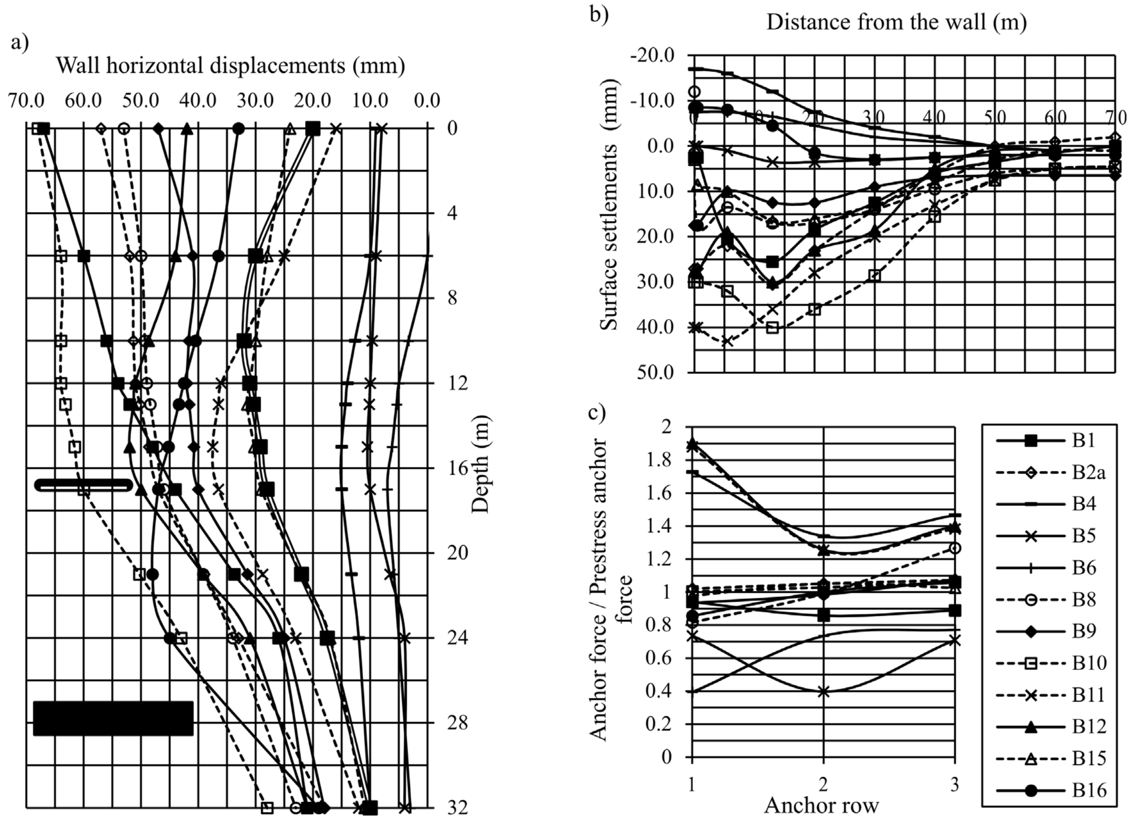

Figure 13 - Calculated final values: a) wall horizontal displacements; b) surface settlements; c) forces on the three anchor rows (Schweiger, 2002).

half) than the measured values. Also with regard to the anchors forces (Fig. 13 c) the forecasts fluctuation is very marked. The same is true with regard to the prediction of the wall bending moments.

This wide discrepancy in the calculations results is due, among other reasons, to the fact that participants use different numerical models. So, it may be argued that because of this diversity it doesn't make sense to compare the results. However, as Schweiger (2002) points out, one cannot ignore the fact that this is what happens in practice and that the aim of the exercise was to test the methodologies applied in professional practice. Moreover, according to Schweiger (2002), most analysts made reasonable choices, whether in relation to the values assumed for the basic parameters and as regarding to the modeling details. Since it doesn't seem reasonable that the results of analyzes carried out by able and experienced people show a variation "dependent on the author" of 100% or more, it is concluded that the complexity of geotechnical problems requires a deepening of knowledge and methodologies, which also involves the establishment of recommendations and standards when possible.

3.4. Knowledge gaps

The difficulties determining the appropriate geotechnical parameters, particularly those featuring the deformability, constitute an undesirable situation but represent what happens in current practice. As illustrated by the first case reported in the previous section, this is not only due to the fact that, in most practical cases, geotechnical investigations and reports do not have the necessary depth essential to *feed* properly the most sophisticated numerical models. Indeed, in the present state of knowledge and practice, deficiencies in the following areas are unequivocally clear:

- Ability to adequately explore and characterize soil masses; actually the most important current need of geoengineering is perhaps to improve the capacity to *see inside the Earth*, whatever the specific problem to be solved may be; faster underground characterization techniques are needed, more accurate and less invasive and with better cost-benefit ratios, (NRC, 2006);
- Methodologies for proper consideration of heterogeneities and discontinuities;
- Ability to determine the spatial variability of soil and rock properties, the uncertainty of these properties and of soil and rock masses behavior and, hence, the reliability of systems;
- Characterization and understanding of the behavior of geomaterials that do not fit the classical Soil and Rocks Mechanics paradigms; characterization of materials that are between hard soils and soft rocks;

- Knowing the effects of non-saturation on the behavior of soil masses and its relevancy for the performance of geotechnical structures;
- Understanding geotechnical structures behavior taking into account the actual stress paths on the involved soil masses;
- Establishing procedures and standards for the reliable application of numerical models in geotechnical engineering practice (Schweiger, 2002).

Apart from these, the following weaknesses are also identified (NRC, 2006):

Improved methods of detection and monitoring, including best geophysical and remote control technologies, most reliable and precise instrumentation, more advanced techniques of data collection, processing and storage.

- Understand and predict long-term behavior of geotechnical structures; properties and other conditioning factors change over time, but the ability to accurately predict what will happen is limited, even for short periods of time.
- Understand the biogeochemical processes of soils and rocks with two purposes: (1) a better understanding of the composition and properties of soils and rocks and how they may change over time; (2) this improved knowledge may lead to the development of new remediation processes for environmental applications and of innovative and sustainable applications of existing techniques for stabilization and improvement of earth masses.
- Better methods and techniques for soil stabilization and improvement; now, more than ever before, it is necessary to deal with inadequate subsoil conditions, especially in urban areas and in megacities, both in developed and developing countries.
- Improve the prediction capacity of geomaterials' behavior under extreme loads and in extreme environments; understanding the behavior of geomaterials in extreme environments, including the ocean floor, the polar regions, the Moon or Mars provides new opportunities and both technical and scientific challenges.

Develop databases and models for the underground space, including geological and geotechnical data, information about the built environment (eg, location of underground utilities), issues related to natural resources, environmental data and monitoring results of natural hazards and environmental conditions.

- Application of advanced computing technologies, information and communication systems; these technologies will condition what can be investigated and how.

Finally, it should be noted that to improve the predictive abilities of real works behavior, the benchmarking of models and methodologies acquires a significant importance in geotechnical engineering, probably greater than in other areas of engineering, because (adapted from Schweiger, 2002): i) the domain to analyze is generally not well defined; ii) it is not always clear whether to use continuous or discontinuous models; iii) there are many constitutive models but there is no approved model for each type of soil; iv) in many cases, the construction details cannot be modeled very closely in space and time; v) in general, soil-structure interaction is important and requires adoption of special treatments; vi) implementation details and solution methodologies (of nonlinear problems, which in general terms constitute the geotechnical ones) may affect the results of certain types of problems.

4. Needs

4.1. Introduction. The importance of infrastructures

Infrastructures are essential to the functioning of modern societies. Infrastructures ensure, on the one hand, the distribution of goods and services, essential for the promotion of prosperity and growth and, consequently, quality of life, health and safety of citizens, and, on the other hand, the quality of environments. Infrastructures played in the past and will continue to play in the future a vital role on economic and social development. Furthermore, the various infrastructure systems increasingly interact with each other, generating interdependencies and complementarities, as well as increasing vulnerabilities, presenting new challenges of interoperability and reliability (OECD, 2007).

Infrastructures provide the foundations underpinning the prosperity and well-being of nations: they facilitate movement and contacts, promote communications, provide energy and water, contribute to people's health and education and enable the economy as a whole to thrive. Infrastructure construction and maintenance costs are high, but the costs of not conducting the essential investments are incalculable; quality infrastructures may yield benefits for the economy, the environment and the social progress (WEF, 2012). So it is not surprising that, as shown in Fig. 14, countries with the higher quality of infrastructures are also more competitive (OECD, 2011).

However, many countries, developed and developing, face significant infrastructure deficits, due to population growth, urbanization, new needs and aging of existing infrastructures. Brief specific references to global needs of drinking water, energy and transport are made in the following sections and some relevant data on the importance of investments in infrastructures in the developing - mainly new infrastructures - and developed - mainly renovation of existing ones - countries is summarized.

4.2. Brief characterization of the needs in some sectors

4.2.1. Water

Water and sanitation is a key sector to human life, public health and the economy, the use of which requires appropriate infrastructures. Table 4 shows the distribution of water in the world and Table 5 the daily water consump-

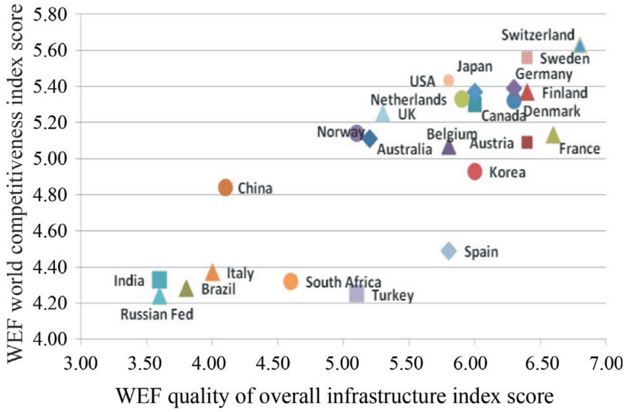

Figure 14 - Correlation between quality of infrastructure index and competitiveness index; both indices are set by the WEF - World Economic Forum (OECD, 2011).

tion per capita in several countries. Note that consumption is extraordinarily variable, between the high consumption of Americans and Australians and the low consumption of most African countries inhabitants.

In El País Semanal report (March 15, 2014) the following data characterizing the current situation is also referred: a) 20% of the world's aquifers are over-exploited; b) the collected water is consumed 70% in irrigation (agriculture), 20% in industry and 10% in household; c) the percentage of population with access to safe water is 100% in industrialized countries, 57% in sub-Saharan Africa and between 76 and 87% in the other world's regions; d) it is predicted that by 2030 water shortages may affect half the world's population; e) 1/3 of the population has no access to sanitation; f) 80% of waste water is not treated and is dumped into rivers and lakes; g) 70% of industrial waste is poured into water courses.

4.2.2. Energy

Energy and quality of life (child mortality, education, life expectancy, etc.) are closely linked, as demonstrated by the correlation between HDI (Human Development Index) and per capita energy consumption, shown in Fig. 15. HDI index is the average of three indices: life expectancy index, education index and GDP index. Data shows that human development is closely related to energy consumption, but also shows that similar life quality levels can be achieved with huge differences in energy consumption levels, which allows anticipating an increased efficiency in the use of energy.

A significant increase in energy demand over the next 25 years due to economic development and population growth is expected. According to Fragaszy *et al.* (2011) the growth will be of 17% if consumption and population grow at current pace, but it will reach 66% if consumption in developing countries increases to the level necessary for an adequate standard of living. This will exacerbate current environmental, political and social problems caused by dependence on fossil combustibles. Indeed, currently, over 80% of all energy consumed in the world is obtained from fossil fuels, mainly due to its low cost in current market conditions.

As stated above, burning fossil fuels releases carbon dioxide into the atmosphere, which is the main cause of greenhouse effect. Thus, the reduction of CO_2 emissions in the coming decades is a pressing need and a central task of applied research for years to come. The contribution of geotechnical engineers in finding innovative solutions that meet this overall objective can be and certainly is very broad and diverse. As examples, refer to geothermal energy and CO_2 capture and storage.

4.2.3. Transport

A recent OECD (2011) study states that global GDP is expected to double by 2030; the highest economic growth should occur in the Asia / Pacific region, with the leadership of China and India; in developed regions, US GDP should grow 50% and Europe GDP 40% by 2030.

The growth of economy, international trade and population (particularly urban) are important drivers of the increase in passenger and goods flow. With the doubling of world GDP by 2030, OECD expectations for the period 2010-30 are that, worldwide, the following annual increases should occur: i) around 4.7% in air traffic; ii) around 5.9% in air cargo; iii) more than 6% in maritime

Table 4 - Distribution of water in the world (10^6 km^3).

Atmosphere and soil moisture	0.9%	0.3
Rivers and lakes	0.3%	0.1
Groundwater	30.1%	9.8
Ice and snow perpetual	68.7%	22.3
Freshwater	2.5%	32.5
Saltwater	97.5%	1267.5
Total		1300.0

Source: El País Semanal No. 1955, March 15, 2014.

Table 5 - Water consumption per day per capita (in liters).

Angola, Cambodia, Ethiopia, Haiti, Rwanda	15
Ghana, Nigeria	35
China	85
United Kingdom, Brazil, India	135-150
Portugal	170
Italy, Japan, Mexico	365-385
Australia	495
USA	575

Source: El País Semanal No. 1955, March 15, 2014.

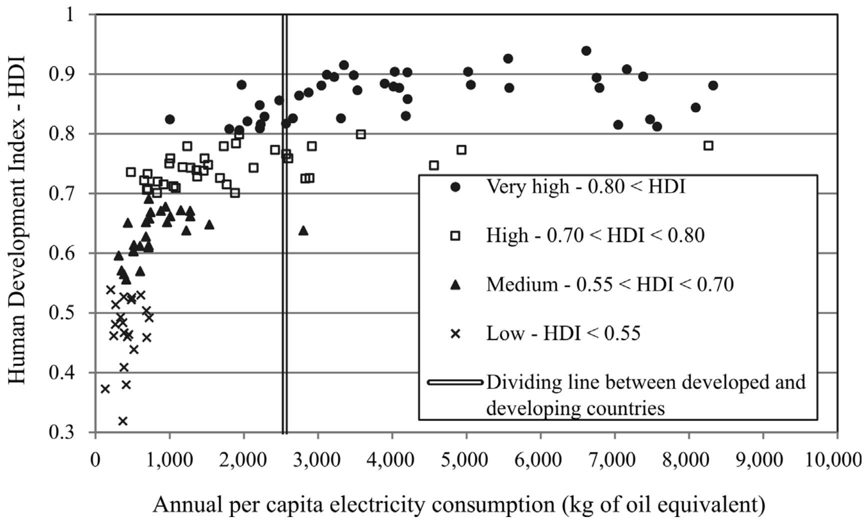

Figure 15 - Relationship between HDI and per capita primary energy consumption.

traffic of containers; iv) 2-3% in railway passenger and freight. These growths will lead to the doubling of air transportation of passengers in 15 years, the tripling of air freight within 20 years and the multiplication by 4 of shipping containers by 2030. Current infrastructures are not able to support growths with this magnitude, so major investments will be essential.

4.3. Estimates of future investments in infrastructures worldwide

In report "Infrastructure to 2030" (OECD, 2007) it is estimated that infrastructure needs (additional and renewals) worldwide by 2030 imply a cumulative total investment of US$ 71 x 10^{12}, between 2007 and 2030 (Table 6), not including airports and ports. A later report (OECD, 2011) concludes that it will be necessary an amount of US$ 11 x 10^{12} from 2009 to 2030 to meet global needs in transport infrastructures. Therefore, the average global annual investment should be around US$ 3.4 x 10^{12}, similar to the value pointed out by the McKinsey Global Institute (2013). Bearing in mind that the world GDP in 2013 was US$ 73.9 x 10^{12}, it is concluded that the aforementioned amount is greater than 4% of world GDP. This means that investments in infrastructures may reach high percentages of the GDP in countries with economies in strong development and lacking infrastructures.

A very recent document from the United Nations (UN, 2013) collects various estimates that have been made about overall annual investment needs worldwide, most of it to finance investments in infrastructures (Fig. 16). In each sector or cluster the variation of published estimates is very large, ranging from simple to 3-10 times more. This wide variation reflects (UN, 2013) differences of date, scope, methodology, references and other factors, including the uncertainty inherent to this type of exercises. With regard to infrastructures, probably the value estimated by OECD

Table 6 - Estimated investment in infrastructures until 2030, according to OECD.

OECD (2007) - Infrastructures to 2030	2007-2030
Rail, road, telecoms, electricity transmission & distribution, water	53 x 10^{12} US$
Electricity generation	12 x 10^{12} US$
Other energy-related investments (*e.g.* oil, gas, coal)	6 x 10^{12} US$
Airports and ports	-
	71 x 10^{12} US$
OECD (2011) - Strategic Transport Infrastructure Needs to 2030	**2009-2030**
Airports capital expenditure	2 . x 10^{12} US$
Port infrastructure facilities capital expenditure	0.8 x 10^{12} US$
Rail "new construction" (including maintenance)	5 x 10^{12} US$
Oil and Gas - transport & distribution	3.3 x 10^{12} US$
	11.3 x 10^{12} US$

(2007, 2011), intermediate between the extreme values included in Fig. 16, is a reasonable estimate. This means that the average annual investment in infrastructures in the world by 2030 will be something above 4% of the global GDP.

5. Global Outlook

5.1. Introduction

Shaping geotechnical engineering future is both a challenge and a problem. The size of this challenge stems from the fact that geotechnics, perhaps more than any other engineering branch, being a technical and scientific field which has a major contribution in developing the infrastructures necessary to human progress, is strongly affected and conditioned by the societal factors briefly stated in the previous chapters. Moreover, despite the fact that geotechnics is, in many aspects, a mature technical and scientific field, able to address and solve many serious and complex problems, there are still many problems / difficulties of various kinds to face, resulting from the specificity and extreme variability of natural materials, the very wide range of issues with which geotechnics deals and the constant appearance of new challenges (more complex problems, new materials, new technologies, etc.).

On the other hand, geotechnical engineers must have a perception, as clear as possible, of the economic, social and environmental implications of their actions.

In what the definition of prospects for geotechnics future evolution is concerned, there are global / societal perspectives, which are directly related to the economic, social and environmental constraints (described in Chapter 2), as well as to the infrastructural needs generated by these constraints (summarily set out in Chapter 4), and there are more particular / professional perspectives, specific of geotechnics, dependent on its state of development, but also conditioned by some of the societal factors.

In any case, there is one factor that will certainly affect all future developments. As stated in a NRC (2006) report, there are no activities isolated in this rapidly changing world; decision-making in a given place has repercussions elsewhere, sometimes even dramatic and unforeseen consequences; many practical decisions at all scales are having a strong impact on the environment. In order to effectively respond to the problems caused by human interactions with Earth systems, it is necessary to extend the scope of geo-engineering: sustainable development is a new paradigm for the practice of geo-engineering. Geo-engineering has made significant progress in response to societal needs; however, it is necessary to change perspectives, from the national to the global point of view, and to include the social, economic and environmental dimensions in the development of robust solutions to meet those needs. Greater attention to anthropogenic effects on the environment and to sustainable development are important manifestations of this change in perspective.

Therefore, all engineering projects and more generally all infrastructure planning actions, should bear in mind the issue of sustainability (Sterling, 2012; Nelson, 2013; etc.), whose overall objective, defined as broadly as possible, is to ensure the satisfaction of society's current needs without compromising the ability of future generations to meet their own needs (Brundtland, 1987).

Sustainability and also resilience - some consider this concept integrated in the first - are two key concepts to ensure a safer future for human development. Ensuring the sustainability of all activities undertaken and the resilience of the designed solutions implies that such desiderata are taken into account in the conceptual and constructive methods, procedures and processes to be applied.

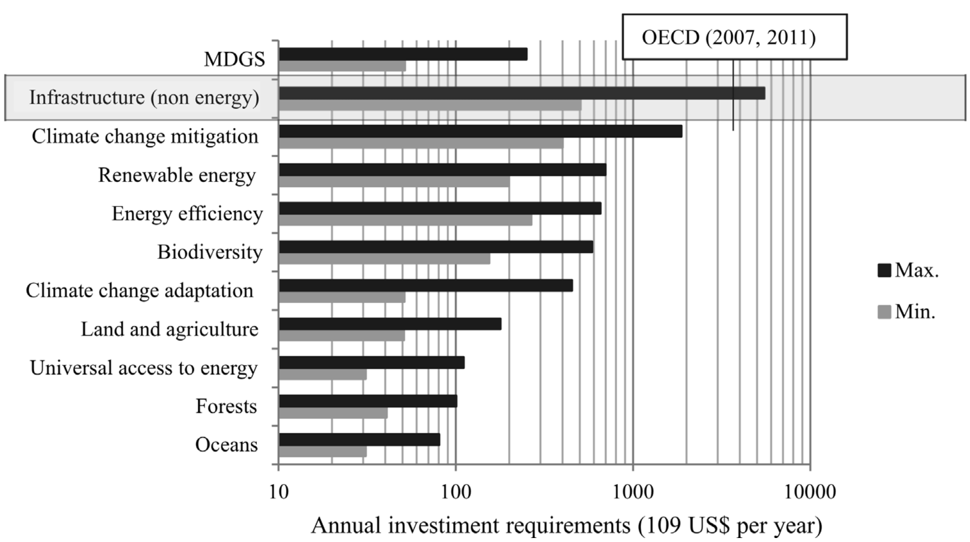

Figure 16 - Order of magnitude of annual investment needs - literature search (adapted from UN, 2013, Chapter 1).

In the remainder of this chapter global / societal perspectives are discussed. The specific perspectives of geotechnical engineering development are treated in the next chapter.

5.2. Global perspectives

As stated previously, the general prospects of the future development of geotechnical engineering derived from reflections discussed in Chapters 2 and 4. They are the following, among others: i) growth and urbanization of the population as well as economic and social development generate major infrastructures needs, therefore geotechnical engineers will be heavily involved in its planning, design and construction; ii) human activities and needs put enormous pressure on natural systems, posing new problems for the solving of which engineering involvement is essential; iii) the solutions will have to be defined bearing in mind the perishability of resources, the imbalances that human actions can cause - these imbalances can have serious consequences, for instance the increase of natural disasters that can seriously affect human populations - and the need to ensure that future generations have the resources essential to them, that is, in a word, the solutions will have to be sustainable; iv) new technologies will be a valuable aid in finding the best solutions, since they provide forecasts of increased quality (increased capacity of data collection and processing and of phenomena modeling, etc.) and the advent of innovative and environmentally more appropriate solutions; v) interventions should be environmentally responsible and economically beneficial, seeking holistic solutions to problems.

Humanity depends on natural resources in order to survive. They support the functioning of the global economy and our quality of living depends on them. Natural resources include raw materials such as fossil fuels and minerals but also food, soil, water, air, biomass and ecosystems. However, resources are limited and, according to some experts, some of the natural basic resources are on the way to exhaustion. Demand growth and competition for natural resources put pressure on the environmental and ecological balances. Hence the need <u>to improve the efficiency of resource usage</u>, such as, for example, water or certain minerals, essential for life (see, for example, Rijnaarts, 2010). The efficient use of limited resources means using them in a sustainable way, *i.e.*, taking into account the capacity of resources regeneration (Breedeveld, 2012).

The contributions to design the appropriate solutions that engineers and, in particular, geotechnical engineers have to make, should (Long, 2006): i) take into account new technologies and new approaches to solve problems better, quicker and in a cheaper way.; ii) bear in mind that the problems whose solution they seek, such as the consequences of global change, supply of energy free of environmentally aggressive emissions, water supply and urban systems are socially and economically very important for human populations and <u>involve issues that require multi- and interdisciplinary approaches</u>.

6. Specific Perspectives for Geotechnical Engineering Development

6.1. Fundamental basic areas

Geotechnical fundamental basic areas are addressed in this section. Subsequently, perspectives concerning other areas more directly related to problem solving are analyzed, not trying to be exhaustive, which given the vast fields covered by geotechnics, would in fact be impossible.

In 1936 Terzaghi wrote: “In soil mechanics the accuracy of computed results never exceeds that of a crude estimate, and the principal function of the theory consists in teaching us what and how to observe in the field”. 80 years later it is obvious that some of the conditioning factors that, to date, contributed to make this judgment a reality have been overcome, but others have not. Indeed, although since then there has been a huge development of geotechnical concepts and theories and of calculation capabilities, the fundamental difficulty of characterizing ground variability remains, which justifies why geotechnical engineers continue to suffer from lack of information. Therefore, even the results of calculations using very sophisticated numerical models still remain more or less rough estimates of reality.

Thus, with the aim of improving compliance between forecasts and reality, it is easy for a geotechnical engineer to outline the key challenges of his technical-scientific work field:

1) Geotechnical ground characterization, including its spatial variability; the characterization should include all variables important to the problem addressed;
2) Better understanding of the complex behavior of soils and rocks, including the influence of time; to a complete and comprehensive understanding of soils and rocks characteristics and behavior as well as to the development of new effective, efficient and economic solutions for geotechnical problems it’s important to consider not only mechanical but also thermal, chemical and electrical interactions (NRC, 2006); within this scope are the soils that do not fit the traditional paradigms (residual soils, unsaturated soils, etc.) and local soil (Terzariol, 2009; Francisca, 2011); in some circumstances it is essential to acknowledge the behavior of geomaterials under extreme environments (NRC, 2006);
3) Improving uncertainty estimations (taking into account the spatial distribution and time effects) that affect the decision process and developing better methods to assess the potential impact of these uncertainties on the engineering decisions, *i.e.*, on the risk analysis that support engineering decisions; indeed, it is still diffi-

cult to translate fundamental knowledge of soils and rocks physics and chemistry and of certain systems behavior in methodologies and processes that allow to quantify the properties required for engineering analysis; in face of these constraints, the paradigms to deal with the resulting uncertainties are poorly understood and even more poorly practiced.

I personally believe that there is nowadays already the possibility of finding good answers to these three problems based on:

- the use of geophysical methods in field and laboratory;
- the use of laboratory tests with ability to control different paths and to measure with high precision what is going on, with a minimum interference of measuring equipment;
- the use of methods of analysis that allow modeling particles set, enabling a better study of phenomena at local level and with consequent repercussions at macroscopic level; for now these studies are mostly theoretical, aiming for a better understanding of phenomena;
- the development of methodologies to assess variability in analysis and design procedures;
- the incorporation of risk analysis in the project development processes.

6.3. Other areas

The future of geotechnical engineering is not confined to the key areas mentioned in the previous section. Indeed, other diversified perspectives appear when examining the gaps that remain and continue to challenge the practice of geotechnical engineering.

In a text entitled Geotechnics: the next 60 years, Simpson & Tatsuoka (2008) predict that the future of geotechnical construction will be very active, addressing the application of processes and methodologies currently in use and many developments and innovations, with the common and primary objective of reducing energy consumption and dioxide carbon emissions. More specifically they indicate that: 1) advances in all types of geotechnical works are to be expected, including underground and foundation works; 2) soil improvement and reinforcement techniques should have a particularly important development, together with more advanced techniques to reuse land that was previously used (NRC, 2006), including bio-nano-geotechnical technologies (Nelson, 2013); 3) developments in computing, communications and instrumentation will provide new opportunities for improving existing procedures (NRC, 2006; ASCE, 2007).

There is a coincidence of views (NRC, 2006; Chowdhury & Flentje, 2007; Simpson & Tatsuoka, 2008; Francisca, 2011; Brandl, 2011; Misra & Basu, 2011; Nelson, 2013; etc.) regarding the promising future of ground improvement and reinforcement technologies. It should be referred that 3 of the 5 French geotechnical research projects presented at the 18th ICSMFE (Schlosser *et al.*, 2013) relate to soil improvement and reinforcement techniques - soil nailing (CLOUTERRE), micropiling (FOREVER) and strengthening of foundations with rigid inclusions - and the fourth, on dynamic pile driving (VIBROFONÇAGE), also has applications in sandy soils improvement, although its scope is wider.

Clough (2006) draws attention to the fact that advances in technology allow addressing fundamental problems that could not be addressed before because there were no means to do it. Some examples: i) improving the understanding of complex multiphase systems such as soils through molecular simulation of components, water, air, solid particles, clay minerals, organic matter, etc.; ii) studying the behavior of complex geotechnical structures at different scales, from basic nanostructure, through microscopic scale (for example, to understand how earth masses mobilize resistance in some areas while in others resistance decreases to residual levels) until macro scale (for example, to visualize how deformations are mobilized by the different construction methods); iii) advances in computing power allows for the creation of online systems for collection and processing of information in order to improve the ability to adjust the projects to local conditions, totally exposed only during implementation (observational method).

With respect to underground structures, Nelson (2013) reports the necessity for: i) computational models alternative to expensive tests in order to study the effect of scale present in most rock formations and to better understand the mechanics of fracture; ii) advances in the understanding of underground structures behavior over time, a key aspect for evaluating sustainability and resiliency, which necessarily involves long term; iii) the behavior of underground works waterproofing systems need to be better understood, including the long-term (life cycle); iv) use of new materials and technologies for the rehabilitation and life extension of existing underground infrastructure; v) development of probabilistic models for the design of underground structures contemplating the lifespan and incorporating costs, impacts, necessary resources, contingencies and risks.

In the future, world will be characterized by a social and environmental situation with high levels of risks of various kinds. Civil engineers are called to be in the forefront of the development of appropriate methodologies and procedures to manage and mitigate risks (ASCE, 2007). It is a complex and deeply multidisciplinary task for, on the one hand, it requires the development of robust methodologies for determining probability of occurrence of adverse events - which implies, in particular, to improve ability to characterize soils and rocks spatial and temporal uncertainties, that condition catastrophic ruptures caused by extreme natural events such as earthquakes, storms, etc. (Chowdhury & Flentje, 2007). On the other hand, it requires the establishment of reliable and robust procedures for evaluating consequences of any nature - social, economic, technological, etc.

Francisca (2011) points out that geotechnical engineering will have to make major contributions to solve central problems of current civilization: i) urban population increase poses complex environmental problems as a result of land-use change, increasing air, water and soil pollution and waste generation and accumulation; ii) congestion in urban areas makes it necessary to design and build geotechnical structures in difficult conditions (unstable soils, steep and unstable slopes, erosion problems, ground waterproofing, flood risk, etc.) and to recycle materials resulting from demolitions; iii) in short, the scope of geotechnical engineering profession will be expanding in the near future to meet demand generated by new problems such as climate change, demand for drinking water and energy, population growth and the need for rational and optimized use of resources in order to achieve sustainable development.

NRC (2006) believes that geoengineering should focus on the problems associated with the recovery of global resources and the global effects of their use. In addition to those already mentioned, the following are also questions raised by sustainability (NRC, 2006; Misra & Basu, 2011): i) application of alternative materials; ii) re-use and recycling of materials (Nelson, 2013); iii) development of "environment-friendly" ground improvement techniques ; iv) efficient use of underground space; v) re-use of foundations; vi) energy geotechnology.

Energy geotechnology is a sub-area of geotechnics recently proposed in order to aggregate all issues that have to do with energy, thus constituting an essential component of a strategy to energy sustainable development. The topics included are (Santamarina & Cho, 2011; Fragaszy *et al.*, 2011):

a) Energy production: 1) exploration and exploitation of fossil fuels (oil, gas and coal); 2) geotechnical issues associated with the use of nuclear energy; 3) developing structures for production of renewable energy (mainly wind); 4) geothermal energy (drilling, fracturing, heat transfer, energy piles, optimization, etc.); Nelson (2013) suggests the integration of geothermal heat pumps in the foundations and lining of tunnels and other underground structures; 5) in this context, offshore geotechnical engineering becomes relevant (Randolph 2005; Randolph *et al.*, 2011; Jardine, 2014);
b) Geological storage: 1) CO_2 sequestration; 2) energy storage (compressed air contained in underground tanks to meet peak demands, etc.); 3) waste, including radioactive waste;
c) Geo-environmental remediation (bio-chemo-geological phenomena and methods);
d) Efficiency and conservation: 1) energy efficient building technologies; methods to reduce energy involved in engineering projects development (*life cycle assessment*); 2) bio-mimetic (tree roots, processes used by plants and animals, etc.).

The technical issues involved in this field require analysis at very different scales, considera-tion of large spatial and temporal dimensions and consideration of coupled hydro-bio-chemo-thermo-mechanical processes (Santamarina & Cho, 2011; Santamarina, 2012 and 2014).

Shackelford (2005) lists some geotechnical problems associated with environmental issues: i) long-term behavior of waste containment systems (landfills); ii) application of alternative materials in impermeable barriers; iii) development of innovative materials and barriers; iv) new waste profiles; v) biological processes (landfills with improved conditions for waste decomposition, bio-remediation, etc.); vi) modeling and forecasting capacity.

The list of what Brandl (2011) regards as key challenges for civil and geotechnical engineering is vast and includes many of the issues already mentioned above: i) transport and traffic infrastructures (construction and maintenance); ii) water management; iii) resource management; iv) waste management (solid and liquid); v) prevention and risk mitigation; vi) management of watercourses; vii) energy production; viii) irrigation systems; ix) urban and industrial ecology; x) land regeneration; xi) remediation of derelict and contaminated land; xii) renaturation of mining areas; xiii) environmentally sound underground construction technologies; xiv) marine engineering (port, coastal, etc.).

The contributions to the design of appropriate solutions that engineers and, in particular, geotechnical engineers have to make, should take into account new technologies and new approaches to solve problems better, quicker and in a cheaper way. . Nevertheless, as well pointed out by Long (2006), despite the new contexts and conditions, we should not forget that traditional problems solved in the past still need to be solved and that many of the techniques and technologies used then retain their validity. This should be properly addressed in engineer's education programs.

It is also engineer's responsibility to inform / educate society about the limitations of new technologies, contributing to the proper management of expectations and to well support decisions about the way infrastructures can be built (ASCE, 2007).

Acknowledgments

The author greatly appreciates the invitation of the Portuguese Geotechnical Society to present the 31th Manuel Rocha Lecture. He is indebted to the colleagues António Topa Gomes, Nuno Guerra and Pedro Alves Costa who have read the manuscript from which the lecture and this text have been extracted.The very kind introduction of the lecturer done by Professor Manuel de Matos Fernandes is justified by the intense cooperation, during the last thirty years, in all aspects of the academic activities and by the

friendship that has been established between them. Great recognition is due to Professor Laura Caldeira for her final vote of thanks.

References

ASCE - American Society of Civil Engineers (2007). The vision for Civil Engineering in 2025 (based on the Summit on the Future of Civil Engineering, June 21-22, 2006). Task Committee to Plan a Summit on the The Future of the Civil Engineering Profession.

Brandl, H. (2011). Importance of geotechnics in today's and future civil engineering - Public image, risks and responsibilities and future aspects of civil/geotechnical engineering. Stranice, Broj 3, p. 120-136.

Breedeveld, J. (2012). Future position of Geotechnical Engineering. (http://www.kiviniria.nl/eygec/papers/keynote_breedeveld.pdf).

Brundtland, G. H. (1987). Our Common Future. Oxford University Press, Oxford UK.

Cardoso, A.S. (2013). Questões de segurança. Revista Geotecnia, 127:5-43.

Chowdhury, R., & Flentje, P. (2007). Perspectives for the future of Geotechnical Engineering. Proc. of the International Conference on Civil Engineering for the New Millennium: Opportunities and Challenges, Bengal Engineering College, Shibpur, India, Plenary Papers & Abstracts Volume, pp. 59-75.

CIOB - The Chartered Institute of Building (2013). Corruption in the UK Construction Industry, September 2013.

Clark, G. (2007). A Farewell to Arms - A Brief Economic History of the World. Princeton University Press, 432 p.

Clough, G.W. (2006). The Past and Future of Computing in Geotechnical Engineering: The Inside-Out View. Geo Institute's 2006 Geo Congress, Atlanta, Georgia.

Day, P. (2009). What is failure. Chapter 2 of Forensic Geotechnical Engineering. V.V.S. Rao (ed) TC40 - Forensic Geotechnical Engineering. International Society for Soil Mechanics and Geotechnical Engineering, October 2009.

Delatte, N. (2006). Learning from failures. Civil Engineering Practice Fall/Winter 2006, Boston Society of Civil Engineers Section/ASCE, Boston, pp. 21-38.

El País Semanal (2014). El tesoro transparente. Por Isabel Valdés Aragonés y Artur Galocha, n° 1955, 15 de Marzo de 2014 (in Spanish).

Flyvbjerg, B. (2006). From Nobel prize to project management: getting risks right. Project Management Journal, 37(3):5-15.

Flyvbjerg, B. (2014). What you should know about megaprojects and why: An overview. Project Management Journal, 45(2):6-19.

Flyvbjerg, B.; Holm, M.K.S. & Buhl, S.L. (2005). How (in)accurate are demand forecasts in public works projects? The case of transportation. Journal of the American Planning Association, 71(2):131-146.

Fragaszy, R.J.; Santamarina, J.C.; Amekudzi, A.; Assimaki, D.; Bachus, R.; Burns, S.E.; Cha, M.; Cho, G.C.; Cortes, D.D.; Dai, S.; Espinoza, D.N.; Garrow, L.; Huang, H.; Jang, J.; Jung, J.W.; Kim, S.; Kurtis, K.; Lee, C.; Pasten, C.; Phadnis, H.; Rix, G.; Shin, H.S.; Torres, M.C. & Tsouris, C. (2011). Sustainable development and energy geotechnology - Potential roles for geotechnical engineering, KSCE Journal of Civil Engineering, 15:4, p. 611-621.

Francisca, F.M. (2011). About the future of geotechnical engineering: a view from South America. Proc. of the 2011 Pan-Am CGS Geotechnical Conference, Paper 1211.

Haack, A. (2009). Construction of the North-South-Metro Line in Cologne and the Accident on March 3rd, 2009. International Symposium on Social Management Systems, Kochi, pp. 120-124.

Hajra, M.G. (2012). Sustainability in geotechnical engineering: current and future trends in research, education & professional practice. Louisiana Civil Engineering Conference and Show 2012, Pontchartrain Center Kenner.

Hansford, P. (2011). Delivering value. Proceedings of the Institution of Civil Engineers. Civil Engineering, 164(1):3-8.

Hardoon, D., & Heinrich, F. (2011). Bribe Payers Index 2011. Report of the Transparency International - The Global Coalition Against Corruption. Transparency International, Berlin, 30 p.

IITG / IGS - Indian Institute of Technology Guwahati / Indian Geotechnical Society (2012). Proc. of the National Wokshop on Emerging Trends in Geotechnical Engineering, organized by Department of Civil Engineering Indian Institute of Technology Guwahati and Indian Geotechnical Society Guwahati Chapter (NE), Guwahati, 135 p.

IPCC - Intergovernmental Panel on Climate Changes (2000). Emissions Scenario. Spacial Report. Summary for Policymakers.

IPCC - Intergovernmental Panel on Climate Changes (2007). Climate Change 2007, Fourth Assessment Report of the Intergovernmental Panel on Climate Change: 1) Synthesis Report, Contribution of Working Groups I, II and III, Core Writing Team. R.K. Pachauri, & A. Reisinger (eds) IPCC, Geneva, 104 p; 2) The Physical Science Basis, Contribution of Working Group I. S. Solomon, D. Qin, M. Manning, Z. Chen, M. Marquis, K.B. Averyt, M. Tignor & H.L. Miller (eds) Cambridge University Press, Cambridge, 996 p.; 3) Impacts, Adaptation and Vulnerability, Contribution of Working Group II. M.L. Parry, O.F. Canziani, J.P. Palutikof, P.J. van der Linden, & C.E. Hanson (eds) Cambridge University Press, Cambridge, 976 p.; 4) Mitigation, Contribution of Working Group III, B. Metz, O.R. Davidson, P.R. Bosch, R. Dave & L.A.

Meyer (eds) Cambridge University Press, Cambridge, 851 pp.

Jardine, R. (2014). Advanced laboratory testing in research and practice: the 2nd Bishop Lecture. ICE - Geotechnical Research, 1(1):2-31.

Kenny, C. (2009). Why Do People Die in Earthquakes? The Costs, Benefits and Institutions of Disaster Risk Reduction in Developing Countries. Policy Research Working Paper 4823, WPS4823, Sustainable Development Network, Finance Economics & Urban Department, The World Bank.

Lambe, T.W. (1973). Predictions in soil engineering. Géotechnique, 23(2):149-202.

Long, J.C.S. (2006). Preface of Geological and Geotechnical Engineering in the New Millennium. Opportunities for Research and Technological Innovation. Board on Earth Sciences and Resources, Division on Earth and Life Studies, National Research Council, The National Academies Press.

Maddison, A. (2014). Maddison Historical GDP Data. (http://www.worldeconomics.com/Data/MadisonHistoricalGDP/).

Marr, W.A. (2006). Geotechnical engineering and judgment in the information age. Proc. of the GeoCongress 2006, Geotechnical Engineering in the Information Technology Age.DeGroot, D.J.; DeJong, J.T.; Frost, J.D. & Baise, L.G. (eds) The Geo-Institute of the American Society of Civil Engineers, pp. 1-17.

Matos Fernandes, M.A. (2010). Deep urban excavations in Portugal: Practice, design, research and perspectives. Soils and Rocks, 33(3):115-142.

McKinsey Global Institute (2013). Infrastructure productivity: How to save $1 trillion a year. McKinsey and Company, 90 p.

Misra, A. & Basu, D. (2011). Sustainability in geotechnical engineering , Internal Geotechnical Report 2011-2, Department of Civil and Environmental Engineering, University of Connecticut, 49 p.

Nelson, P.P. (2013). Uncertainty and Resilience as Key Frameworks for the Future of Urban Geotechnical Engineering. A Presentation to the Geotechnical Group of the ASCE Metropolitan Section, October 31, 2013.

Nicholson, D.; Tse, C. & Penny, C. (1999). The Observational Method in Ground Engineering - Principles and Applications. Report 185, CIRIA, London, 80 p.

NRC - National Research Council (2006). Geological and Geotechnical Engineering in the New Millennium. Opportunities for Research and Technological Innovation. Committee on Geological and Geotechnical Engineering, Board on Earth Sciences and Resources, Division on Earth and Life Studies, National Research Council, National Academies Press.

NRC - National Research Council (2010). Advancing the Science of Climate Change - America's Climate Choices. Panel on Advancing the Science of Climate Change, Board on Atmospheric Sciences and Climate, Division on Earth and Life Studies, National Academies Press.

OECD - Organization for Economic Co-operation and Development (2007). Infrastructure to 2030. Main findings and policy recommendations. OECD Futures Project on “Global Infrastructure Needs: Prospects and Implications for Public and Private Actors”.

OECD - Organization for Economic Co-operation and Development (2011). Strategic Transport Infrastructure Needs to 2030. Main Findings. International Futures Programme. OECD Futures Project on Transcontinental Infrastructure Needs to 2030/50.

Randolph, M.F. (2005). Challenges of offshore geotechnical engineering. 16th ICSMGE, Osaka, Japan, pp. 123-176.

Randolph, M.F., Gaudin, C., Gourvenec, S.M., White, D.J., Boylan, N. & Cassidy, M.J. (2011). Recent advances in offshore geotechnics for deep water oil and gas developments. Ocean Engineering, 38(7):818-834.

Reddy, K.R. (2011). Emerging trends in remediation of contaminated sites in the United States. Proc. of the US-Japan Workshop on Geoenvironmental Engineering, Kyoto, Japan, pp. 35-45.

Rijnaarts, H.H.M. (2010). The Olympic Game of Eco-Innovation and Technology. Inaugural Lecture upon taking up the post of Professor of Environment and Water Technology at Wageningen University on 8 April 2010. (http://edepot.wur.nl/170203).

Rzevski, G. & Skobelev, P. (2014). Managing Complexity, WIT Press, Southhampton, 216 p.

Santamarina, J.C. (2012). Energy Geotechnology: The Role of Geotechnical Engineers in the Energy Challenge. The British Geotechnical Association BGA Touring Lecture 2012. (http://www.ice.org.uk/ICE_Web_Portal/media/northernireland/Santamarina---Energy-Geotechnology---BGA-2012---DISTRIBUTION.pdf).

Santamarina, J.C. (2014). Energy geotechnology: Enabling new insights into soil behavior. Karl Terzaghi Lecture, Geo-Congress 2014, Geo-Characterization and Modeling for Sustainability. A.J. Puppala, P. Bandini & T.C. Sheahan (eds) Geotechnical Special Publication N° 235, Geo-Institute, ASCE, 181 p.

Santamarina J.C. & Cho, G.C. (2011). Energy geotechnology. KSCE Journal of Civil Engineering, 15(4):607-610.

Schlosser, F.; Plumelle, C.; Frank, R.; Puech, A.; Gonin, H.; Rocher-Lacoste, F.; Simon, B. & Bernardini, C. (2013). Innovations Françaises en Géotechnique: les Projets Nationaux de Recherche. Proc. of the 18th ICSMGE, Paris, p. 163-182.

Schweiger, H.F. (2002). Benchmarking in geotechnics 1 - Part I: Results of benchmarking. Computational Geotechnics Group, CGG_IR006_2002.

Shackelford, C.D. (2005). Environmental issues in geotechnical engineering. Proc. of the 16th ICSMGE, Osaka, Millpress, v. 1, p. 95-122.

Simpson, B. & Tatsuoka, F. (2008). Geotechnics: The next 60 years. Géotechnique 58:5, p. 357-368.

Sterling, R.L. (2012). Understanding the Sustainability and Resiliency Implications of Underground Space Use. Geotechnical Aspects of Tunneling for Infrastructure Development, Proc. of the 32nd Annual Seminar Geotechnical Division, The Hong Kong Institution of Engineers, pp. 1-6.

Terzaghi, K. (1936). Relation between soil mechanics and foundation engineering. Proc. 1st ICSMFE, Harvard University, v. 3, pp. 13-18.

Terzariol, R.E. (2009). 40 años de Estudio de los Suelos Loessicos en Córdoba, Argentina. Desafíos y Avances de la Geotecnia Joven en Sudamérica. Francisca, F.M. (ed), Alejandría, Córdoba, 337 p. (in Spanish).

UN - United Nations (2010). World Urbanization Prospects. The 2009 Revision. Highlights. Department of Economic and Social Affairs, Population Division, ESA/P/WP/215.

UN - United Nations (2013). UN Task Team on the Post-2012 UN Development Agenda, Working Group on Financing for Sustainable Development - Background Papers: Chapter 1. Financing for sustainable development: Review of global investment requirement estimates; Chapter 2. The variety of national, regional and international public sources for development finance; Chapter 3. Challenges in raising private sector resources for financing sustainable development; Chapter 4. Public support to private investment for sustainable development: challenges and opportunities, with emphasis on the environmental pillar; Executive Summary. UN System Task Team on the Post-2015 UN Development Agenda Working Group on "Financing for sustainable development". (http://www.un.org/esa/ffd/sdf/firstsession/index.htm).

UNFCCC - United Nations Framework Convention on Climate Change (1992). United Nations Conference on Environment and Development (UNCED), Rio de Janeiro. (http://unfccc.int/resource/docs/convkp/conveng.pdf.).

UNFCCC - UN Framework Convention on Climate Change (2009). National Adaptation Programmes of Action. (http://unfccc.int/national_reports/napa/items/2719.php.).

USGCRP - US Global Change Research Program (2009). Global Climate Change Impacts in the United States. New York, Cambridge University Press, 196 p.

Viana da Fonseca, A. & Santos, J. (2008). Internacional Prediction Event - Behaviour of Bored, CFA and Driven Piles in Residual Soil - ISC'2 Experimental Site, 670 pp.

WB / UN - The World Bank / The United Nations (2010). Natural hazards, unnatural disasters: the economics of effective prevention. The International Bank for Reconstruction and Development / The World Bank.

WDR - World Development Report (2009). Reshaping Economic Geography. The International Bank for Reconstruction and Development / The World Bank.

WEF - World Economic Forum (2011). A vision for managing natural disaster risk - Proposals for public/private stakeholder solutions.

WEF - World Economic Forum (2012). Global Agenda Council on Infrastructure 2012-2014. (http://www.weforum.org/reports/global-agenda-council-infrastructure-2012-2014).

Articles

Climatic Effects on In-Situ Soil State Profiles Considering a Coupled Soil-Atmosphere Interaction Model

K.V. Bicalho, G.P.D. Vivacqua, Y.-J. Cui, C. Romanel

Abstract. The influence of soil-atmosphere interactions on an unsaturated soil in water-limited environment is investigated using a coupled heat-water flow model with a balance of net solar energy at earth's surface. The paper also presents the governing equations for soil-atmosphere interaction analysis which, although important, are still rare in geotechnical applications. Numerical results were obtained by approximating the governing partial differential equations through a 1D finite difference scheme representing the soil as a two-layer system. Soil state profiles (temperature, moisture and suction) were predicted using daily meteorological data collected in France, from 2004 to 2005. Parametric analyses estimated the effects on soil state profiles caused by changes in initial conditions (soil temperature), hydraulic properties (saturated hydraulic conductivity), model geometry (upper layer thickness), ratio of reflected to incident solar radiation (soil albedo) and characteristics of meteorological data (sampling frequency). For the investigated site, the zone of seasonal fluctuations (ZSF) where the moisture and corresponding suction profiles is influenced by climatic conditions is about 1.5 m. The results also show that calculated average month meteorological values as daily inputs modify significantly the ZSF (about 100%). Predicted soil temperature profiles were in good agreement with measured values.

Keywords: soil suction, soil temperature, soil moisture, unsaturated flow, evaporation, soil-atmosphere interaction.

1. Introduction

The exchange of water between the soil surface and the atmosphere is governed by two processes: infiltration and evaporation. The process of infiltration is reasonably well understood and depends primarily on the hydraulic conductivity of the soil while the evaporation flux from a soil surface is more difficult to quantify since it is a function of both the soil properties and climatic conditions.

To estimate evapotranspiration rates engineers have traditionally used the term potential evaporation, which may be understood as the maximum rate of evaporation from a pure water surface under given climatic conditions. The actual rate of evapotranspiration from a soil surface depends on the availability of water (Penman, 1948; Priestley & Taylor, 1972) and the maximum potential rate occurs only when the soil surface is fully saturated and water is present on the ground surface. The actual rate of evapotranspiration begins to decline once the soil surface becomes unsaturated and its determination is much more difficult because the analysis becomes indeterminate since there are more unknowns than unique equations.

The solution to this problem requires an approach where the flow of water from an evaporating unsaturated soil surface is represented as a coupled soil-atmosphere interaction (SAI) model taking into account the variation of suction along the soil profile due to spatial and temporal changes in soil moisture and temperature caused by micro-climate conditions above the soil-atmosphere boundary. Studies with consideration of SAI effects in civil engineering problems are rare, especially in the geotechnical area, even though this subject has already been the topic of two Rankine Lectures (Blight, 1997; Gens, 2010).

Evapotranspiration from soil occurs in the form of combined liquid and vapour transport. Under field conditions it is not possible to separate evaporation from transpiration totally and the term actual evapotranspiration is used herein to describe the amount of total water loss. When the available soil moisture is depleted, the actual evapotranspiration will be limited by the monthly precipitation (lower limit) and the potential evapotranspiration (upper limit); in months when the potential evapotranspiration is less than the rainfall, the actual evapotranspiration is closer to the potential value (Fetter, 1994). Many regions have become drier and more drought-affected during recent decades (Dai *et al.*, 2004) and in water-limited regions (high soil suction) the ratio of the actual to the potential evaporation may be lower than 1 (Skidmore *et al.*, 1969; Blight, 1997).

Soil moisture varies depending on the actual evapotranspiration from soil surface which can be estimated by either field measurement based on water balance, energy balance or numerical analysis using meteorological data (Federer *et al.*, 1996). This former approach is desirable due to difficulties in direct measurements of soil suction us-

Kátia V. Bicalho, Ph.D., Associate Professor, Departamento de Engenharia Civil, Universidade Federal do Espírito Santo, Vitória, ES, Brazil. e-mail: kvbicalho@gmail.com.
Gabriel P.D. Vivacqua, M.Sc., Rechercher, Departamento de Engenharia Civil, Universidade Federal do Espírito Santo, Vitória, ES, Brazil. e-mail: gpd.vivacqua@hotmail.com.
Yu-Jun Cui, Ph.D., Full Professor, ENPC (CERMES, UR Navier), Université Paris Est, Marne-la-Vallee, France. e-mail: yujun.cui@enpc.fr.
Celso Romanel, Ph.D., Associate Professor, Departamento de Engenharia Civil, Pontifícia Universidade Católica do Rio de Janeiro, Rio de Janeiro, RJ, Brazil. e-mail: celso.romanel@gmail.com.
Submitted on February 1, 2012; Final Acceptance on May 12, 2015; Discussion open until December 31, 2015.

ing suction probes, such as tensiometer cavitation and psychrometer temperature effects.

In this paper changes of the in-situ soil state (moisture, suction and soil temperature) profiles due to climatic effects were predicted considering soil-atmosphere interactions in a water-limited environment. The principle of mass and energy conservation was applied to describe 1D water (liquid and vapour) and 1D heat flows in an unsaturated soil and a surface energy balance was imposed to the evaporation fluxes from a wet bare soil surface (Choudhury *et al.*, 1986; Xu & Qiu, 1997). A 1D explicit finite difference program (SAIAFDM model) developed at Ecole Nationale des Ponts et Chaussees (Gao, 2006) was used for numerical calculations.

The numerical calculations were carried out using the daily meteorological data collected by a French weather station, from 2004 to 2005. The soil parameters were determined from laboratory measurements by Fleureau *et al.* (2007) on soil specimens obtained at three different depths at studied region. Parametric analyses were carried out to estimate the influence of several parameters (soil albedo, saturated hydraulic conductivity, initial soil temperature profile, meteorological data) on the profile distributions, including fluctuations in the superficial zone of seasonal soil profile. Computed results were also compared with in situ soil temperature measurements in 2005 in Mormoiron, France.

2. Transient Water Flow in Unsaturated Soils

Consider a porous material, consisting of a solid matrix with a continuous pore space filled with fluid, a mixture of liquid water and vapour. For the particular case of one-dimensional water flow (along the vertical z direction), the flow of liquid water q_{wz} occurs in response to a hydraulic gradient that can be described by Darcy's law,

$$q_{wz} = -k_w(h_m)\frac{\partial(h_w)}{\partial z} \tag{1}$$

where the hydraulic conductivity k_w is a function of the matric suction head h_m. In the absence of an osmotic pressure head, the total hydraulic head h_w is defined as the sum of the matric head and the elevation head z,

$$h_w = h_m + z \tag{2}$$

The flow of water vapor q_{vz} in an unsaturated soil can be described by Fick's law (Fredlund & Dakshanamurthy, 1982) as:

$$q_{vz} = -\frac{1}{\rho_w} D_v \frac{\partial P_v}{\partial z} \tag{3}$$

where ρ_w is the water density at 20 °C (1000 kg/m^3), D_v the diffusion coefficient of the water vapour through the soil and P_v is the partial pressure due to water vapour.

Hence, the total flow of water q_z may be expressed as the sum of the liquid water flow q_{wz} and water vapour flow q_{vz} as:

$$q_z = -k_w \frac{\partial(h_w)}{\partial z} - \frac{1}{\rho_w} D_v \frac{\partial P_v}{\partial z} \tag{4}$$

Fredlund & Morgenstern (1976) suggested that the change in volumetric water content $\Delta V_w/V$ may be estimated through the following constitutive relationship:

$$\theta_w = \frac{\Delta V_w}{V} = [m_1^w d(\sigma_z - u_a) + m_2^w d(u_a - u_w)] \tag{5}$$

where σ_z is the vertical stress component, u_a the pressure in the air phase, u_w the pressure in the water phase, m_1^w the slope of the $d(\sigma_z - u_a)$ *vs.* volumetric water content plot for $d(u_a - u_w) = 0$ and m_2^w the slope of the $d(u_a - u_w)$ *vs.* volumetric water content plot for $d(\sigma_z - u_a) = 0$.

Assuming that there is no change in both vertical stress and air pressure,

$$d(\sigma_z - u_a) = 0 \tag{6a}$$

$$d(u_a - u_w) = -d(u_w) = -\rho_w g d(h_m) = -\rho_w g d(h_w - z) \tag{6b}$$

then the change in volumetric water content with respect to time may be written as:

$$\frac{\partial \theta_w}{\partial t} = -\rho_w g m_2^w \frac{\partial(h_w - z)}{\partial t} = -\rho_w g m_2^w \frac{\partial(h_w)}{\partial t} \tag{7}$$

However, the divergence of the total water flux in the one-dimensional space $\partial q_z / \partial z$ is equivalent to the change of volumetric water content with respect to time $\partial\theta_w / \partial t$. Hence from Eqs. 4 and 7 the following mass balance equation can be written,

$$\frac{\partial(\theta_w)}{\partial t} + \frac{\partial(q_z)}{\partial z} = 0 \tag{8}$$

$$\frac{\partial(h_w)}{\partial t} = C_w \frac{\partial}{\partial z}\left(k_w \frac{\partial h_w}{\partial z}\right) + C_v \frac{\partial}{\partial z}\left(D_v \frac{\partial P_v}{\partial z}\right) \tag{9}$$

where the modulus of volume change of the liquid water phase is given as:

$$C_w = \frac{1}{\rho_w g m_2^w} \tag{9a}$$

and the modulus of volume change of the vapour phase is defined as:

$$C_v = \frac{1}{(\rho_w)^2 g m_2^w}\left(\frac{P + P_v}{P}\right) \tag{9b}$$

The term $(P + P_v)/P$ is a correction factor introduced by Wilson (1990) to account for combined flow due to vapour diffusion and bulk air advection, where P is the total atmospheric pressure and P_v the partial pressure in the soil due to water vapour. According to Wilson *et al.* (1994) this correction factor in most applications is approximately equal to unity and has little effect on the solution.

The two unknown variables of Eq. 9, namely the hydraulic head h_w and partial vapour pressure P_v, are not independent and may be related through a thermodynamic relationship (Edlefsen & Anderson, 1943),

$$P_v = P_{vs} h_T \tag{10}$$

where P_{vs} is the saturation vapour pressure at the soil temperature T and h_T is the relative humidity defined as:

$$h_T = \exp(h_m W_v / RT) \tag{11}$$

considering h_m the matric suction head, W_v the molecular mass of water (0.018 kg/mol), R the universal gas constant (8.314 J/(mol.K)) and T the absolute temperature (K).

Observe that calculation of the partial vapour pressure in Eq. 10 depends on the temperature, whose variation along the soil profile must be accounted for. Wilson (1990), Philip & De Vries (1957) and De Vries (1987) suggested the following equation for heat flow,

$$C_h \frac{\partial(T)}{\partial t} = \frac{\partial}{\partial z}\left(\lambda \frac{\partial T}{\partial z}\right) - L_v \frac{P+P_v}{P} \frac{\partial}{\partial z}\left(D_v \frac{\partial P_v}{\partial z}\right) \tag{12}$$

where C_h is the volumetric specific heat (J/(m^3 °C)), λ the apparent thermal conductivity of soil (W/(m^3 °C)) and L_v the latent heat of vaporization for water (J/kg) determined as:

$$L_v = 4.186 \times 10^3 (607 - 0.7T) \tag{13}$$

where T is given in °C.

The volumetric specific heat of the soil can be defined as follows (De Vries, 1963):

$$C_h = C_s \theta_s + C_w \theta_w + C_a \theta_a \tag{14}$$

where θ_w, θ_a and θ_s are the volumetric fractions of water, gas and solid materials, respectively, and C_w (4.15 x 10^6), C_a and C_s (2.24 x 10^6) their volumetric specific heat (J/m^3. °C). The value of C_a can be negligible (Gao, 2006).

The apparent thermal conductivity of soil λ can be also determined from De Vries (1963),

$$\lambda = \frac{f_s \theta_s \lambda_s + f_w \theta_w \lambda_w + f_a \theta_a \lambda_a}{f_s \theta_s + f_w \theta_w + f_a \theta_a} \tag{15}$$

where the thermal conductivity of water is λ_w = 0.57 W/m °C, the thermal conductivity of solids varies between $2.0 \leq \lambda_s \leq 7.7$ W/m °C depending on the quartz volumetric fraction (Johansen, 1975) and the thermal conductivity of the gaseous phase is composed by the conductivity of the dry air (λ_{dryair} = 0.025 W/m °C) plus the conductivity of the water vapour ($\lambda_{vapourr} = 0.608\theta_w$ W/m °C). The weighting coefficients $f_w = 1$ and f_a, f_s are estimated as (Gao, 2006):

$$f_s = \left[1 + \left(\frac{\lambda_s}{\lambda_w} - 1\right)\right]^{-1} \tag{16}$$

$$f_a = \frac{1}{3} \sum_{i=1}^{3} \left[1 + \left(\frac{\lambda_a}{\lambda_w} - 1\right) g_i\right]^{-1} \tag{17}$$

where the shape factors g_1, g_2 and g_3 may be estimated from the following correlations:

$$g_1 = g_2 = \frac{0.105 - 0.015}{0.121} \theta_w + 0.015 \quad \text{for } \theta_w \leq 0.121 \tag{17a}$$

$$g_1 = g_2 = \frac{0.333 - 0.105}{0.236 - 0.121} (\theta_w - 0.121) + 0.105 \quad \text{for } \theta_w > 0.121 \tag{17b}$$

$$g_1 + g_2 + g_3 = 1 \tag{17c}$$

The governing equation for heat flow (Eq. 12) does not include the heat transfer by convection but several publications (Andersland & Anderson, 1978; Jame & Norum, 1980) point out that this contribution is negligible for most engineering applications.

Hence, the transfer of liquid, water vapour and heat in a porous medium is described by Eqs. 9, 10 and 12, respectively. The vapour pressure variable P_v is the common variable to all three equations.

3. Soil-Atmosphere Boundary Condition

The most direct method of estimating evapotranspiration is considering a surface energy balance. The net incoming solar radiation at any location is converted into heat energy, which warms the air above the surface and the soil itself, and into latent heat of evapotranspiration from the soil surface.

Consider R_n as the net radiation at the earth's surface, discounting the part of the incoming solar radiation R_{si} reflected by the surface albedo. Conservation of energy requires that the energy consumed by evaporation must equal that supplied, while conservation of mass requires that the rate at which water evaporates from the surface be equal to the rate at which it is dispersed into the atmosphere. According to Blight (2002, 2013) the surface energy balance, i.e. the way R_n is converted at the ground surface, may be expressed as:

$$R_n = L_e + H + G \tag{18}$$

where L_e is the latent energy transfer (positive for evaporation and negative for condensation), H is the sensible heat flux, the energy consumed in heating the air above the surface ("sensible" because this is the heat sensed or felt by the observer) and G is the soil heat flux (positive when energy is transferred to the near-surface soil and negative when energy is transferred to the atmosphere).

Equation 18 refers only to solar energy. If energy from an additional source is present (e.g. wind energy) a term describing this kind of energy should be included. For instance,

$$R_n + W_e = L_e + H + G \tag{19}$$

where W_e is the effective energy flux arising from the wind. In the case of landfills the heat supplied from the decomposing waste may also influence evaporation and should be added as a new term in the surface energy balance (Bendz & Bengtsson, 1996).

The net radiation flux R_n can be measured directly or estimated. Cui *et al.* (2010) calculated it from the incoming solar radiation R_{si} and the long-wave radiation emitted by soil surface and atmosphere, suggesting the following expression:

$$R_n = (1-a)R_{si} - \varepsilon_s \sigma T_s^4 + \varepsilon_a \sigma T_a^4 \tag{20}$$

where a is the soil albedo, ε_s the soil-surface emissivity, ε_a the air emissivity, σ the Stefan-Boltzmann constant (5.67 x 10^{-8} Wm^{-2} K^{-4}); T_s (K) and T_a (K) are the absolute soil surface and air temperatures, respectively. The soil albedo represents the ratio of reflected to incident solar radiation and it is a function of several surface parameters including soil color, water content, roughness and vegetation cover, usually being lower for wet and rough conditions. The albedo value ranges from 0 to 1. The value of 0 refers to a blackbody, a theoretical media that absorbs 100% of the incident radiation. Albedo ranging from 0.1 to 0.2 corresponds to dark-colored, rough soil surfaces, while the values around 0.4-0.5 indicate smooth, light-colored soil surfaces. The value of 1 refers to an ideal reflector surface in which all the energy falling on the surface is reflected. Solar altitude angle and soil moisture are the two main factors that influence the albedo value (Li & Hu, 2009).

In Eq. 18 the sensible heat flux H between soil and air is given by (Choudhury *et al.*, 1986; Kalma,1989):

$$H = \frac{\rho_a C_{pa} (T_s - T_a)}{r_a} \tag{21}$$

where ρ_a is air density, C_{pa} the specific heat of air at constant pressure equal to 1.013 x 10^3 J/(kg.K), T_s the absolute soil surface temperature (K) and T_a the absolute air temperature (K) at height z_a. The aerodynamic resistance r_a is the diffusion resistance to sensible heat transfer between the surface and height z_a; a reliable estimation of this parameter is important for soil-atmosphere interaction problems. Kalma (1989) observed good agreement between estimated and measured aerodynamic resistance over bare soil surface using Eq. 22 developed by Choudhury *et al.* (1986), based on an exact solution for stable conditions ($T_s < T_a$ and Richardson number $R_i > 0$) and on an approximate solution under unstable condition ($T_s > T_a$ and Richardson number $R_i < 0$) with a claimed 95% accuracy.

$$r_a = r_{a0} \frac{1}{(1 + R_i (T_s - T_a))^n} \tag{22}$$

where the exponent $\eta = 0.75$ is used for unstable conditions and $\eta = 2$ for stable conditions. The aerodynamic resistance r_{a0} is obtained from a logarithmic wind profile and may be calculated as:

$$r_{a0} = \frac{\left[\ln\left(\frac{z_a - d}{z_0}\right)\right]^2}{k^2 u_z} \tag{22a}$$

where u_z is the wind speed measured at height z_a, d the zero plane displacement equivalent to the vegetation height, z_0 the roughness length for momentum (wind) transfer and k the von Karman constant (0.41). When no vegetation is considered $d = 0$.

The Richardson number R_i in Eq. 22 is defined as:

$$R_i = \frac{g(T_a - T_s)(z_a - d)}{u_z^2 T_a} \tag{22b}$$

where g is the acceleration of gravity.

In Eq. 18 the latent heat flux L_e may be determined as (Xu & Qiu, 1997),

$$L_e = \frac{L_v M_w (P_{vz0} - P_{vza})}{RTr_a} \tag{23}$$

where L_v is the latent heat of vaporization, M_w the molecular mass of water equal to 0.018 kg/mol, P_{vz0} the partial vapour pressure at the soil surface, P_{vza} the partial vapour pressure in the air at height z_a, R the universal gas constant (8.314 J/(mol.K)) and T (K) the average absolute temperature $T = (T_a+T_s)/2$;

Finally, the soil heat flux G may be calculated from the energy balance equation (Eq. 18), considering the net radiation flux R_n (Eq. 20) and the energy fluxes calculated with Eqs. 21 and 23.

4. Constitutive Equations

Since in Eq. 1 the unsaturated hydraulic conductivity k_w depends on the matric suction head h_m, the following equation proposed by Juarez-Badillo (1975) was used in this research:

$$k_w = \frac{k_s}{1 + \left(\frac{k_s}{k_{w1}} - 1\right)\left(\frac{s}{s_1}\right)^{\xi}} \tag{24}$$

where k_s is the saturated hydraulic conductivity at suction $s = 0$, k_{w1} the unsaturated hydraulic conductivity at suction s_1 and ξ a parameter that controls the shape of the suction vs. unsaturated hydraulic conductivity curve s-k_w .

The equation for heat flow (Eq. 12) is a function of the volumetric specific heat C_h and the apparent thermal conductivity of soil λ which, by their turn, depend on the volumetric water content θ_w (Eqs. 14 and 15). Hence, it is necessary to establish a relationship between suction s *vs.* volumetric water content θ_w that, according to Juarez-Badillo (1975), may be written as:

$$\theta_w = \frac{\theta_{ws} - \theta_r}{1 + \left(\frac{\theta_{ws} - \theta_r}{\theta_{w1} - \theta_r} - 1\right)\left(\frac{s}{s_1}\right)^{\varsigma}} + \theta_r \quad (25)$$

where θ_{ws} is the saturated volumetric water content, θ_r the residual volumetric water content, θ_{w1} the volumetric water content corresponding to suction s_1 and ς a parameter that controls the shape of the suction vs. volumetric water content curve s - θ_w called the soil-water characteristic curve or the soil water retention curve (SWRC). A number of equations have been suggested for the SWRC and almost all the equations suggested can be derived from a single generic form as presented by Leong & Rahardjo (1997). The equations represent the general sigmoidal shape of the SWRC as observed on the Eq. 25 used in this research.

5. Computer Program Based on a Finite Difference Method

In order to estimate the rate of evaporation at the ground surface, the computer program SAIAFDM was used to simultaneously solve the coupled equations of mass balance (liquid water and vapour), heat flow and energy balance between the soil and atmosphere. It was originally developed by Gao (2006) based on a 1D finite difference scheme and subsequently modified by Cui *et al.* (2005, 2010). The model assumes no variation in volume of voids as a function of the variation in suction or, in other words, the soil is considered as a rigid material.

The governing Eqs. 9 and 12 and can be rewritten as:

$$\frac{\partial(h_w)}{\partial t} = C_w\left(\frac{\partial k_w}{\partial z}\frac{\partial h_w}{\partial z} + k_w\frac{\partial^2 h_w}{\partial z^2}\right) + C_v\left(\frac{\partial D_v}{\partial z}\frac{\partial P_v}{\partial z} + D_v\frac{\partial^2 P_v}{\partial z^2}\right) \quad (9)$$

$$C_h\frac{\partial(T)}{\partial t} = \frac{\partial\lambda}{\partial z}\frac{\partial T}{\partial z} + \lambda\frac{\partial^2 T}{\partial z^2} - L_v\frac{P+P_v}{P}\left(\frac{\partial D_v}{\partial z}\frac{\partial P_v}{\partial z} + D_v\frac{\partial^2 P_v}{\partial z^2}\right) \quad (12)$$

Considering the forward difference scheme for first-order derivatives and a central difference scheme for second-order derivatives, the differential governing equations (Eqs. 9 and 12) can be approximated as:

$$\frac{h_w^{i,j+1} - h_w^{i,j}}{\Delta t} = C_w\left(\frac{k_w^{i+1,j} - k_w^{i,j}}{\Delta z} \times \frac{h_w^{i+1,j} - h_w^{i,j}}{\Delta z} + k_w\frac{h_w^{i+1,j} - 2h_w^{i,j} + h_w^{i-1,j}}{\Delta z^2}\right) + C_v\left(\frac{D_v^{i+1,j} - D_v^{i,j}}{\Delta z} \times \frac{P_v^{i+1,j} - P_v^{i,j}}{\Delta z} + D_v\frac{P_v^{i+1,j} - 2P_v^{i,j} + P_v^{i-1,j}}{\Delta z^2}\right) \quad (26)$$

$$C_h\frac{T^{i,j+1} - T^{i,j}}{\Delta t} = \frac{\lambda^{i+1,j} - \lambda^{i,j}}{\Delta z} \times \frac{T^{i+1,j} - T^{i,j}}{\Delta z} + \lambda\frac{T^{i+1,j} - 2T^{i,j} + T^{i-1,j}}{\Delta z^2} - L_v\frac{P+P_v}{P}\left(\frac{D_v^{i+1,j} - D_v^{i,j}}{\Delta z} \times \frac{P_v^{i+1,j} - P_v^{i,j}}{\Delta z} + D_v\frac{P_v^{i+1,j} - 2P_v^{i,j} + P_v^{i-1,j}}{\Delta z^2}\right) \quad (27)$$

where the index i is associated to the vertical coordinate z and the index j to time.

The advantage of using the approximate Eqs. 26 and 27 is that $h_w^{i,j+1}$ and $T^{i,j+1}$ can be calculated explicitly but, as its main disadvantage, the numerical solution may become unstable when time and space increments are not well chosen. In this research the time increment was selected as $\Delta t = 5$ s and the space increment was delimited by 5 mm $\leq \Delta z \leq$ 50 mm for stable and accurate results. Figure 1 gives a general view of the program framework.

6. Data Presentation

6.1. Site description and input data

The investigated site is located in Mormoiron, department of Vaucluse, in the southeast of France. It has a Mediterranean climate. The site was instrumented by the French research office on geology and mines (BRGM) and the measured soil temperature is used to evaluate the numerical simulations. Cui *et al.* (2010) mention that previous geotechnical investigations to a depth of 10 m showed that the soil layer is relatively uniform, composed of clay of green colour.

The daily meteorological data were available from a French weather station, called Carpentras station, that is located at about 10 km from Mormoiron site. The data include precipitation, relative humidity of the air, air temperature, solar radiation and wind speed measured at 2 m from the soil surface from January 1964 to December 2000 (a total of 42 years). The Mormoiron site was selected for studying because a water deficit is observed in most of time throughout the monitored years where the recharge of the

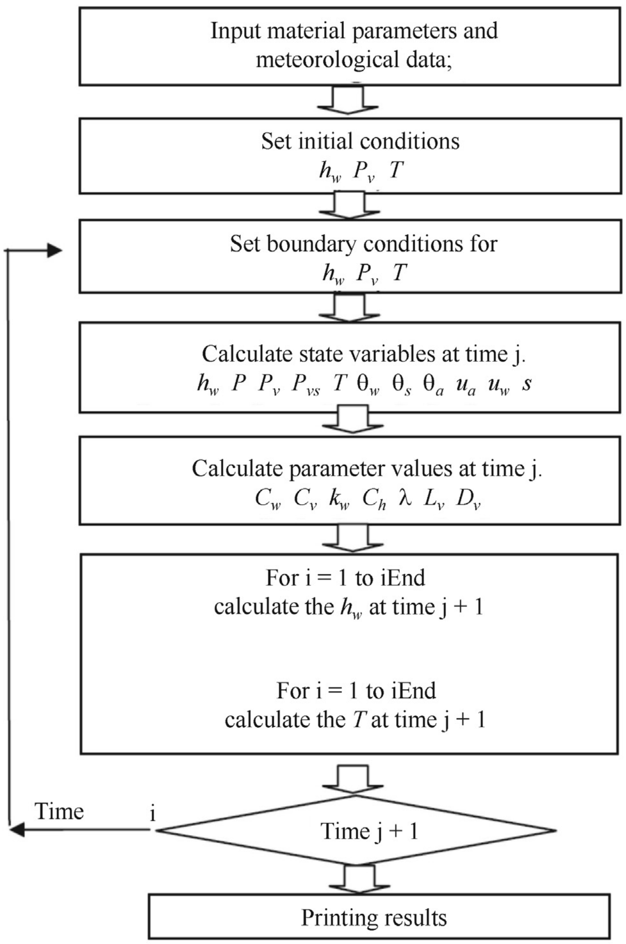

Figure 1 - The program framework used in the present study.

water table did not take place and the zone of unsaturated soil assumed a much greater significance. Examination of the recorded meteorological data showed that a seasonal warming trend is observed in the recorded data after the year 2000 (mean maximum and minimum annually air temperatures equal to 21.2 °C and 8.3 °C respectively).

The climatic data at the Mormoiron site in France was recorded daily from December 1, 2003 to December 31, 2005, consisting of solar radiation (0.05 to 0.35 kWm^2), rainfall (0 to 60 mm), air temperature (0 to 25 °C), air relative humidity (40 to 90%) and wind speed (2 to 14 m/s), as shown by plots in Fig. 2 where the average monthly values were also indicated by the horizontal bars. It should be observed that the air temperature changes correlate well with solar radiation while the air relative humidity does not necessary follow the rainfall pattern. The air relative humidity depends not only on precipitation, but also on air temperature and wind speed (Cui & Zornberg, 2008). A water deficit is observed in most of time throughout the two years, except for brief periods in December 2003, October 2004, April 2005 and October 2005. Thus, the years of 2004 and 2005 correspond to drier conditions where the recharge of

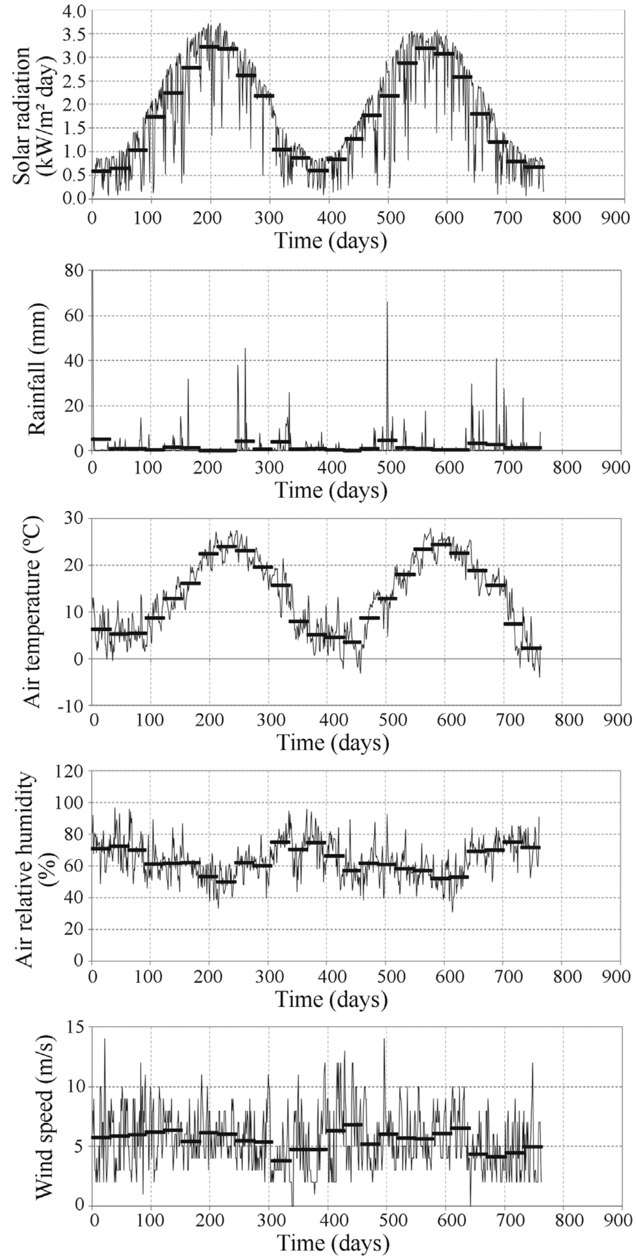

Figure 2 - Variation of the daily measured solar radiation, rainfall, air temperature, air relative humidity and wind speed for the 2 year time period.

the water table did not take place and the zone of unsaturated soil assumed a much greater significance.

The actual land soil cover was represented by a two-layer system of homogeneous soils with an upper layer thickness Z_1 = 3.45 m, maximum depth Z_{max} = 5.25 m (Fig. 3) and soil albedo 0.15. For both layers the parameters related to the flow of liquid and water vapour are listed in Tables 1 to 4. The initial temperature profile and the initial volumetric water content profile, corresponding to the beginning of the analysis on December 1, 2013 (late Fall), are shown in Figs. 4 and 5, which have been estimated from field measurement taken at the Mormoiron site.

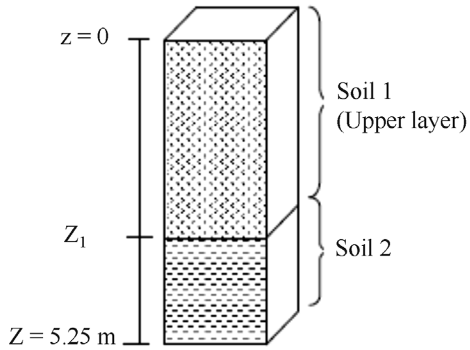

Figure 3 - The two-layer system of homogeneous soils.

7. Parametric Analyses

In the following sensitivity analyses, only one parameter is changed independently at each time while the remaining parameters are kept constant ignoring the effects of parameters interactions and output or responses interdependences. This simple approach facilitates a preliminary identification of potentially important parameters for further researches that will take into account the interdependence between model parameters or the interactions between model outputs or responses. Moreover the interdependence of the investigated parameters is not observed for the considered magnitude variations.

7.1. Influence of the initial temperature profile

In order to investigate the effects of the initial temperature profile on the volumetric water content and soil temperature distribution, a 5 °C increase was prescribed to all points along the profile of Fig. 4, based on an expected daytime temperature oscillation. However, as can be observed in Fig. 6 the volumetric water content profile remained insensitive to the initial temperature variation (T and T + 5 °C). Values for the volumetric water content (and suction) were practically constant for depths $z > 1.5$ m. The dependence of the soil temperature on the soil water retention curve was not considered.

Figures 7 and 8 present the predicted soil temperature profiles from January to July 2004 considering the two hypotheses for the initial temperature profile. It can be observed that close to the surface (0-10 cm) the soil temperatures are slightly affected (1 °C to 2 °C only) by the initial profiles, adjusting to the air temperature quickly. At deeper depths ($z > 1.5$ m) the temperatures tend to become stable over the year and preserving the original difference of 5 °C imposed on the initial temperature profiles. For instance, at $z = 3$ m the soil temperature approaches the initial

Table 1 - Soil-water retention function input variables.

Parameter	$Z \le Z_1$	$Z_1 < Z \le Z_{max}$	Unity
Saturated volumetric water content θ_{ws}	0.490	0.400	m^3/m^3
Suction s_1	700	200	kPa
Residual volumetric water content θ_r	0.080	0.080	m^3/m^3
Volumetric water content θ_{w1} at suction s_1	0.240	0.240	m^3/m^3
Shape parameter ς	1.1	1.1	-

Table 2 - Unsaturated hydraulic conductivity function input variables.

Parameter	$Z \le Z_1$	$Z_1 < Z \le Z_{max}$	Unity
Saturated hydraulic conductivity k_s	1.2×10^{-11}	2.4×10^{-10}	m/s
Suction s_1	40	40	kPa
Unsaturated hydraulic conductivity k_{w1} at suction s_1	1.2×10^{-14}	1.2×10^{-14}	m/s
Shape parameter ξ	1.25	1.25	-

Table 3 - Volumetric specific heat input variables.

Parameter	$Z \le Z_1$	$Z_1 < Z \le Z_{max}$	Unity
Solid specific heat C_s	2.24×10^6	2.24×10^6	J/m^3 °C
Water specific heat C_w	4.15×10^6	4.15×10^6	J/m^3 °C
Air specific heat C_a	0	0	J/m^3 °C

Table 4 - Thermal conductivity input variables.

Parameter	$Z \leq Z_l$	$Z_l < Z \leq Z_{max}$	unity
Thermal conductivity λ_s of solids	3.92	3.92	W/m °C
Thermal conductivity λ_w of water	0.57	0.57	W/m °C
Thermal conductivity λ_a of air	$0.025+0.608\theta_w$	$0.025+0.608\theta_w$	W/m °C

temperatures 12 °C < T < 13 °C and 16 °C < $T + 5$ < 17 °C. These results suggest that for the soil near the surface it is not relevant to know the values of initial temperature with high accuracy, but for deeper layers this is an important question.

7.2. Influence of the saturated hydraulic conductivity

The saturated hydraulic conductivities of the two-layer system were modified in order to verify their effects on the volumetric water content and suction profiles. The values listed in Table 2 were increased a hundredfold passing from $k_S^A = 1.2\times10^{-11}$ m/s for $Z \leq 3.5$ m and $k_S^A = 2.4\times10^{-10}$ m/s for $Z > 3.5$ m (herein identified as case A) to $k_S^B = 1.2\times10^{-9}$ m/s for $Z \leq 3.5$ m and $k_S^B = 2.4\times10^{-8}$ m/s for $Z > 3.5$ m (denominated as case B). McCartney & Parks (2009) reported that empirical predictions can lead to an error in hydraulic conductivity of 1 to 4

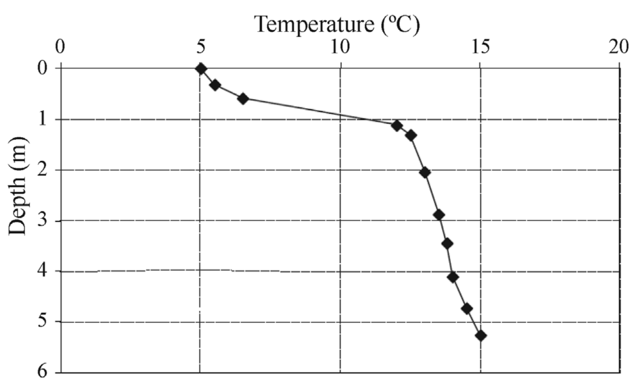

Figure 4 - Initial temperature profile on December 1, 2003.

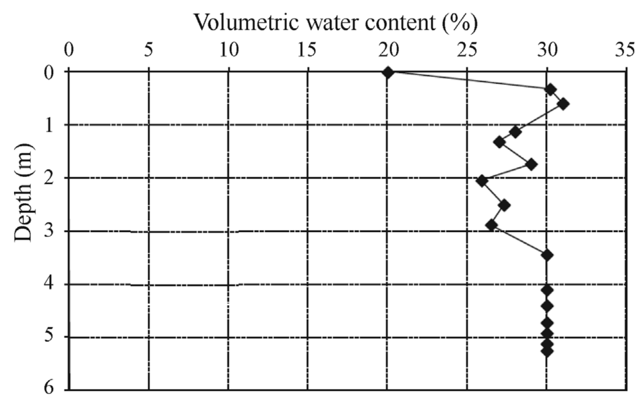

Figure 5 - Initial volumetric water content profile on December 1, 2003.

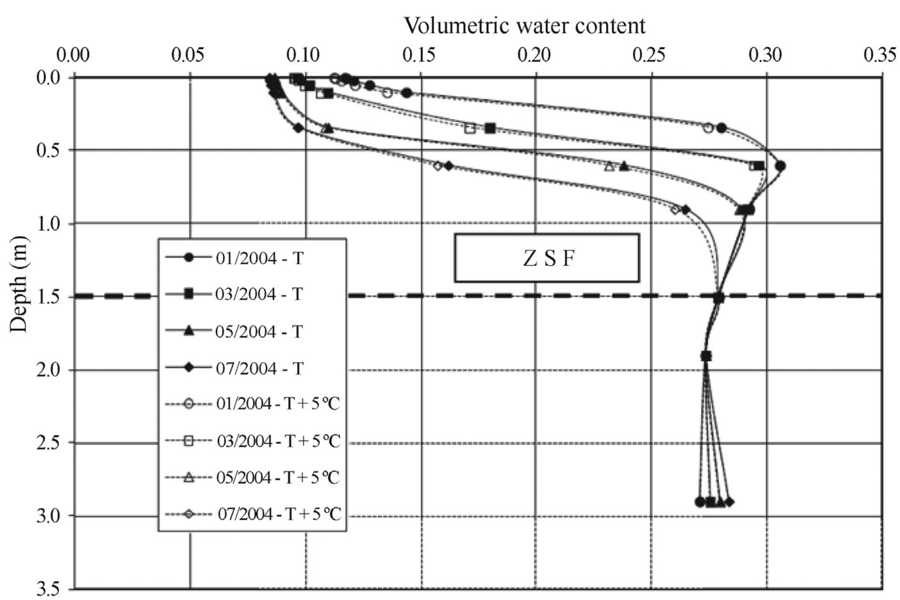

Figure 6 - Volumetric water content profile from January to July/2004 considering the initial temperature profiles T (solid line) and $T + 5$ °C (dotted line).

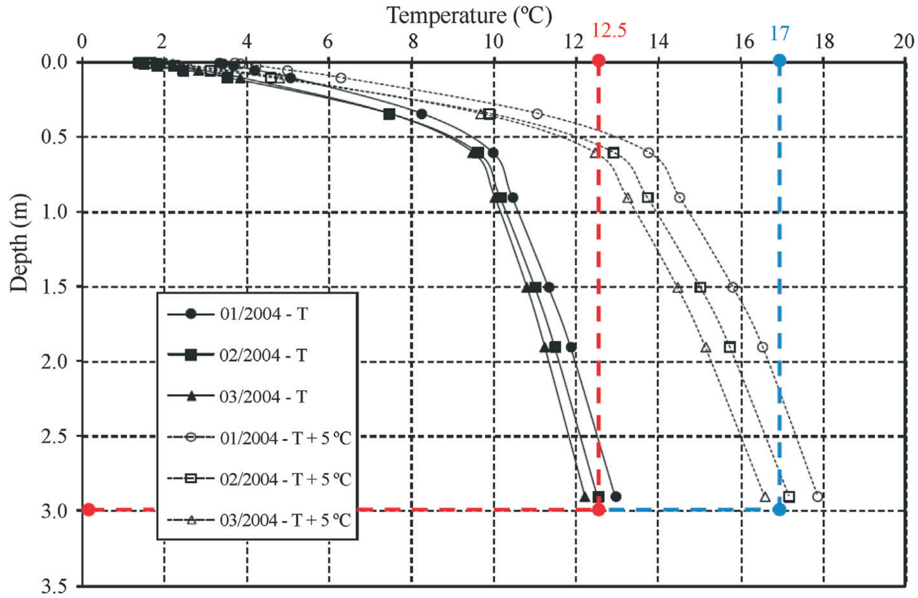

Figure 7 - Soil temperature profile from January to March/2004 considering the initial temperature profiles T (solid line) and $T + 5$ °C (dotted line).

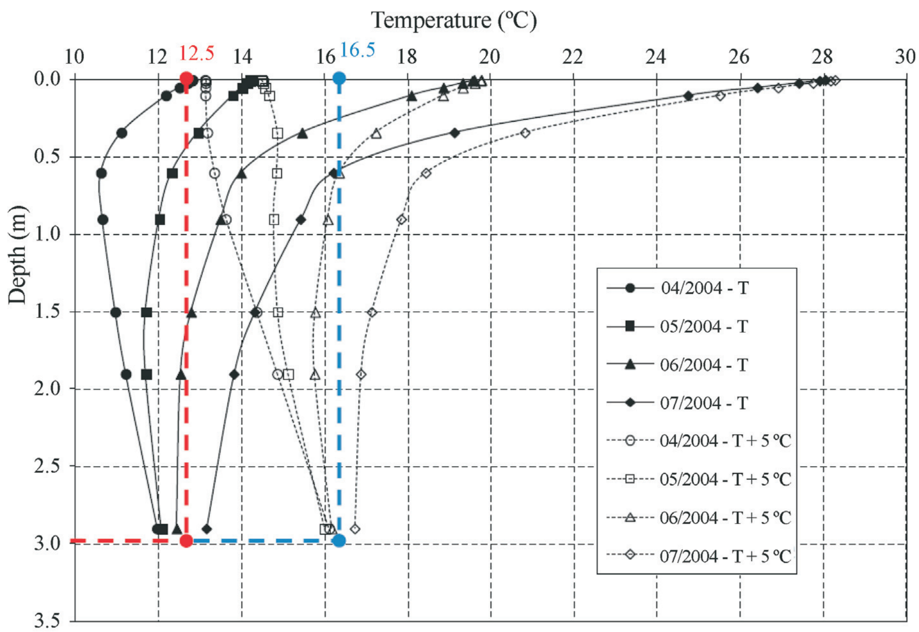

Figure 8 - Soil temperature profile from April to July/2004 considering the initial temperature profiles T (solid line) and $T + 5$ °C (dotted line).

orders of magnitude, with the greatest discrepancies at low moisture contents.

The results are presented in Fig. 9 in terms of suction profiles. Their insensitivity to changes of the saturated hydraulic conductivities is quite apparent since curves from both cases are coincident. The same behavior was observed when comparing the volumetric water content and soil temperature profiles. Although the computed evaporative fluxes are very sensitive to the permeability of the soil (Wilson, 1990), the years of 2004 and 2005 correspond to drier conditions (high suction values), and it seems that changes of this magnitude on the saturated hydraulic conductivities have not significant effect on the suction-unsaturated hydraulic conductivity relationship.

7.3. Influence of the upper layer thickness

This parametric analysis investigated the influence of the upper layer thickness (Fig. 3), considering in case A a

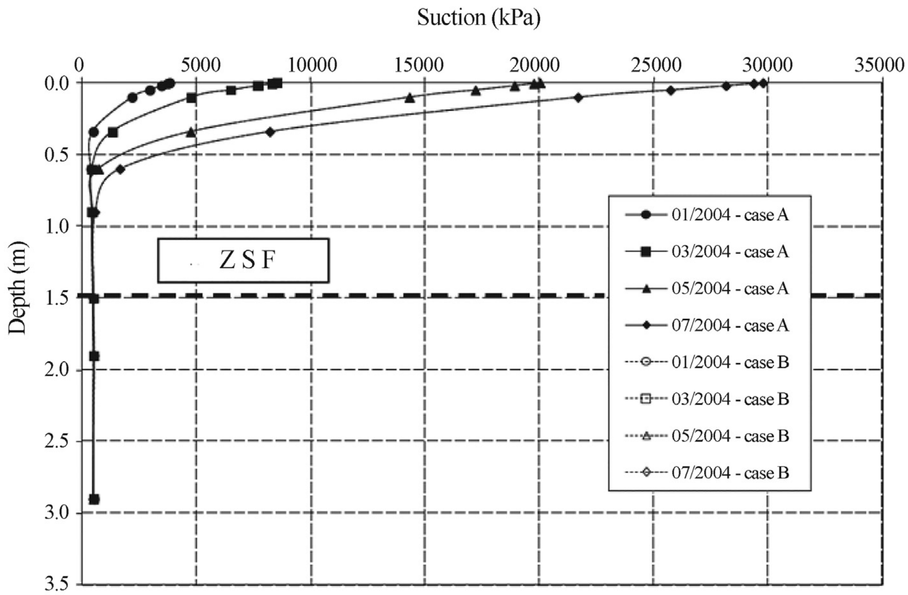

Figure 9 - Influence of the saturated hydraulic conductivity on suction profiles from January to July/2004.

thickness $Z_1 = 3.45$ m and in case C a new value $Z_1 = 0.5$ m. With respect to previous analyses, this means that the soil between depths 0.5 m < z < 3.45 m had its hydraulic properties changed (soil-water retention function and unsaturated hydraulic conductivity function) according to the values listed in Tables 1 and 2. The soil was divided into two layers with variable thickness to account for the observed changes of the hydraulic properties in the laboratory measurements.

Predicted results for both cases can be seen in Fig. 10. It can be concluded that the differences observed between distributions are small except in the superficial region between 0.40 m < z < 0.90 m (marked in blue) that was more affected by the climatic conditions. The results also indicated that the expected hysteresis in the functions due to the variation of the wetting and drying processes in the field has not significant effect on the predicted soil profiles in Mormoiron, France.

7.4. Influence of the soil albedo

The changes in soil profiles during a given period depend on the ratio of reflected to incident solar radiation (i.e., the soil albedo value). The sensitivity of predicted temperature changes to variations of soil albedo is studied next,

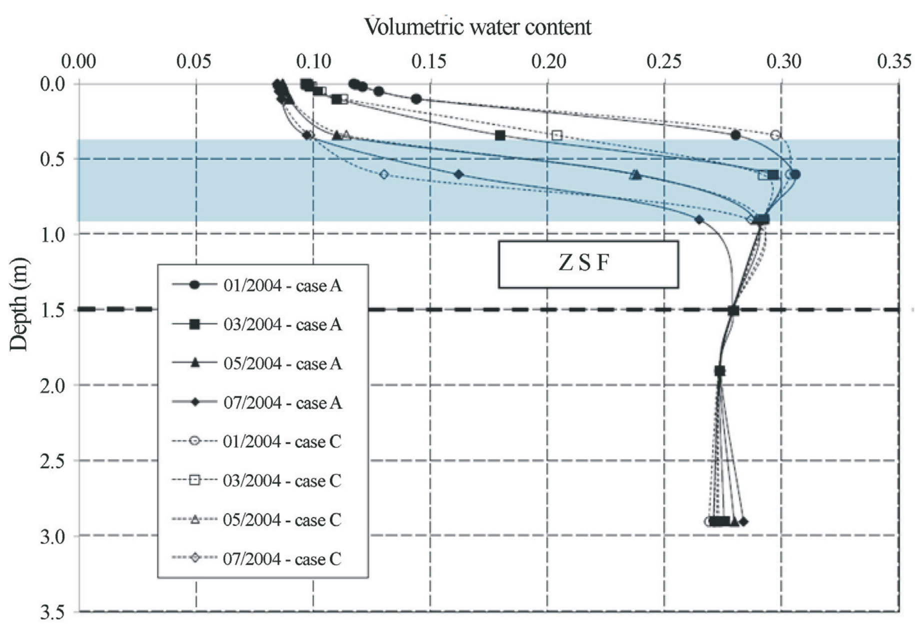

Figure 10 - Influence of upper layer thickness on volumetric water content profiles from January to July/2004.

considering soil albedo values of 0.15 (case A) and 0.05 (case D).

Figures 11 shows that the soil temperatures profiles are not significantly affected by the soil albedo values, mainly during the cold season (from January to March, 2005). During the warmer months (from April to August 2005) it may observed for case D small temperature increases (approximately 1 °C) probably due to the higher incident solar radiation that made the soil albedo parameter more relevant for analysis of temperature distributions.

7.5. Influence of the climatic data frequency

Figures 6, 9 and 10 show that the soil layer where moisture and corresponding suction profiles influenced by climatic conditions is about 1.5 m deep but Figs. 7 and 8 indicate that the layer where the soil temperature profile is affected by climate is thicker (3 m). Therefore the zone in which the interchange of water between the atmosphere and the soil occurs is different from the one in which the interchange of heat between the atmosphere and the soil takes place.

Whereas the impact of thermal variation on the soil behavior is recognized and especially significant for fined grained soils and higher temperature values (Lingnau *et al.*, 1996, Tang & Cui, 2005), Franchomme *et al.* (2013) demonstrated that temperatures variations from 1 °C to 30 °C do not significantly affect the measured soil shear stress parameters for a kaolinite-sand mixture.

For the particular site of Mormoiron, France, the zone of seasonal fluctuations (ZSF) in which water contents change seasonally due to climate changes can be established as 1.5m deep considering the variations through the cold and warm seasons (January to July 2004). For London clay with vegetation the ZSF is about 1.0 m according to Smethurst *et al.* (2006).

In order to investigate the influence of the climatic data frequency (input data), some analyses were repeated considering data sampled at a monthly frequency (case E) instead of the daily frequency adopted in Case A. The monthly frequency refers to the average values shown in Fig. 2 as horizontal bars.

Predicted results for suction profiles are shown in Fig. 12. It can be observed that for the monthly frequency case the ZSF doubled in size, reaching the depth of 3 m, and the suctions profiles for cases A and E are quite discrepant. Similar results were predicted for soil temperature and volumetric water content profiles.

These unexpected results have probably come from the simple and rather naïve choice of converting a daily time series into a monthly time series just by averaging the recorded values within a 30-days period. Specific conversion functions must be applied for an adequate collapse of a daily data sequence to a monthly time series, but it is quite common in the practice of engineering to represent a monthly interval by its average value. When dealing with time series, this issue may be quite important especially when the recorded climatic data (rainfall, wind speed, air temperature, air relative humidity) are not all sampled at the same frequency.

7.6. Comparison between predicted and measured soil temperatures

Figure 13 presents the comparison between predicted and measured changes in soil temperature at three different depths (0.5 m, 1.5 m, and 2.5 m) from January to August 2005 in Mormoiron, France. The results suggest that near the soil surface the predictions were less satisfactory, due probably to vegetation or other effects, such as soil cracking, not considered in the computational model. A sensitivity analysis of soil temperature and water content profiles to

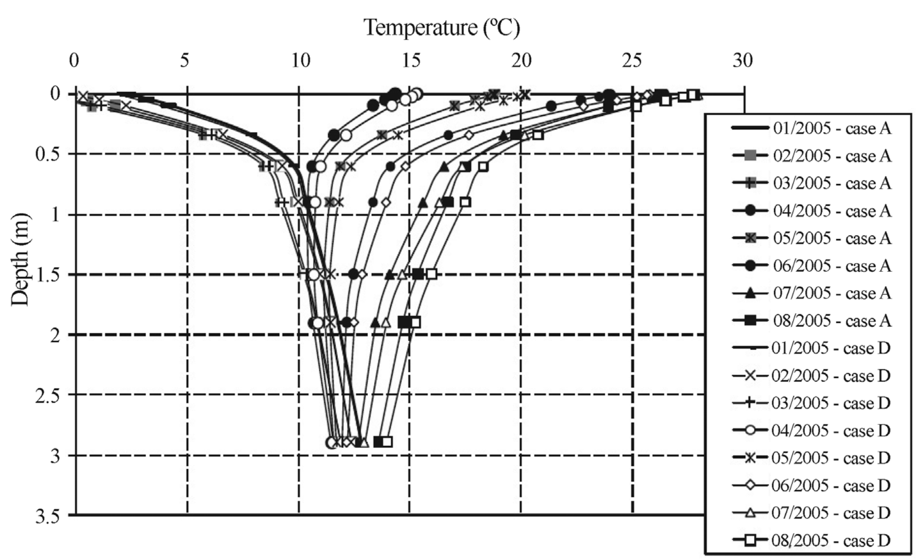

Figure 11 - Influence of soil albedo values on soil temperature profiles from January to August/2005.

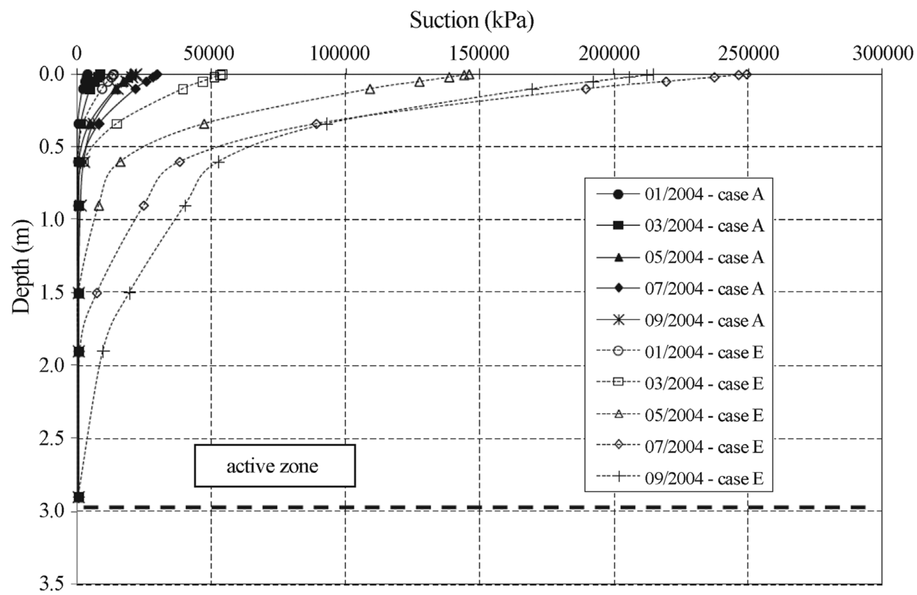

Figure 12 - Influence of climatic data frequency on suction profiles from January to September/2004.

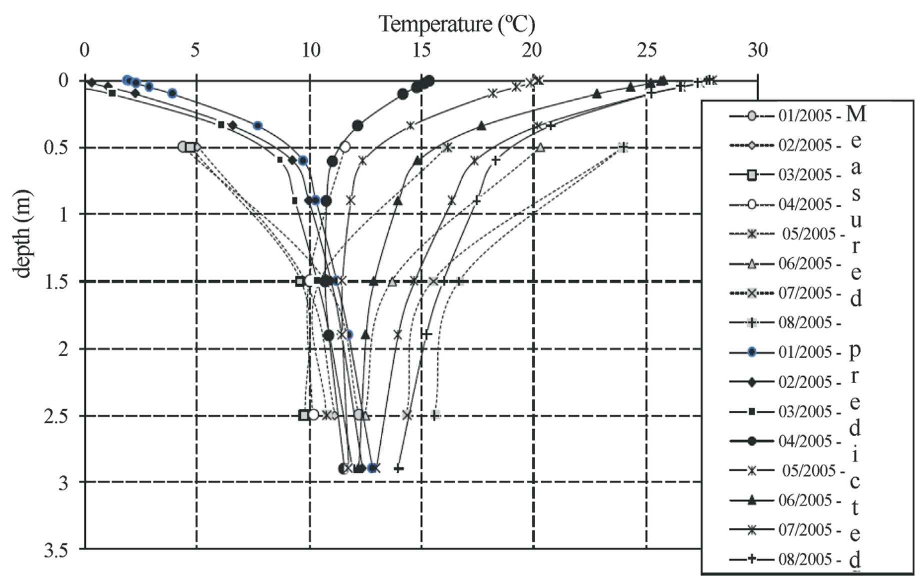

Figure 13 - Comparison between predicted and measured soil temperatures from January to August/2005.

variations of other unknown parameters (such as soil water content that depend on the soil temperature) should also be investigated. Cui *et al.* (2005) suggested considering the superficial zone as an independent layer with its own and particular values of soil parameters.

8. Conclusion

This paper investigated the influence of soil-atmosphere interactions on an unsaturated soil in water-limited environment using a coupled heat-water flow model with a balance of net solar energy at earth's surface. The numerical calculations were carried out using the daily meteorological data collected by a French weather station, from 2004 to 2005. The soil parameters were determined from laboratory measurements on soil specimens obtained at three different depths at the studied region.

Numerical results were obtained by approximating the governing partial differential equations through a 1-D finite difference scheme representing the soil as a two-layer system. Parametric analyses estimated the effects on soil state profiles caused by changes in initial conditions, hydraulic properties, model geometry, ratio of reflected to incident solar radiation and characteristics of meteorological data.

The results suggest that for the soil near the surface it is not relevant to know the values of initial temperature with high accuracy, but for deeper layers this is an important question. For the investigated site, the zone of seasonal fluctuations (ZSF) where the moisture and corresponding suction profiles are influenced by climatic conditions is about 1.5 m although the layer where the soil temperature is affected by climatic conditions is twice this value (3 m). The results also show that calculated average month meteorological values as daily inputs significantly modify the ZSF (about 100%) but the response depends on the statistical procedure to convert a daily time series into a representative monthly sequence.

The comparison of predicted and measured changes in soil state temperature profiles suggest that in near the surface layers the simulations are less satisfactory probably due to vegetation effects or other mechanical phenomena such as soil cracking. Further investigations, including experimental studies and numerical simulations, are needed to better understand climate effects on soil state profiles and their influence on geotechnical engineering problems.

Acknowledgments

The first authors are grateful for sponsorship by the Brazilian government agencies CNPq and CAPES. This work has been performed within the French ANR-RGCU project: ARGIC. The meteorological data was provided by Météo France and the soil data by BRGM. The helpful comments and corrections by the reviewers are also appreciated.

References

Andersland, O. & Anderson, D. (1978). Geotechnical Engineering for Cold Regions. McGraw-Hill. Inc., New York.

Bendz, D. & Bengtsson, L. (1996). Evaporation from an active, uncovered landfill: Journal Hydrology, 182:1, p. 143-155.

Blight, G.E. (1997). Interactions between the atmosphere and the earth. Géotechnique, 47:4, p. 715-767.

Blight, G.E. (2002). Measuring evaporation from soil surfaces for environmental and geotechnical purposes. Water SA, 28:4, p. 381-394.

Blight, G. E. (2013). Unsaturated Soil Mechanics in Geotechnical Practice. CRC Press, Taylor & Francis Group, London, 597 p.

Choudhury, B.J.; Reginato, R.J. & Idso, S.B. (1986). An analysis of infrared temperature observations over wheat and calculation of latent heat flux. Agric. For. Meteorol., 37:2, p. 75-88.

Cui, Y.J.; Lu, Y.F.; Delage, P. & Riffard, M. (2005). Field simulation of in site water content and temperature changes due to ground-atmospheric interactions. Géotechnique, 55:7, p. 557-567.

Cui, Y.J. & Zornberg, J. (2008). Water balance and evapotranspiration monitoring in geotechnical and geoenvironmental engineering. Geotechnical and Geological Engineering, 26:6, p. 783-798.

Cui, Y.J.; Gao, Y. B. & Ferber, V. (2010). Simulating the water content and temperature changes in an experimental embankment using meteorological data. Engineering Geology, 141:3, p. 456-471.

Dai, A.; Lamb, P.J.; Trenberth, K.R.; Hulme, M.; Jones, P. D. & Xie, P. (2004). The recent Sahel drought is real. Int. J. Climatol., 24:11, p.1323-1331.

De Vries, D.A. (1963). Thermal properties of soils. In: W.R. Van Wijk (ed) Physics of Plant Environment. North-Holland, Amsterdam, pp 210-235.

De Vries, D.A. (1987). The theory of heat and moisture transfer in porous media revisited. International Journal of Heat and Mass Transfer, 30:7, p.1343-1350.

Edlefsen, N.E. & Anderson, A.B.C. (1943). Thermodynamics of soil moisture. Hilgardia 15:2, p. 31-298.

Federer, C.A.; Vörösmarty, C. & Fekete, B. (1996). Inter comparison of methods for calculating potential evaporation in regional and global water balance models. Water Resources Research, 32:1, p. 2315-2321.

Fetter, C.W. (1994). Applied Hydrogeology. 3rd ed. Macmillan College Publishing, Inc., New York, 616 p.

Fleureau, J.M.; Guellati, Z.; Nguyen, D. & Souli H. (2007). Synthèse des essais réalisés au LMSSMat sur le matériau du site de Mormoiron, Annexe de rapport BRGM, Projet ANR-05-PRGCU-005, Rapport d'activité n° 3, École Centrale de Paris.

Franchomme, G.; Rosin-Paumier, S. & Masrouri, F. (2013). Evaluating the impact of thermal variations on the penetration test parameters, Proc. The 1st Pan American Conference on Unsaturated Soils, Cartagena de Indias, Colombia , pp. 371-376.

Fredlund, D.G. & Morgenstern, N.R. (1976). Constitutive relations for volume change in unsaturated soils, Canadian Geotechnical Journal, 13:3, p.261-276.

Fredlund, D. G. & Dakshanamurthy, V. (1982). Transient flow process in unsaturated soils under flux boundary conditions. Proc. the 4th International Conference on Numerical Methods in Geomechanics, Edmonton, Canada, pp. 307-317.

Gao, Y.B. (2006). From Meterological Data to the Predication of Embankment Stability. Technical report, CERMES-ENPC, Paris, 180 p.

Gens, A. (2010). Soil-environment interactions in geotechnical engineering. Géotechnique, 60:1, p. 3-74.

Jame, Y.W. & Norum, D.I. (1980). Heat and mass transfer in a freezing unsaturated porous medium. Water Resources Research, 16:4, p. 811-819.

Johansen, O. (1975). Thermal Conductivity of Soils. Ph.D. Thesis, Trondheim, Norway, CRREL Draft Translation 637, ADA 044002.

Juárez-Badillo E. (1975). Constitutive relationships for soils, Proc. Symposium on Recent Developments in the Analysis of Soil Behavior and their Application to Geotechnical Structures, University of New South Wales, Australia, pp. 231-257.

Kalma, J.G. (1989). A Comparison of Expressions for the Aerodynamic Resistance to Sensible Heat Transfer. CSIRO Division of Water Resources, Technical Memorandum, 89/6, 18 p.

Leong, E.C. & Rahardjo, H. (1997). Permeability functions for unsaturated soils. J. Geotech. Geoenviron. Eng., 123:12, p. 1118-1126.

Li, Y. & Hu, Z. (2009). A study on parameterization of surface albedo over grassland surface in the northern Tibetan Plateau, Adv. Atmos. Sci., 26:1, p. 161-168.

Lingnau, B.E.; Graham, J.; Yarechewski, D.; Tanaka, N. & Gray, M.N. (1996). Effects of temperature on strength and compressibility of sand-bentonite buffer, Engineering Geology, 41:1, p. 103-115.

McCartney, J. S. & Parks, J. (2009). Uncertainty in predicted hydraulic conductivity functions of unsaturated soils. Proc. 17th International Conference on Soil Mechanics and Geotechnical Engineering, Alexandria, Egypt. Taylor & Francis Group, London, pp. 1618-1621.

Penman, H.L. (1948). Natural evaporation from open water, bare soil and grass. Proceedings of the Royal Society of London, Series A, 193:1032, p. 120-145.

Philip, J.R. 7 de Vries, D.A. (1957). Moisture movement in porous materials under temperature gradients. Transactions American Geophysical Union, 38:2, p. 222-232.

Priestley, C.H.B. & Taylor, R.J. (1972). On the assessment of surface heat flux and evaporation using large-scale parameters. Monthly Weather Review, 100:2, p. 81-92.

Skidmore, E.L.; Jacobs, H.S. & Powers, W.L. (1969). Potential evapotranspiration as influenced by wind. Agron. J., 61:4, p. 543-546.

Smethurst, J.; Clarke, D. & Powrie, W. (2006). Seasonal changes in pore water pressure in a grass covered cut slope in London Clay. Géotechnique, 56:8, p. 523-537.

Tang, A.M. & Cui, Y.-J. (2005). Controlling suction by the vapour equilibrium technique at different temperatures and its application in determining the water retention properties of MX80 clay, Canadian Geotechnical Journal, 42:1, p. 287-296.

Wilson, G.W. (1990). Evaporation from Bare Soil Surfaces. Ph.D. Thesis, University of Saskatchewan, Saskatoon, Canada.

Wilson, G.W.; Fredlund, D.G. & Barbour S.L. (1994). Coupled soil-atmosphere modeling for soil evaporation. Canadian Geotechnical Journal, 31:2, p.151-161.

Xu, Q. & Qiu, C.-J. (1997). A variational method for computing surface heat fluxes from ARM surface energy and radiation balance system. J. of App. Meteorology, 36:1, p. 3-11.

Laboratory Evaluation of Electrokinetic Dewatering of Bauxite Tailings

L. De Leon Ferreira, R.C. Gomes

Abstract. The mining tailings disposal system is often associated to the construction of large retaining systems, either for the great volume of materials generated by industrial plants or for the impossibility or difficulty of grants for new disposal areas. Due to increasing demand, these impoundments have become much more significant, triggering considerable increase of risk associated to them. In this context, new techniques must be developed aiming to decrease the volume of tailings produced and the optimization of disposal systems for these materials, particularly in terms of systems including tailings dewatering techniques. An alternative solution consists in dewater and consolidate mine tailings under current intermittence, technique called electroosmosis. This paper presents the development of an electroosmotic cell to measure the electrokinetic flow and the consolidation process of fine tailings under specified boundary conditions. The tailings are generated by the process of treatment of bauxite from BPM (Bauxita Paragominas Mining/Brazil), which consist of fine-grained materials, with initial solid content of 31%. The results of this experimental study are analyzed and discussed based on the principles of electrokinetic theory and has shown that the proposed technique would significantly accelerate the consolidation process of fine tailings (an average solid content of 58% was reached, within a 12-hour period), besides providing adequate design parameters for field applications.

Keywords: tailings, consolidation, electro-osmosis, electrokinetic phenomena.

1. Introduction

Activities of mineral exploitation are divided basically in the processes of mining extraction, corresponding to the direct exploration of the mineral deposit (often surface mining methods in Brazil), and in beneficiation processes, characterized by the physical and/or chemical operations necessary to change the mineral assembly in form and/or composition, in order to make them suitable to the desired industrial applications. The final product resulted from all this industrial process accounts for only a small part of all material extracted from the deposit, therefore it is necessary the proper disposal of residues generated by all the activities related to mining. Overburden, the soil and rock material that overlies the mine area, removed to expose the ore deposit, are stored in piles. Tailings as water containing suspended solids and dissolved materials are commonly stored in retaining dams.

One of the main processes which results in great environmental impacts from mining activities is related to the large volume of residues generated, in the extraction as well as in the ore beneficiation processes. So, there is need of large areas to dispose these materials, fact which, just by itself, would imply great concern with this sector of the production process. In addition to this fact, there are socio-economic and environmental risks associated to the large retaining structures usually built to store tailings (Vick, 1990). On the other hand, tailings are relatively low-density materials with a high degree of saturation and such conditions can generate problems of liquefaction (Gomes *et al.*, 2002; Pirete & Gomes, 2013).

The disposal of mining tailings can be made on the surface of the ground in the form of piles or in disposal basins formed by retaining dams or dikes, or it is even possible to be made in underground cavities or in exhausted mines. The tailings disposal techniques have developed significantly in past years, for instance the use of consolidation methods, aiming to dewatering the water content in the mine pulp and the acceleration of the global process. It is an interesting way to reduce the total volume to be disposed, with positive consequences in terms of increasing the capacity of preservation of available areas. However, one problem linked to tailings thickening is the transportation of these materials until the disposal site. Because it is a more viscous material, in the form of paste or thickened tailings, the transportation by pumping becomes much more expensive in energy consumption as well as in the logistics for the implantation of the pumping system itself.

It is an unquestionable fact that the commodities production has great importance in the Brazilian economic and social development, especially considering the high volume of exports currently presented by these products of mineral extraction. However, it has become increasingly surprising the proportions that the so called tailings-retaining structures (especially tailings dams) have gained. Some recent failures of tailings dams in Minas Gerais State

Lucas De Leon Ferreira, Msc., Assistant Professor, Núcleo de Geotecnia da Escola de Minas, Universidade Federal de Ouro Preto, Ouro Preto, MG, Brazil. e-mail: lferreira@em.ufop.br.
Romero César Gomes, DSc., Professor, Núcleo de Geotecnia da Escola de Minas, Universidade Federal de Ouro Preto, Ouro Preto, MG, Brazil. e-mail: romero@em.ufop.br.
Submitted on September 11, 2013; Final Acceptance on September 15, 2014; Discussion open until August 31, 2015.

(Mineração Rio Verde, 2001; Indústria Cataguases de Papel, 2003; Mineração Rio Pomba Cataguases, 2007), involving serious economic and environmental impacts, demonstrate the need for developing more thorough systems for tailings disposal in order to identify, reduce and manage the possible risks of accidents in a more effective way, besides the constant quest for optimization of operational costs and monitoring these structures during their useful lives and after their closure.

New approaches for mining tailings disposal systems have been developed all over the world seeking to suit these procedures to the currently existing demands. One of these alternative approaches for fine tailings disposal, which has a long consolidation process, is the technique to accelerate the consolidation process of this material in the form of pulp through the application of an external electric field (electro-osmosis). The fine tailings is a byproduct of the ore beneficiation process, which usually presents granulometry below 400# and low percentage of solids, being, therefore, material associated to large volumes of water. Electrokinetic consolidation is based on the application of an electric potential difference inside a soil mass, through electrodes inserted in this mass, inducing the movement of the liquid phase in the direction of one electrode and enabling the removal of this corresponding flow of water.

The present study aims to improve the knowledge of the electro-osmotic consolidation technique applied to the fine tailings, theme of incipient research in Brazil (Mello *et al.*, 2011). In order to do so, laboratory experiments were carried out, using one special equipment called electrokinetic cell, and using some bauxite tailings samples from BPM (Bauxita Paragominas Mining/Brazil).

2. Electro-Osmosis Phenomena

The combination between hydraulic and electric flows, with their respective gradients, may result in four well-known electrokinetic phenomena in materials which present fine granulometry and electrostatically charged solid particles, as in the case of clay soils and colloidal systems. These four electrokinetic phenomena are: electrophoresis (movement of particle in a stationary fluid by an applied electric field), electro-osmosis (movement of liquid past a surface by an applied electric field), streaming potential (creation of an electric field as a liquid moves along a stationary charged surface and sedimentation potential (creation of an electric field when a charged particle moves relative to stationary fluid). All the electrokinetic phenomena involve, essentially, a difference of electric potential, particles with surfaces electrostatically charged and a liquid phase.

Electro-osmosis refers to the movement of bulk liquid relative to a stationary charged surface due to an applied electric field that is primarily generated in the electrical double layer (EDL). The mobile portion of the EDL tends to migrate towards the cathode or anode depending on its polarity. This electromigration of ions constituting the EDL causes viscous shearing of the adjacent bulk-liquid molecules, ultimately resulting in bulk-liquid motion. For thin EDL's, the bulk-liquid motion or electro-osmotic flow is characterized by a plug-like velocity profile (Fig. 1).

Among many theories which describe electro-osmotic flow, the Helmholtz-Smoluchowski theory is the most accepted and widely adopted by geotechnical engineers. This theory is based on a model proposed by Helmholtz (1879) and later refined by Smoluchowski (1914). In this conception, the pore radii are relatively large in comparison to the thickness of the diffuse double layer and the mobile ions are concentrated near the soil-water interface.

The zeta potential (ζ) and the charge distribution in the fluid adjacent to soil surface play important roles in determining the electro-osmotic flow. The ζ is the electric potential developed at solid-liquid interface in response to movement of colloidal particles; *i.e.*, it is the electrical potential at junction between the fixed and the mobile parts of the electrical double layer. The ζ is less than the surface potential of a particle and shows the value at the slip plane, which is located at a small unknown distance from the colloidal surface (Hunter, 1981; Jones *et al.*, 2008).

In this model, the electro-osmotic flow (q) becomes a function of the electro-osmotic permeability of the soil (k_e), of the applied electrical gradient (i_e), which is the ratio between the potential difference (E) by the distance between the electrodes (L), and of the area of the section transversal to the flow direction (A) as established in the following equation (Haussmann, 1990):

$$q = k_e i_e A \tag{1}$$

The coefficient of electro-osmotic permeability is given by:

$$k_e = -\frac{\zeta \varepsilon n}{\mu} \tag{2}$$

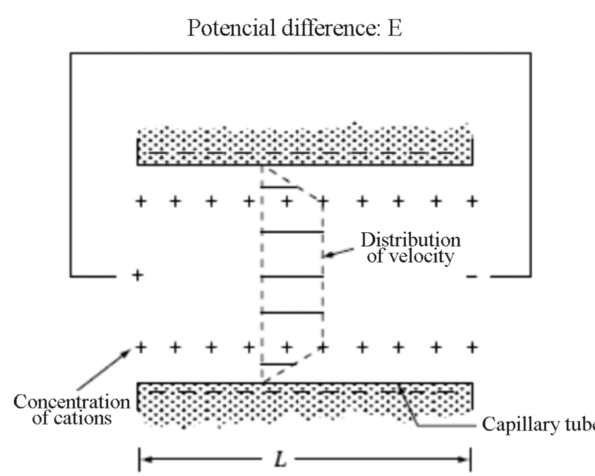

Figure 1 - Helmholtz-Smoluchowski model for electro-osmosis.

in which ζ is the zeta potential in V (usually negative for clay soils), ε is the soil electric permittivity (F/m in SI units), μ is the fluid viscosity (N.s /m^2 in SI units) and n is the soil porosity.

The factors of the mineralogy which have a positive effect for good electro-osmotic phenomena potential (Fig. 2) include: high water content (*w*), clay minerals with low cation exchange capacity (CEC), low valence exchange cations, high surface charge density, a high surface area and nature of water. In terms of water composition, the main aspects are low conductivity (σ), low salinity, high pH and low surface charge density per unit pore volume (A_0).

Electrochemical reactions associated with the electrical field application in tailings are very complex, including electrolysis of water (generation of oxygen and hydrogen gases), reduction at the cathode and oxidation process at the anode. As a result, the pore water pH of tailings decreases at the anode and increases at the cathode; the anode corrodes and/or deteriorates quickly if it is made of a material highly susceptible to corrosion effects.

Besides the parameters associated to the mineralogy of the soil or tailings, and the physico-chemical conditions of the interstitial fluid, there are still factors related to the arrangement (set up) of the external electric field applied (especially concerning the intensity of electric current and potential difference), and to the nature, geometry and distance between electrodes (Shang, 1997). This makes the technique of electrokinetic consolidation a complex process based on several variables and demanding, therefore, previous studies in reduced models or laboratory tests, evaluating as many of these variables as possible, in order to establish parameters to provide applications in field scale.

3. Electrokinetic Cell

In laboratory, the mechanisms of the electrokinetic process can be analyzed under well controlled and varied conditions in test columns or in the electrokinetic cells (called EK-cells), equipment which simulates, in reduced scale, the field setup. The EK-cell tests provide information on the electro-osmotic permeability as a function of material density (porosity), applied dc current (current density), voltage (voltage gradient), time and water chemistry. In addition, the EK-cell tests provide information on voltage losses at interfaces of electrodes and materials (for example, soils or tailings).

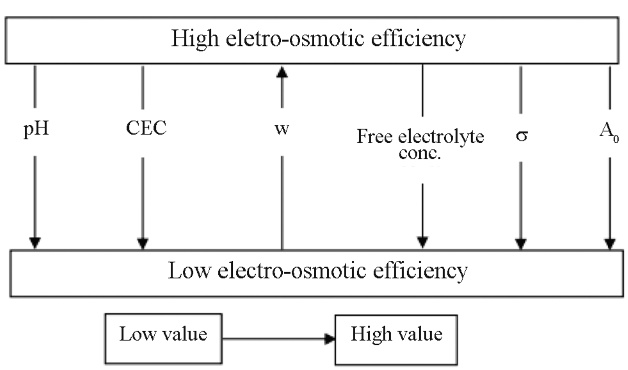

Figure 2 - Influence of soil variables on E-O efficiency (Jones *et al.*, 2008).

The electrokinetic cell shown in Fig. 3 has been developed to measure the electro-osmotic permeability in tailings (or soils) under well-controlled boundary conditions (according to Hamir *et al.*, 2001), consisting basically of the following devices (Ferreira, 2011):

- acrylic cell;
- electrodes;
- load application system;
- input system and electricity control device;
- water circulation system;
- monitoring system;
- data gathering system.

A pair of electrodes and a specimen compartment compose the electrokinetic cell (Fig. 3). The cell is made of 10-mm thick acrylic and bases of polyacetal (polyoxymethylene) material with the inside dimensions of 15 cm of diameter and 35 cm high. The tailings are placed in the specimen compartment and o-rings are placed on the top and bottom of the cell in order to guarantee the complete sealing of the whole system. The water flow through the tailings sample in the cell is essentially one-dimensional (vertical).

The electrodes are placed at both ends of the specimen compartment. In this study, two types of electrodes in the form of circular plates were used in the tests for comparison: copper and stainless steel (SS316). SS316 is the highest grade of corrosion resistant stainless steel commercially

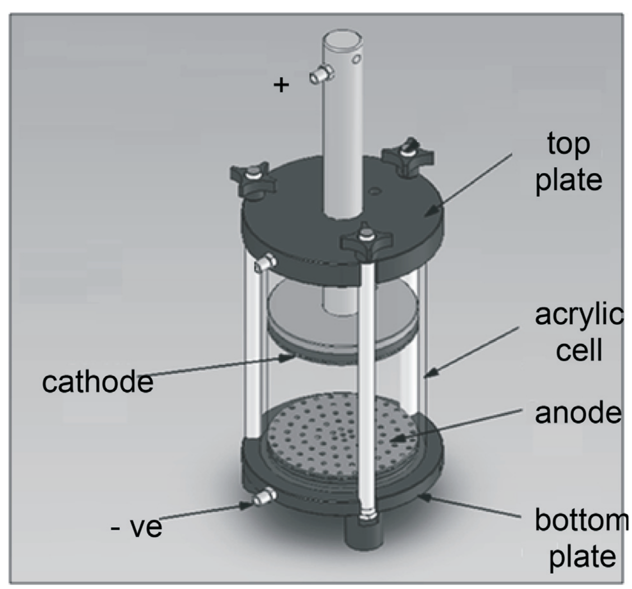

Figure 3 - Electrokinetic cell and electrodes.

available. The lower electrode has a diameter of 148 mm, while the diameter of the upper electrode is 134 mm (due to the characteristics of this sealing of the cell). The plates used in the tests have a thickness of 2.0 mm and specific opening areas between 8.0 and 8.7%. In the tests, the electrodes are wrapped with geotextile or a filter paper for filtering and drainage.

A special designed loading plate (50 cm long x 10 cm wide) equipped with dia1 gauge was placed on the top of the specimen compartment to apply a surcharge through the dead weights. The water in both reservoirs in the cell is controlled at the same level via recharge and discharge tubes to ensure different hydraulic gradients or water flow due solely to the applied dc current. The electrodes were connected to a dc power supply (Instrutherm FA 3005 model, with 0-32 V and 0-3 A ranges); the dc current and voltage were measured using a high precision multimeter. The measuring apparatus consists in three main parts: the transducers (of displacement, pressure, load and volume measurement), data acquisition board and the management software.

Polarity inversion, *i.e.* the change between the anode and cathode has been applied in the performed tests. Under the normal polarity (NP) mode, the lower electrode of the EK-cell is the anode and upper electrode is the cathode. Under the reversed polarity (RP) mode, the applied dc voltage is reversed, *i.e.*, the electrodes are inverted, whereas all other conditions remain the same. The water flow in the tailings reverses direction after the polarity change but the water discharge was measured through a drainage valve at the upper part of the cell in both setups (NP or RP modes).

In the experiments performed in this research, other following design criteria for EK-cell system were considered (Micic, 1998):

- EK-cell had to be water-tight and electricity insulated;
- EK-cell had to be big enough to allow a measurable flow of fluid and electricity through the tailings sample under combined influences of imposed hydraulic and electrical gradients;
- to achieve consolidation by electro-osmosis, the drainage should have been available at the cathode, while the anode could be impermeable;
- an accurately controlled DC electrical potential could be applied across the sample; voltage distribution in the soil sample and the electrical current passing through the sample could be measured as a function of time;
- volume of flow rate of water through the soil sample could be measured accurately as a function of time;
- measurements to be made during electrokinetic treatment could not interfere with the process.

The EK-cell apparatus (Ferreira, 2011), as shown in Fig. 4, was designed and manufactured for the electrokinetic bench-scale experiments performed in this study.

4. Tailings Characterization and Properties

The electrokinetic tests were performed with tailings samples from a bauxite mine (MBP) at Paragominas in the north of Brazil. Morphologically, the bauxite is thin layer, which covers tens of square kilometers. It lies beneath 5 to 20 m of overburden along vast plateaus, which characterize the ore bodies and were created by differential erosion of the plain where the laterites developed. On average, the ore is about 1.5 meters thick and the overburden is 12 m thick. The overburden consists of a thick oxisol and the top 1.5 to 2 m of the laterites, of which the bauxite layer is a part. The main constituents of the overburden are silt and clay.

Paragominas bauxite is washed to remove the free clay that it contains, before shipping to refineries. Washing leaves about 30% of the run-of-mine ore at the mine, in the form of clay rich tailings, which would otherwise reduce the alumina content of the product, increase the refinery cost and increase the volume of red mud for disposal at the refinery site.

In the MBP concept, run-of-mine bauxite is reduced below 8 inches through two stages of double roll crushers. The crushed ore is fed to a SAG mill, usually part of the primary stage in the grinding process in mining operations, which continues reduction and slurries the ore with water. From the SAG mill, most of the slurry goes to a ball mill, which adjusts the particle size distribution of the solids to meet the specification for pipeline transport. Between the two mills, larger pebbles exiting the SAG mill are crushed to control the ball mill feed top size and the greater mass of the slurry is diluted and then classified by hydro-cyclones into three streams. The first stream, with particles greater

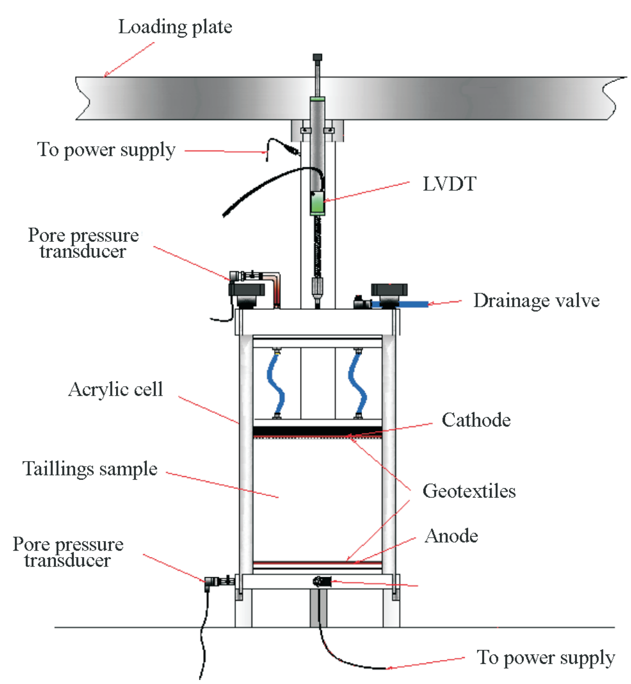

Figure 4 - Schematic of electrokinetic testing cell.

than 150# is directed to the ball mill and the second stream, with particles between 150# and 400#, bypasses the ball mill directly to the product tank. The third stream, with particles below 400#, is waste and proceeds to the tailings thickener. Tailings are approximately 30% of the dry mass of ore, or about 0.38 million tons for each million ton of product, or 220 million tons over the project lifetime.

The deposition area is located in a valley not far from the plant. Tailings are confined laterally by the valley sides and longitudinally by dykes, which divide the total area into four storage basins. Dumping is cyclic; each basin is used for 10 days then allowed to rest for 30 days before repeating the cycle. During the resting time, the tailings consolidate and dry to reach solids content of 70 to 80%, at which point they should be stable and occupy their minimum volume. However, further expansion and production for 40 years at the maximum rate require extensions to the current technique, and so, electrokinetic consolidation can be an interesting alternative solution.

The tailings and original supernatant were directly collected from the spigot and sent to the laboratory in sealed plastic containers, and used in all tests. Table 1 and Table 2 present the main geotechnical and chemical properties of the tailings (obtained by the ICP technique), respectively.

The results show the predominant presence of the elements: iron (Fe), aluminum (Al), titanium (T_i), zirconium (Z_r) and sulfur (S) with all the other elements presenting much lower concentrations. There is no silicon (S_i) in the chemical analysis of the tailings due to the technique of preparation of the sample for test performance. In this case, the sample, air dried, was solubilized in fluoridic acid (HF), which causes the elimination of the silicon by evaporation.

The grain size distributions, with and without use of deflocculant during the test, are shown in Table 3. The results enable us to verify the effective action of the additive incorporated to the tailings in relation of clay particle flocculation (in situ situation), indicating that the tailings solids consist essentially of fines particles. The tailings have high plasticity with a plasticity index of 33.1%.

The results of X-ray of tailings using a powder diffractometer are indicated in Fig. 5, plotted as 2θ angle on the x axis vs. X-ray intensity as measured by the detector on the y axis, usually expressed as counts per second. Peaks are labeled by d-spacings (Å) indicating the predominant presence of kaolinite, goethite, gibbsite and hematite.

5. Electrokinetic Dewatering Tests

The tailings slurry was agitated by a mixer to a uniform consistency, and then it was poured into the cell with preinstalled electrodes. After the cell was filled, the slurry was allowed to settle by gravity until the water flow through the bottom drains stopped and a soft sediment was formed. During the sedimentation stage, the drain valves at the top of the cell were open and drainage water was collected. Electrokinetic tests were performed immediately after sedimentation stage. In the electrokinetic tests, the applied voltage in all tests was 15 V in order to ensure an uniform voltage gradient along the tailings samples of 95 V/m.

Tests were conducted to study the combined effect of surcharge and electro-osmosis, using the following termi-

Table 1 - Tailings geotechnical properties.

Specific gravity	2.67
Liquid limit	64%
Plasticity Limit	31%
Plasticity Index	33%
pH	5.33
CEC (cation exchange capacity)	4.88 cmol/kg
Hydraulic conductivity (for initial solids content= 30%)	5.7×10^{-7} m/s

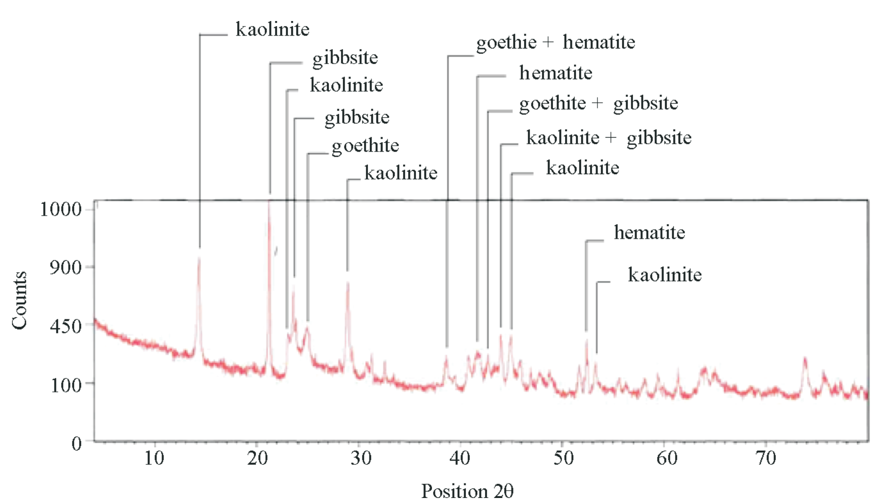

Figure 5 - X-ray diffraction pattern for bauxite tailings.

nology: EKC tests for the electrokinetic consolidation tests with copper electrodes (standard tests); EKS test for the electrokinetic consolidation test with steel electrodes (for comparison) and CCT for the conventional static consolidation test (control test, without electrokinetic effects, using only surcharge for consolidation). Prefixes to represent the filter element used in the test setup were insered to those tests (F for tests performed only with paper filter and G when the filtering element adopted was a layer of a nonwoven polyester geotextile with apparent opening size of 0.17 mm according to ASTM D4751). Six tests were performed on the bauxite tailings as summarized in Table 4 (prefixes T and B are explained hereafter). The initial parameters of each test, such as water content (w_i), solids content (ψ_i) and initial height (H_i) are presented. Solids contents were calculated by subtracting the mass of collected filtrate from the original mass of sample and the results were checked against changes in the volume of the sample, which were determined using an LVDT measurement of the cylinder piston displacement.

Table 2 - Tailings chemical properties by ICP (Inductively Coupled Plasma).

Elements	Concentration (µg/kg)
Al	240134
Ba	26.8
Ca	101
Co	17.1
Cr	110
Fe	103904
K	127
Mg	49.6
Mn	153
Na	92
P	178
S	356
Sc	4.6
Sr	27.4
Th	51.6
Ti	8997
V	265
Y	18.1
Zn	16.7
Zr	559

Table 3 - Particle size distribution of bauxite tailings.

Grain size	With deflocculant (%)	Without deflocculant (%)
Clay	49.1	2.5
Silt	48.8	89.8
Sand	2.0	7.7

During the test, the application of the static load, due to the drainage imposed next to the upper base of the sample, produces an upward axial flow in the slurry sample. On contact with the bases of the sample, the two electrodes (cathode with the upper base and anode with the lower one) generate an electro-osmotic flow parallel to that generated by the static load.

So the original prescriptions for the boundary condition for drainage were that the anode would remain closed and the cathode open. In this condition, the continuous supply of water was not made and the drainage valves in the anode remained closed during the entire test, with the drainage being made through a drainage valve in the cathode. However, during the tests, it was observed that the electro-osmotic flow happened in bigger proportions in the direction of the anode and not the cathode, unlike the commonly reported results in several scientific works.

This fact, which will be discussed ahead, led to the inversion of electrodes placement in the boundary condition previously described in some tests. These variations generated some changes in the nomenclature of the tests, with new inclusion of prefixes T and B to the codes (see Table 4), according to the position of the cathode at the top or bottom of the electrokinetic cell, respectively.

As initial prescription, it was defined for the interruption of the test whenever two consecutive readings of the volume of drained water, done by a calibrated burette, re-

Table 4 - Summary of the bauxite tailings tests.

Test	Cathode position	Filtering element	$w_{initial}$ (%)	$\psi_{initial}$ (%)	$H_{initial}$ (cm)	Voltage (V)
EKC-TF1	top	paper filter	208.73	32.39	16.0	15.0
EKC-BF2	bottom	paper filter	222.04	31.06	15.7	15.0
EKC-TG1	top	geotextile	223.33	30.94	15.7	15.0
EKC-BG2	bottom	geotextile	230.54	30.26	14.6	14.0
EKS-BF2	bottom	paper filter	218.85	31.36	16.0	15.0
CCT-F1	-	paper filter	218.25	31.42	16.0	-

mained constant within an interval of 2 h. Such procedure resulted in a standard time for test of 24 h, which was then adopted as reference for all the series of tests. As exposed previously, the voltage applied to the electrodes was kept constant (over a voltage gradient of 95 V/m) and without polarity inversion during the execution of all tests.

The results obtained are graphically presented according to the variation of the following magnitudes with the time and during the EK-treatment period:

- Volume of drained water;
- Electric current variation;
- Axial deformation;
- Porepressures generated at the base of the electrokinetic cell;
- pH of drained water.

The results of the tests are presented in next sections, for EKC tests, respectively (using for comparison the results from EKS test and CCT control test). They are reported in terms of changes of sample volume (settlement and expelled water), porepressures, current magnitudes and chemical properties of collected water at the completion of the tests. During the tests, the variations of water contents and of solids contents were also registered at three distinct regions of the sample: near the top electrode, in the middle of the sample, and near the bottom electrode.

6. EKC Test Results

Figure 6 presents the scheme for a one-dimensional electrokinetic consolidation test type T on a saturated specimen (Tamagnini*et al*., 2010), *i.e.*, assuming free drainage at the cathode and no hydraulic flow at the anode (impervious boundary).

By imposing a constant potential difference through the specimen, a uniform water flow is induced due to electro-osmosis. In this case, a uniform water flow tends to be recovered from the cathode if the material is assumed to be saturated. But, in reality, water hydrolysis at the electrodes develops oxygen gas at the anode, and hydrogen gas at the cathode. The oxygen produced at the anode remains entrapped by the inward water flow and slowly penetrates into the sample, affecting substantially the flow conditions. Thus the initial flow rate tends to decrease as the duration of the test increases associated to the progressive unsaturation at the anode due to gas production. By increasing the amount of gas produced at the anode, an unstable outflow rate is generated at the cathode.

As water drainage at the anode is prevented, a pore pressure gradient must develop to counteract locally with the electro-osmotic induced flow. Water can flow out from the sample at the draining boundary (cathodic interface) only if an equal amount of pore volume reduction is induced by soil skeleton deformation. As the drainage process is controlled by the volumetric deformation rate of the soil skeleton, which in turns depends on the changes in vertical effective stress, the specimen undergoes a time-dependent deformation process whose time evolution is ruled by soil hydraulic conductivity, soil stiffness and specimen thickness (Tamagnini *et al.*, 2010). Similar considerations can be applied to the B tests based on the effects due to hydrogen gas produced at the cathode.

Figure 7 shows the accumulated water flow induced by the dc current for all EKC tests (in comparison with results from CCT control test).

The tests were performed with normal polarity (without periodical inversion of the electrodes during the experiments). The water flow was collected at the drainage system coupled at the upper part of the cell and measured in real time by a graduated cylinder. The water flow tended to stabilize after about 24 h in all tests.

The general configuration of the curves shows that there is no relevant effect of preloading when comparing results from the electrokinetic tests. The effects of electrokinetic process in the dewatering become more evident around one hour after the start of the tests and were essentially similar in all tests, regardless the filtering interface used (paper filter or nonwoven geotextile). The best response was obtained in the tests where the bottom electrode was the cathode (EKC-BF2 and EKC-BG2). The limit behavior was obtained for EKC-TF1 test; in this case, the sample presented lower initial water content and higher solids content, thus showing the great influence of these parameters on the electro-osmotic dewatering process.

The electrokinetic effects are better observed by the results of collected water during the period of electro-osmotic application (Table 6). In relation to the total volume of expelled water during the tests, more than 90% had

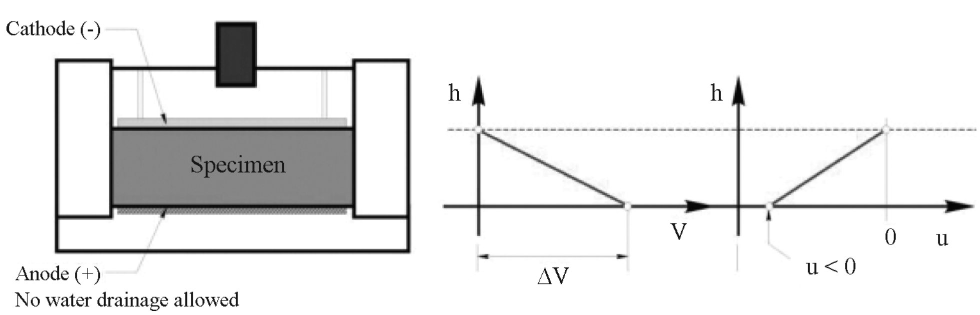

Figure 6 - Scheme of one-dimensional electrokinetic consolidation (EKC-T Tests).

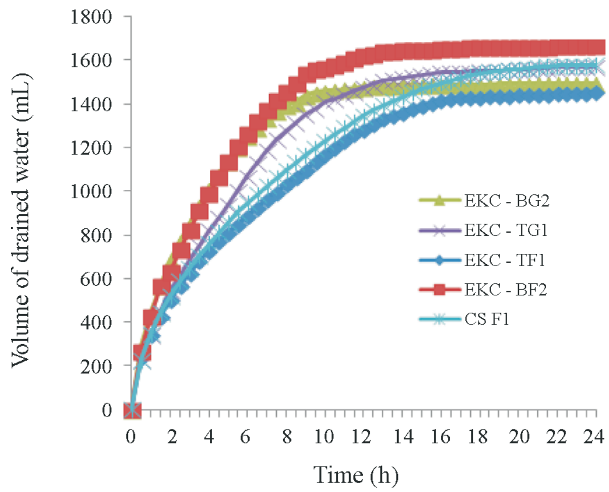

Figure 7 - EKC Tests: Volume of drained water *vs.* time of electrokinetic treatment.

already been extracted in all electrokinetic arrangements after the first 12 h of the test. For the sake of comparison, this table also shows the percentage of drained water during the first 8 hours of test.

The consolidation process under static load (15 kPa) and electric potential(0.95 V/cm) is associated with a deformation in the medium which only occurs in the vertical direction (settlements). The settlements of the tailings specimens during the EKC tests (compared with results from CS control test under static load only) are shown in Fig. 8. In all tests, the settlements of the tailings specimens were measured by a LVDT attached on the top of the loading plate.

Except for test TF1, which presented a discrepant performance (as already evidenced by the results of the test concerning the volume of drained water), all other tests provided final deformations equivalent and of the same order of magnitude as the value obtained in the conventional consolidation test (deformations in the range 57% to 59% after 24 h). On the other hand, the results indicate that the consolidation process is considerably accelerated when an electric field is applied to the tailings sample (Fig. 9). The research showed that the application of the electric gradient of 0.95 V/cm reduces the consolidation time by up to 60%.

Figure 10 shows the distribution of the excess pore pressures at the bottom of the cell in the tests when both static load and electric field are applied. The results show significant variations of pore water pressures at the bottom of the cell in the electrokinetic tests, in comparison with the conventional consolidation test (rising flow inside the cell as exclusive effect from loading). The initial value of the pore pressure at the bottom of the cell (about 20 kPa) corresponds to the sum of the excess of pressure generated by applying the vertical load (15 kPa) and due to the weight of tailings sample and water column pressure from the upper drainage tube of the cell.

It can be seen that pore pressure progressively decreases near the lower electrode region. The null values of pore water pressures (indicated over the t-axis) should be considered only like the final of positive pore water pressures; in reality, from this point on, negative pore water pressures tend to be developed. The consolidation process is directly related to the development of negative excess pore pressure in later stages of electrokinetic process.The reduction of excess pore pressures induces the increase in density via the increase of effective stresses.

Electro-osmotic consolidation (and not properly the electrokinetic dewatering) reduced substantially the water content of the testing samples. At the end of each test, the final water contents and solids contents of the tailings sam-

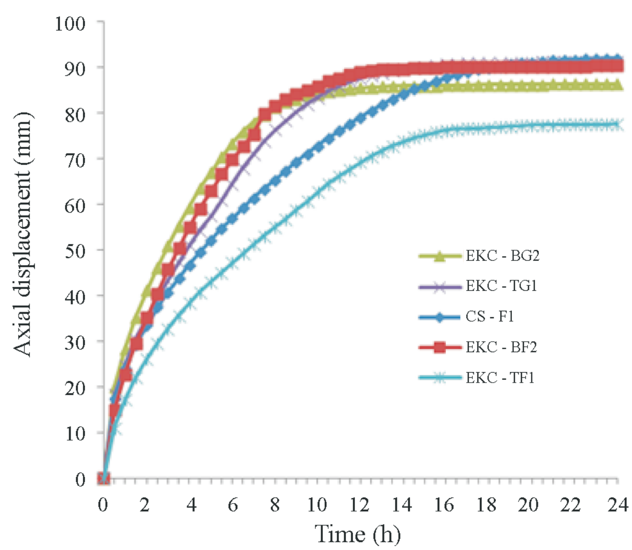

Figure 8 - EKC Tests: Settlements of the tailings specimens *vs.* time of electrokinetic treatment.

Table 6 - Volume of drained water in the tests.

Test	% of volume drained in 8 h	% of volume drained in 12 h	Total volume of drained water (mL)
EKS-TF1	70.96	88.53	1453.0
EKS-BF2	87.38	97.42	1664.0
EKS-TG1	81.53	94.00	1570.0
EKS-BG2	93.44	99.00	1494.0
CCT-F1	69.65	85.24	1579.0

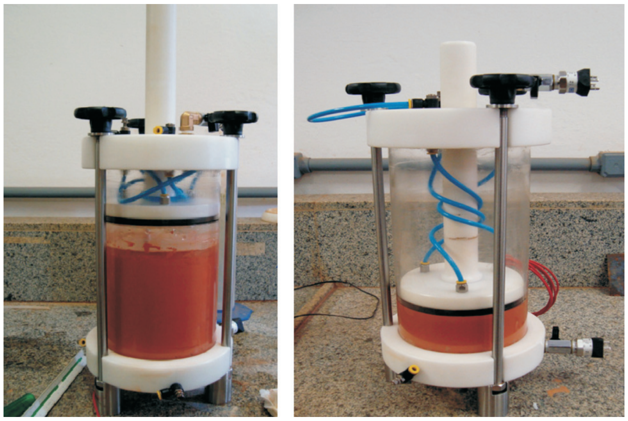

Figure 9 - EKC Test: Example of static and electrokinetic consolidation of bauxite tailings.

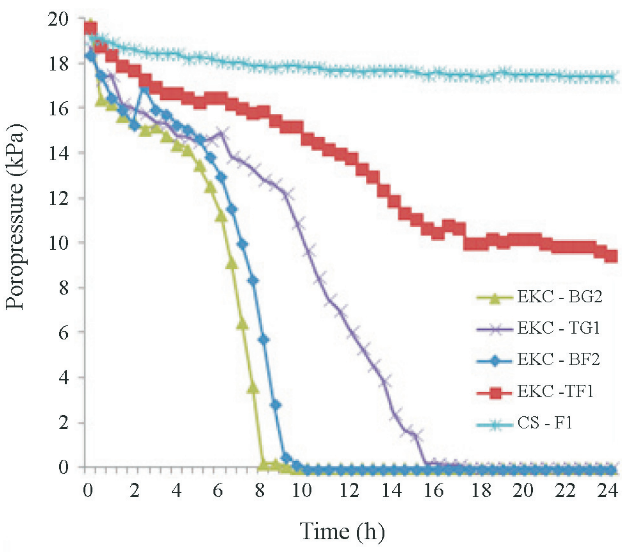

Figure 10 - EKC Tests: Excess pore pressures at the bottom of the cell *vs.* time.

ples were measured in three distinct sections of the specimen (near the upper electrode, in the middle of the sample and near the bottom electrode along the sample axis). The results are presented in Table 7.

In T tests, the water content presented higher values at the anode (sample bottom) and lower values at the cathode (sample top). The results were opposite in the case of G tests, with lower range variation in relation to the previous tests. This behavior happened regardless the initial value of water content of the samples. These experimental results suggest that the general flow is influenced in different ways by the development of pore water and gas pressure gradients generated within the sample in both test configurations. But the main explanation for this fact is due to the inversion of the electro-osmotic flow into the cell. The bauxite tailings presents a specific kaolinite-goethite-gibbsite composition which presents more positive than negative charges in the clayey mineral surfaces that favors anionic absorption (and not a conventional cationic exchange) inducing, as a result, the occurrence of an electro-osmotic reversal flow (cathode-anode direction).

These aspects were observed directly during the electrokinetic tests. Indeed different patterns of cracks were observed along the samples under consolidation, as a result of different conditions of interstitial water flow, induced in combination by the hydraulic flow ϕ_h (surcharge of 15 kPa) and by the electrokinetic flow ϕ_{ek} (indicated in Fig. 11).

These cracks tended to be predominantly parallel to the direction of the interstitial water flow for the tests with the cathode as top electrode and predominantly normal to the flow for the tests with the cathode as bottom electrode (Fig. 12).

The cracks in the test with the cathode at the top of the cell tended to appear in the region near the center of the sample, disappearing as the consolidation advanced. The cracks in the tests with the cathode at the bottom of the cell tended to appear in regions diametrically opposite of the sample, and occasionally remained until the end of the tests. In the region of the cracks, the water content assumed locally maximum values measured in the tests (maximum value of 99.61% for a final solids content of 50.1%). Figure 13 shows the consistency states of the tailings tested, before and after the electrokinetic consolidation process.

The current induced across the sectional area of tailings specimen during the EK-cell tests is shown in Fig. 14 (typical range between 1.5 e 5.0 mA). The pattern indicates a decreasing profile along time as a result of the continuous increase in material resistivity, generation of internal cracks and development of discontinuous gaps near the tail-

Table 7 - EKC Tests: Final water contents and solids contents values.

Test	Final water contents (%)				Final solids contents (%)	
	Top	Middle	Bottom	Top	Middle	Bottom
TF1	76.45	84.23	92.64	56.68	54.26	51.92
BF2	70.00	69.30	65.70	58.82	58.94	60.35
TG1	74.00	75.70	83.88	57.48	56.92	54.38
BG2	73.19	69.63	67.51	57.74	58.95	59.70

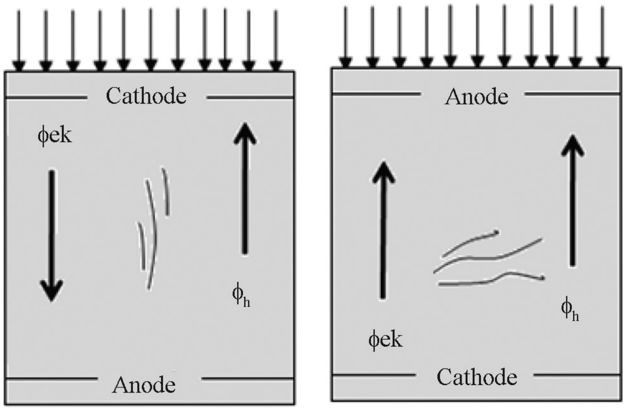

Figure 11 - Cracks pattern and flow conditions in the tested samples.

ings-electrode interfaces due to corrosion effects on the electrode material.

The initial values of electric current were higher in the tests having the cathode as the top electrode. The biggest drop of current was measured in the TG1 test, using geotextile as filtering element at the top of the cell (a reduction of around 77.5% in the current magnitude), whereas the smallest variation occurred in the BG2 test, using geotextile as filtering element and the cathode as bottom electrode (reduction of 50.0% in the electric current during the test).

The changes in the tailings pore water pH are presented in Fig. 15. The values were measured directly from the expelled water during the electrokinetic tests and collected at the drainage system coupled at the upper part of the cell. The tailings pore water pH increases at the cathode and decreases at the anode due to the effects of the electro-osmotic reversal flow and hydrolysis reactions.

Thus, in the surroundings zones of the cathode, the environment tends to become basic (condition observed in the tests TF1 and TG1, with the cathode being the drainage interface). TF1 test presented, in this region, pH values near 10.0, while in TG1 test, water pH reached 9.7. On the other hand, the concentration of hydrogen ions tends to produce acid media in the surrounding zones of the anode (condition

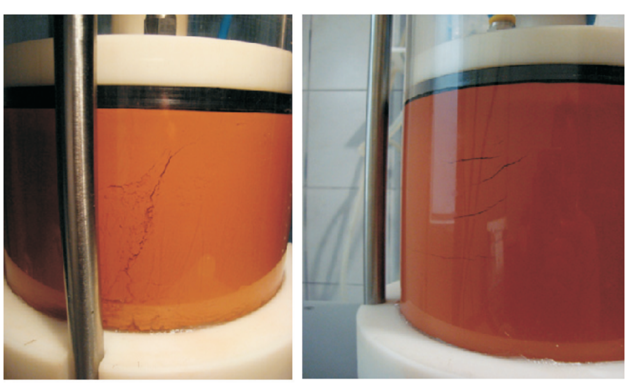

(a) (b)

Figure 12 - Cracks pattern: (a) EKC-TF1 test; (b) EKC-BF2 test.

Figure 13 - Consistency states of the tailings tested (before and after the EKC test).

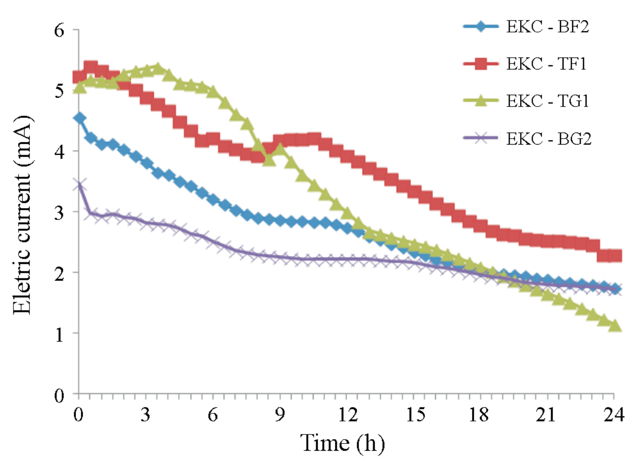

Figure 14 - EKC Tests: Electrical current *vs.* time of electrokinetic treatment.

observed in BF2 and BG2 tests, with the anode being the drainage interface). The values of water pH in this region were practically invariable during the tests, reaching minimum values of 5.17 for BG2 test. The pH control for tailings pore water constitutes a relevant procedure in order to sustain a continuous water flow under dc current.

The coefficients of electro-osmotic permeability (k_e) relate the velocity of the water flow and applied voltage gradient and are calculated from Eq. 1. Because tailings are highly variable in mineralogy, particle size and water chemistry, k_e results also show a great range along the time (Fig. 16). The initial k_e values measured from EKC tests varied between 7.6 x 10^{-8} m^2/Vs and 9.5 x 10^{-8} m^2/Vs, which decreased with time and tended to a mean value of 1.0 x 10^{-10} m^2/Vs after 24 h of voltage application.The mean hydraulic conductivity after the tests was estimated in over 2.1 x 10^{-8} m/s (ψ_{final} = 60%) compared to the initial value of 5.7 x 10^{-7} m/s ($\psi_{initial}$ = 30%). This variation may be attributed to blockage of pores in the tailings sample associated with electrokinetic phenomena.

Chemical analyses results of drained water during the CS-F1 and EKC-BG2 tests are presented in Table 8 for comparison with those obtained intailings. In both tests, the water samples were collected in the first 30 min of the tests.

Comparing the original tailings solution composition (Table 2) and the consolidation tests drained water samples (Table 8), it can be observed a significant reduction of the chemical element concentrations with time in EK tests. The variations on the concentrations of these chemical elements in the drained water happen due to the ionic migration resulting from the potential difference applied, and due to the cationic changes occurring during the electro-osmotic consolidation process.

The exponential increase of copper concentration in the second analysis is a straight result of the high corrosion effects of the copper electrodes used in the tests of electrokinetic consolidation. As a result, in the conventional consolidation test, by action of axial loading only, the copper concentration was 13.3 µg/L of water. In the electrokinetic consolidation test, however, this concentration was 3952 µg/L, approximately 298 times higher than the previous test.

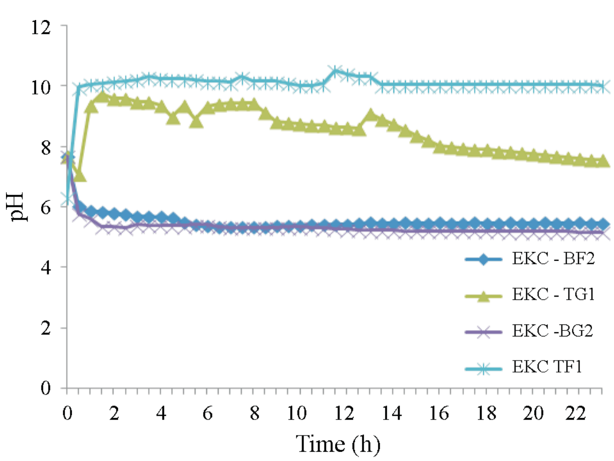

Figure 15 - EKC Tests: Tailings pore water pH *vs.* time of electrokinetic treatment.

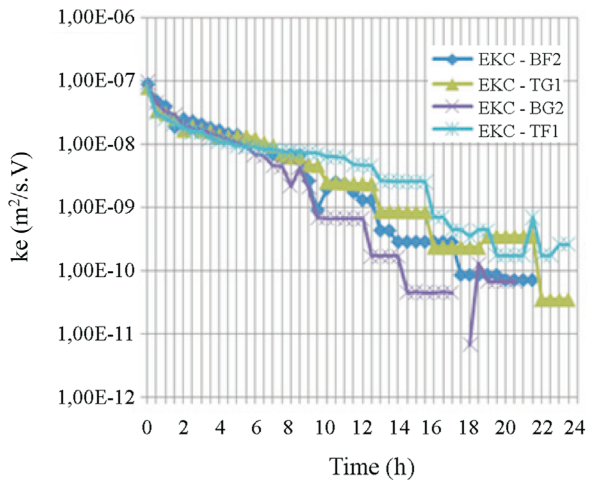

Figure 16 - EKC Tests: coefficients of electro-osmotic permeability (k_e) vs. time.

Due to the substantial effects of corrosion on copper electrodes, the EKC-BF2 test was remade for purpose of comparison using stainless steel (SS316) cathodes which present a higher grade of corrosion resistance (the new test was named as EKS – BF2, whereas all other conditions remained the same). The results show similar behavior between the tests, in relation to the reversal flow and measured quantities, including voltage losses and electric fields generated along the time. Figure 17 presents the corresponding pore pressure profiles induced in both tests. The values of electroosmotic permeability were equivalent and independent of electrode materials but, unfortunately, the new drained water composition was not spared for comparison with previous tests.

7. Conclusions

The processes of electro-osmotic consolidation and dewatering of mining tailings vary according to specific conditions presented by each project, because of the particle mineralogy, the chemical composition of the interstitial fluid, electrodes arrangement, and boundary conditions of drainage. Therefore, the design of structures which use electrokinetic phenomena as accelerators for the process of consolidation of mining tailings requires previous laboratory analyses in order to establish general guidelines for its application to real problems.

It is important to consider the complexity of electrokinetic phenomena in tailings processed in an industrial plant, characterized by milling and addition of several chemical products at different stages of operation. In the specific case of bauxite tailings from MBP (Paragominas -

Table 8 - Chemical analysis of drained water in the CCT-F1 and EKC-BG2 tests.

Element	Concentration (μg/L)	
	CCT-F1 Test	EKC-BG2 Test
Ba	1.13	3.1
Ca	0.978	2.36
Cu	-	3952
K	1.16	1.18
Mg	0.0397	0.0963
Mn	8.06	23.1
Na	4.57	1.9
Ni	-	18.8
P	< QL*	0.282
S	0.187	0.769
Si	0.529	0.917
Sr	4.53	11.2
Zn	10.7	88.8

*QL – Quantification Limit.

PA), very fine residues are generated (particles smaller than 400 #) which are treated with conventional thickeners and enhanced with synthetic flocculants for pH adjustments and optimization of the consolidation processes. This condition is very different of dewatering applications by the electro-osmotic technique for granular tailings (Shang & Mohamedelhassan, 2001).

The conjugation of a specific clay mineral composition, an surcharge of 15 kPa and the application of an external electric field of 0.95 V/cm, induced an electro-osmotic reversal flow in the direction cathode - anode, regardless the different placements and nature of the electrodes (with drainage always made by the superior electrode of the setup). Such flow condition is opposite to the electro-osmotic flow commonly observed, resulting from the mineralogy presented by the tailings used as well as from its pH, fact already observed in other researches related to problems of soils decontamination (Souza, 2002).

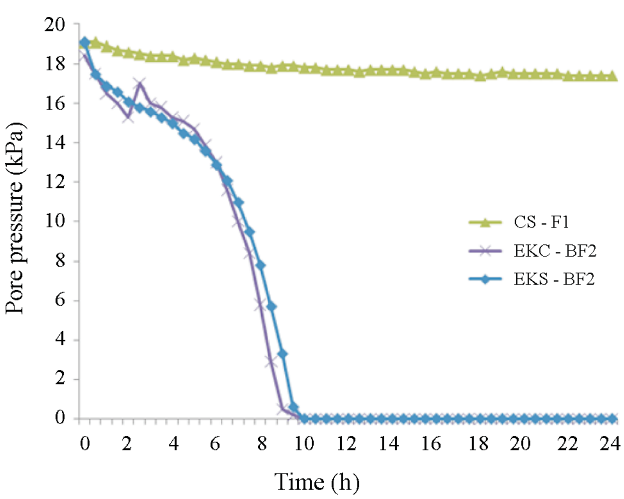

Figure 17 - EKC and EKS Tests: Excess pore pressures at the bottom of the cell *vs.* time.

The device designed and developed in this study enables a large versatility of tests, including the use of electrodes of distinct natures, application of external loadings and adoption of different boundary conditions of drainage of the samples (tailings or soils). The research showed that the application of the electric gradient of 0.95 V/cm reduces the consolidation time by about 60%. The adoption of stainless electrodes material solved the problems due to the high corrosion effects observed in the copper electrodes in the electrokinetic dewatering tests. The results obtained were pertinent, representative of the conditions inherent to the phenomena of electrokinetic nature, liable of repeatability and of direct confrontation among themselves.

References

Ferreira, L.D. (2011). Study of Electrokinetic Phenomena in Consolidation Process of Mining Tailings (in Portuguese). MSc Thesis, Graduate Program in Geotechnical Engineering, Federal University of Ouro Preto, Ouro Preto, 141 p.

Gomes, R.C.; Pereira, E.L.; Ribeiro, L.F.M. & Silva, J.T.G. (2002). Evaluation of liquefaction potential of fine grained tailings. In: 4th International Congress on Environmental Geotechnics - 4ICEG, Rio de Janeiro. Taylor & Francis; Lisse, v. 1, pp 329-333.

Hamir, R.B.; Jones, C.J.F.P. & Clarke, B.G. (2001). Electrically conductive geosynthetics materials for consolidation and reinforced soil. Geotextiles and Geomembranes, 19(8):445-482.

Hausmann, M.R. (1990). Engineering Principles of Ground Modifications. McGraw Hill Publishing Company, New York, 363 p.

Helmholtz, H. (1879) Studien über electrische grenzschichten. Annalen der Physik und Chemie, 243:337-82.

Hunter, J.R. (1981). Zeta Potential in Colloid Science. Academic Press, London, 386 p.

Jones, C.J.F.P.; Lamont-Black, J.;Glendinning, S.; Bergado, D.; Eng, T.; Fourie, A.; Liming, H.; Pugh, C.; Romantshuk, M.; Simpanen, S. & Yan-Feng, Z. (2008). Recent research and applications in the use of electro-kinetic geosynthetics. EuroGeo4; Keynote Paper, 30 p.

Mello, C.M.A.R.; Tibana, S.; Saboya, F.; Reis, R.M.; Del'Aguila, V.M. & Silva, E. Z. (2011). Physical models consolidation by electro-osmosis. In: 14º Panamerican Conference on Soil Mechanics and Geotechnical Engineering, Toronto. 2011 Pan-Am CGS Geotechnical Conference.

Micic, S. (1998). Electrokinetic Strengthening of Soft Marine Sediments. MSc Thesis, University of Western Ontario, Canada, 340 p.

Pirete, W, & Gomes, R.C. (2013). Tailings liquefaction analysis using strength ratios and SPT/CPT Results. Soils and Rocks, 36(1):37-53.

Shang, J.Q. (1997). Electrokinetic sedimentation: a theoretical and experimental study. Canadian Geotechnical Journal, 34,:305-314.

Shang, J.Q. & Mohamedelhassan, E. (2001). Eletrokinetic dewatering of Eneabba West Mine tailings: a laboratory experimental study. Soft Ground Technology Conference, Geotechnical Special Publication No. 112, ASCE, the Netherlands, p. 346-357.

Smoluchowski, M. (1914). In: L. Graetz (ed.), Handbuch der Elektrizitat and Magnetismus, Vol. 2, J.A. Barth, Leipzig.

Souza, M.V. (2002). Electrokinetic Transportation of Gasoline and Oil through a Residual Gneissic Soil and Oil Sludge from Campos Basin. MSc Thesis, Pontifical Catholic University of Rio de Janeiro, Civil Engineering Department, 137 p.

Tamagnini, C.; Jommi, C. & Cattaneo, F. (2010). A model for coupled electro-hydro-mechanical processes in fine-grained soilsaccounting for gas generation and transport. Annals of the Brazilian Academy of Sciences, 82(1):169-193.

Vick, S.G. (1990). Planning, Design, and Analysis of Tailings Dams. BiTech Publishers Ltd, Vancouver, 369 p.

Experimental Investigation of Soil-Atmosphere Interaction in an Instrumented Embankment Constructed with Two Treated Clays

K.V. Bicalho, G.P.D. Vivacqua, Y.-J. Cui, M. Froumentin, D. Mercadier, A.M. Tang

Abstract. This paper discusses the field monitoring of an experimental embankment divided into two symmetrical instrumented sections constructed with two clays treated with lime and/or cement in the northeast of France. The soil-atmosphere interaction is investigated in the monitored embankment. The field instrumentation included spatial and temporal changes of the soil suction, moisture, and temperature at predefined locations within the embankment, as well as measurements of meteorological data, collected from April to November 2011. The data show similarities in the suction daily variations trend in the two treated clays. Maximum changes in suction occur near ground surface. Even at the location of -0.75 m from the slope face the interchange of water between the atmosphere and the ground was observed in the daily soil suction measurements. No significant hydrologic response of the soils to rainfall was observed during the period of water deficit. The rainfall events showed a significant effect on the soil suction changes in the initial period of water surplus after a long period of water deficit. The comparison of the period of water deficit observed in the responses of the mean monthly suction and moisture measurements in the treated soils and the one estimated by simple water balance models based on standard meteorological observations in the region indicate that there is an overall qualitative agreement between the modelling and observational results.

Keywords: field monitoring, suction, temperature, moisture, evaporation, soil- atmosphere interaction.

1. Introduction

Compacted soils are widely used for the construction of earth embankments or earth fills, but the behavior of these soils is not fully understood, mainly because of their unsaturated state. Compacted soils are unsaturated during the construction stage; subsequently the degree of saturation is either increased (*e.g.*, infiltration or loading) or decreased (*e.g.*, evaporation), and the soil properties may change considerably. Understanding these changes in the soil properties, especially the changes in the pore-water pressure, is crucial in optimizing the design of earthen landfill covers and in controlling their long-term performance (Bicalho el al., 2000).

Negative pore-water pressures (or suctions) contribute to increasing the strength of the unsaturated soil, and changes in weather conditions might lead to changes in suctions and in the strength of the soil making it more susceptible to failure. When the water table is at significant depth, soil suction changes are likely to be directly controlled by atmospheric conditions (Toll *et al.*, 2011). In consequence of that, suction should be viewed as an environmental variable (Gens, 2010), and field monitoring results can help engineers to understand the impact of soil surface conditions and soil moisture and temperature on the soil suction profiles.

The interactions between the atmosphere and the soil surface have not been potently addressed by civil engineers, and particularly by geotechnical engineers, even though, it has already been the topic of several publications (Blight, 1997, 2013; Wilson *et al.*, 1997; Cui *et al.*, 2005, 2010; Gens, 2010; Hemmati *et al.*, 2012). Soil suctions can be changed under two principal mechanisms: infiltration or evapotranspiration. The amount of rainfall infiltration into the soil mass depends on external factors as well as intrinsic soil parameters, and the effect of rainfall infiltration on soil instabilities has been studied and published by many researchers (Brand, 1981, Wolle & Hachich, 1989; Lim *et al.*, 1996; Rahardjo *et al.*, 2001, 2005; Springman *et al.*, 2003; and Huang *et al.*, 2009). Evapo-transpiration from soil, on the other hand, is a significantly more complex mechanism,

Kátia V. Bicalho, Ph.D., Associate Professor, Departamento de Engenharia Civil, Universidade Federal do Espírito Santo, Vitória, ES, Brazil. e-mail: kvbicalho@gmail.com.
Gabriel P.D. Vivacqua, M.Sc., Rechercher, Departamento de Engenharia Civil, Universidade Federal do Espírito Santo, Vitória, ES, Brazil. e-mail: gpd.vivacqua@hotmail.com.
Yu-Jun Cui, Ph.D., Full Professor, CERMES UR Navier, ENPC - Université Paris Est, Marne-la-Vallee, France. e-mail: yujun.cui@enpc.fr.
Michel Froumentin, Ph.D., Senior Rechercher, CETE Normandie Centre Departement, Experimentation Recherche Developpement et Innovation, Centre d'experimentation e de Recherche, Le grand Quevilly, France. e-mail: michel.froumentin@developpement-durable.gouv.fr.
Dimitri Mercadier, Ph.D., Rechercher, CETE Normandie Centre Departement, Experimentation Recherche Developpement et Innovation, Centre d'experimentation e de Recherche, Le grand Quevilly, France. e-mail: dimitri.mercadier@developpement-durable.gouv.fr.
Anh Minh Tang, Ph.D., Senior Rechercher, CERMES UR Navier, ENPC - Université Paris Est, Marne-la-Vallee, France. e-mail: anhminh.tang@enpc.fr.
Submitted on May 10, 2014; Final Acceptance on May 11, 2015; Discussion open until December 31, 2015.

occurring in the form of combined liquid and vapor transport both at the depth and ground surface.

Under field conditions it is not possible to separate evaporation from transpiration totally, and the term of actual evapotranspiration is used to describe the amount of evapotranspiration that occurs under field conditions, or the total water loss. Evaporation from the bare soil surface is controlled by atmospheric and soil conditions. When available soil moisture is depleted, the actual evaporation will be limited by the monthly precipitation (lower limit) and the potential evaporation (upper limit). In months when the potential evaporation is less than the rainfall, the actual evapotranspiration is closer to the potential value (Fetter, 1994). In this case, the potential evaporation can be used to estimate the actual evaporation. However, there are some uncertainty regard to the potential evaporation value, which depends on the model structure and input data, to be investigated.

The investigation of soil-atmosphere interactions is a multidisciplinary complex research field, and, results of *in situ* monitoring of soil-atmosphere interactions have improved understanding and modelling descriptions of coupled heat, water vapour, and liquid water fluxes in unsaturated soils (Cui *et al.*, 2005, 2010). Accurate instrumentation of the soil surface in a large-scale and long-term is required for improving hydro-thermal soil profiles predictions especially in different fine-grained soils exposed to the same meteorological conditions.

This paper presents and discusses the on-going field monitoring of a large-scale experimental embankment divided into two symmetrical instrumented sections constructed with two different treated clays in the northeast of France. The objective of the study was to investigate the influence of weather changes on the treated soil responses (*i.e.*, suction, volumetric water content and temperature) to provide an understanding of soil-atmosphere flux in the embankment system over time. The study highlights some features of soil-atmosphere interactions, in particular, the impact of the duration and intensity of rainfall on low permeable soils during dry and wet periods, and examines the use of simple water balance models based on standard meteorological observations to assess soil suction and moisture conditions.

2. Materials and Methods

2.1. Site description and materials used in the experimental embankment

The experimental embankment was constructed at Hericourt, in the Haute-Saone department (Franche-Comte region) in the northeast of France. It is exposed to a continental climate, with oceanic influences. The embankment dimensions are 107 m long by about 5 m high with side slopes of 1 on 2 (Vertical: Horizontal). The embankment was divided into two symmetrical sections, constructed with two different fine-grained soils to represent two types of constructions: a road and a railway embankment. The soils used in the embankment were treated with cement and/or lime in different percentages.

In the experimental program, the *in situ* testing, soil sampling and laboratory testing were undertaken to help characterize the used materials. According to the unified soil classification system, the two natural soils were classified as: CL, an inorganic clay with low plasticity, and CH, an inorganic clay with high plasticity. The French Soil Classification System classifies these soils into A2 and A4 groups, respectively. The same soils were classified by the AASHTO soil classification system as A-2 and A-7, respectively. The soils in this group are fine grained soils and quite common in occurrence in the region. The soils classified as CH group often have an affinity for water. If the compaction is not sufficient or the treatment is not adequate, they may shrink or swell and lose much of their stability (Lund & Ramsey, 1959; Croft 1967; Bell 1996). The grain/particle size distribution, Atterberg limits, and Methylene blue (VBS) mean values of the two natural soils are summarized in Table 1. The specific surface (m^2/g) is about 24 x VBS (Cui *et al.*, 2010).

Figure 1 presents one cross section of the embankment. The section constructed with the silty clay (CL) treated with cement and/or lime (*i.e.*, CEM and/or CaO) in different percentages represents a railway embankment. The top layer consists of a railway-type structure with 0.25 m of gravel, underlain by a layer called CDF of 0.30 of CL + 1% CaO + 5% CEM. The section below called PST consists of three layers of 0.30 m and the natural soil was treated with cement (CL + 3% CEM). The fill of the central area consists of a layer of 0.40 m and eleven layers of 0.30 m of the natural soil treated with lime (CL + 2% CaO). The section constructed with a treated high plasticity clay (CH) represents a road embankment and the top layer consists of a road-type structure with 0.25 m of silt with lime and cement (1% CaO + 5% CEM), underlain by a subsequent layer called CDF of 0.30 m of CH + 2% CaO + 3% CEM. The section below called PST consist of three layers of 0.30 m of CH + 2% CaO + 3% CEM. The fill of the embankment consists of a layer of 0.40 m and eleven layers of 0.30 m and the natural soil was treated with lime (CH + 4% CaO). The locations of the instrumentation (SUC and TDR) discussed in this paper are also shown in Fig. 1.

Tests conducted at IFSTTAR (the French Institute for Transports, Development and Networks, formerly LCPC) of Nantes showed that the mineralogical composition of the CH soil contains mainly micas, montmorillonite and quartz. Only one of the four tested samples showed the presence of carbonates (calcite and dolomite). No phase sulphate (gypsum or anhydrite) or sulphide (pyrite or pyrrhotite) have been observed. The swelling volume of the CH samples treated with 5% lime after immersion for 7

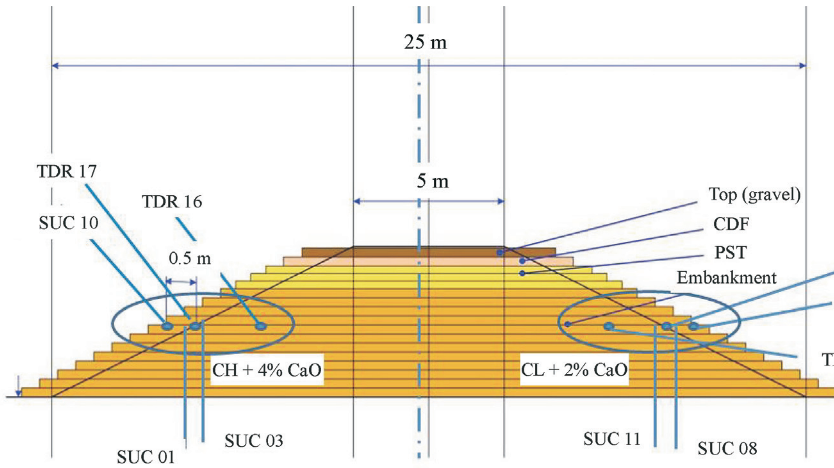

Figure 1 - A cross section of the experimental embankment constructed with two clays treated with lime and/or cement.

days at 40 °C varied from 1% to 6% for which the presence of carbonates was detected (Froumentin, 2012).

A series of laboratory tests of the natural and treated soils were conducted to evaluate the relevance of the chosen treatment formulation and the batching. Standard Proctor compaction tests results show that the addition of lime (CaO) to the soil increases quickly the optimum water content (w_{opm}, standard Proctor test) and decreases the corresponding dry density (γ_{dmax}), and the influence of lime treatment is accentuated in the CH soil (Table 2). The addition of cement (CEM > 3%) provokes the same phenomena but its influence is less than of the influence of lime. For a given water content, the addition of CEM and/or CaO reduces the swelling potential, liquid limit, and plasticity index of the soil, and increases its shrinkage limit (Croft, 1967; Bell, 1996; Le Runigo, 2008; Okyay & Dias, 2010). This is due to the flocculation and cementation of soil particles.

2.2. Field instrumentation program

In the construction of the embankment, 5280 m^3 of silty clay (CL), 4710 m^3 of high plasticity clay (CH), 320 t of lime and 162 t of cement were used. Soil and meteorological conditions on the test plots at the embankment have been monitored since the construction was completed in 2010. The field instrumentation program consists of detailed monitoring of matric suction, volumetric water content, and soil temperature at predefined locations over time within the embankment.

The instrumentation layout was symmetrical for the two sections of the experimental embankment constructed with the two fine-grained soils treated with lime and/or cement. The embankment consists of 17 layers made of the two fill materials compacted to optimum water contents (Standard Proctor tests). The optimum water contents were determined by the intercept of the compaction curve with the degree of saturation line corresponding to 85%. At each layer, the gravimetric water content and soil density were measured at various positions before and after construction, and the measurement variations were quite small. No leachate of lime or cement with rainfall was observed in the monitored area.

A layer of the slope, approximately at mid-slope, was selected for the investigations and analyses in this paper. The selected layer, located at about 1,8 m from the embankment base, is instrumented with sensors, for measuring suction (SUC) and water content (TDR), located close to allow estimation of the *in situ* soil water retention curves (Fig. 1).

Table 2 - Compaction tests results of the two natural and treated soils used in the investigated embankment sections.

Soils	w_{opm} (%)	γ_{dmax} (kN/m^3)
CL	17.9	17.60
CL+2%CaO	20.3	16.80
CH	26.4	15.00
CH+5%CaO	40.0	11.97

Table 1 - Characterization of the two natural soils used in the embankment.

Soils	Grain size distribution		Liquid limit (w_L)	Plasticity index (I_p)	Methylene blue value (VBS)
	≤ 0.075 mm	≤ 0.002 mm			
CL (A2)	50% - 60%	25% - 30%	40	18	2.19
CH (A4)	90%	80% - 85%	79	45	4.2 -6.3

The field instrumentation program generated a large amount of data; therefore, this paper summarizes some of this data in graphical form from April 2011 to November 2011.

The embankment was also equipped with a site-specific meteorology station on the top surface to record the meteorological data every 30 min, including solar radiation, precipitation, atmospheric pressure, wind speed and direction, and air temperature and relative humidity at 0.5 m and 1.5 m above ground level. The soil surface temperature and atmospheric pressure were also monitored. All components were supplied by Delta-T devices Ltd.

Time Domain Reflectometry (TDR) method, a measurement technique for electrical properties (*i.e.*, dielectric constant and electrical conductivity), is used to monitor the volumetric soil water content changes at the investigated embankment. The used sensors are TRIME-PICO 64, of IMKO Micro GmbH, in Germany, which are capable of simultaneously measuring soil temperature and inferring the volumetric water content. A total of 44 called Quasi-TDR based TRIME Pico 64 was used in the embankment in two symmetrical sections. The probes installed were linked to a control panel and data acquisition system, which allowed regular measurements. The readings frequency was usually once every 3 h.

TDR is a relatively accurate and automated method for determining the water content and electrical conductivity of porous media. The water content is derived from the dielectric permittivity of the medium, while the electrical conductivity is inferred from the TDR signal attenuation. Empirical and dielectric mixing models are used to relate water content to measured dielectric permittivity. The success of TDR technique for soil water content measurement originated from the Topp *et al.* (1980)'s universal calibration in which several soils were tested and an empirical equation was obtained by regression for the relationship between apparent dielectric constant and volumetric water content. TRIME measuring system operates with a factory calibration (Topp *et al.*, 1980) for mineral soils as a standard. Material-specific calibration is recommended if one needs accuracy to the last digit.

A total of 24 Watermark soil suction sensors connected to a data acquisition system was used to monitor the matric suction changes over time at the investigated embankment. The readings frequency was usually a value every 24 h. The used sensor is an indirect, calibrated method of measuring soil suction. It is an electrical resistance type sensor. These "Granular Matrix Sensors" electronically read the amount of moisture absorbed through a special "granular matrix", or mix of precisely composed materials. This special mix buffers the sensor against the effects of different salinities and ensures a lifetime much longer than the traditional "gypsum blocks". The readings were calibrated to reflect the same values that would be generated by a Tensiometer. All conversion equations take into account the soil temperature, because as temperature increases resistance decreases (Spaans & Baker, 1992). Variations in soil temperature can affect water potential readings by 1 to 3% per degree Celsius (Irrometer, 2005; Spaans & Baker, 1992). Shock *et al.* (1998) found that as the soil dries, the temperature effect increases. The measurement range of the used Watermark sensor is 0-200 kPa. The Watermark soil suction sensor is a product of the Irrometer Company, Inc.

2.3. Estimation of potential evaporation (ET)

The estimation of the potential evaporation (*i.e.*, the maximum evaporation rate in the case of water availability) of the investigated region is an important component of the hydrological cycle and essential for understanding soil-atmosphere fluxes in the embankment system performance over time. Several methods have been proposed to estimate ET from standard meteorological observations (Xu & Singh, 2001). In this study, the ET was estimated using two methods applied in the year 2011 when the weather data were directly measured in the investigated slope. The used methods, a temperature based equation (Thornthwaite, 1948) and a combination of temperature and air relative humidity based equation (Romanenko, 1961) are briefly summarized here and the cited references are suggested for a more detailed discussion

The empirical Thornthwaite (1948) method is highly used in several publications, even though the method is not recommended for use in areas that are not climatically similar to the developed area, in the eastern region of USA, where sufficient moisture water was available to maintain active transpiration. Moreover one should be aware that the soil temperature fluctuates daily and yearly affected mainly by changes in air temperature and solar radiation. Fetter (1994) reported that the amount of evaporated water is the greatest near the equator where solar radiation is more intense.

Often one chooses a model to estimate ET based on the available data to calculate the model. Thornthwaite (1948) formula is evaluated in this paper due to the advantage that the temperature based method offers in calculating ET by using only temperature. The method for monthly *ET* (mm/month) is:

$$ET\,(\text{mm/month}) = 16\,d\,(10\text{T}/\text{I})^{a};\ \text{for}\ 0 \le T \le 26\ °\text{C} \qquad (1)$$

$$a = 0.000000675\,I^{3} - 0.0000771\,I^{2} + 0.0179\,I + 0.492$$

where T is the mean temperature for the month (in °C), I is the annual thermal index, *i.e.* the sum of monthly indices I [$i = (T/5)^{1.514}$], d is a correction factor which depends on latitude and month. In this paper, d is defined equal to 1 (Xu & Singh, 2001).

Romanenko (1961) derived an evaporation equation based on the relationship using mean monthly temperature, T (in °C), and air relative humidity, R_h (in%):

$$\text{ET}\,(\text{mm/month}) = 0.0018\,(25 + T)^{2}\,(100 - R_h) \qquad (2)$$

The air relative humidity is the ratio of the absolute humidity to the saturation humidity for the air temperature. The saturation humidity is directly proportional to the air temperature, and the evaporation ceases when the air relative humidity approaches to 100%. Xu & Singh (2001) proposed an equation to calculated R_h, but, in this study, the mean monthly relative humidity values measured at the instrumented area are adopted.

Soil moisture at a location varies depending on the amount of precipitation (rain or snow) and evaporation. The atmospheric water balance (B), at a particular locality, can be written as (Blight, 1997):

$$B = P - ET \tag{3}$$

where P is the precipitation, and ET is the potential evaporation. During the period of excess water (B positive), there is moisture available for ground-water recharge and runoff. The uncertainties regard to the potential evaporation value, which depends on the model structure and input data, might result in different B values.

3. Results and Discussion

3.1. Meteorological data

The year of 2011 had a cumulative precipitation (rainfall) of 773 mm recorded by a French weather station at Luxeuil-les-Bains (located about 50 km from the site-specific meteorological station) compared with the average annual precipitation of 619 mm in France. It is observed some difference in the daily total rainfall measurements between these two places due to the great distance between them (see Fig. 2), especially in the months of April, June, August and September 2011 (Table 3). The results demonstrate that meteorological data measured by a site-specific meteorological station is important. The site-specific meteorological data are used in the investigations and analysis in this paper.

Table 3 - Comparison between the monthly rainfall values recorded at Luxeuil-les-Bains (site1) and those recorded at the site-specific meteorological station (site2).

Month (2011)	Monthly rainfall recorded at site 1 (mm/month)	Monthly rainfall recorded at site 2 (mm/month)
April (A)	11.2	0.6
May (M)	37.4	37.2
June (J)	147	85.8
July (J)	149.8	120.4
August (A)	68.2	118.6
September (S)	31.1	72.2
October (O)	71	64
November (N)	7.2	9.8

Storms with heavy rainfall exceeding 50 mm/h were not recorded in 2011 in the investigated site. Some rainy periods of heavy rain (10-50 mm/h) were observed from May to July 2011: one on May, 4 (18.6 mm/ 30 min), two events on June 8 (17.8 mm/30 min and 11 mm/30 min), two events on June 15 (9.6 mm/30 min and 7 mm/30 min), one on June 17 (6.6 mm/30 min), and the other on July 12 (13 mm/30 min). A total of 34 rainfall events of moderate rain (2.5-10 mm/h) was recorded in July 2011, the month with the highest monthly precipitation in 2011. A total of 13 rainfall events of moderate rain (2.5 -10 mm/h) was recorded in June 2011, and only one moderate rainfall event was recorded in May (*i.e.*, May 05, 3 mm/30 min). Cumulative total rainfall in May, June and July were 37.2 mm/month, 85.8 mm/month, and 120.4 mm/month respectively. Figure 2 also presents the total daily rainfall collected from April to November 2011 by the site-specific meteorological station. The largest daily rainfall

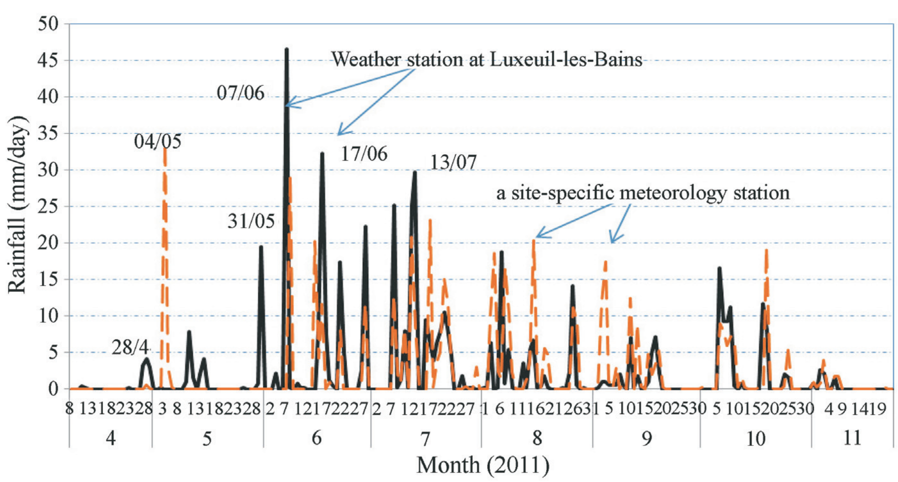

Figure 2 - Comparison between the mean daily rainfall values recorded by a French weather station at Luxeuil-les-Bains and those recorded by the site-specific meteorological station.

totals (34 mm/day) was on May 4, 2011, corresponding to circa of 92% of the month rainfall totals recorded in May, 2011.

The air temperature and relative humidity were recorded at 0.5 m and 1.5 m above the soil surface, which had an average air temperature of 16.3 °C (at soil surface), 13.8 °C (at 1.5 m) and 13.5 °C (at 0.5 m) in 2011. The air temperature varied between -4.3 °C and 34.5 °C and 4.1 °C and 34.3 °C, at 0.5 m and 1.5 m above the soil surface, respectively. At the soil surface, the air temperature varied between -3.6 °C and 44.6 °C. June and August, 2011 were the hottest months and November 2011 was the coldest, with the mean monthly temperatures near soil surface equal to 20.05 °C, 20.49 °C, and 7.24 °C, respectively (see Table 4).

Blight (1997) stated that air temperature and relative humidity gradients are generally not constant with the height above the soil surface, but they are approximately constant at heights of 0.5-2 m above the surface. The results show that the air temperatures are approximately constant at heights of 0.5 m and 1.5 m above the surface. A small difference of about 5-10% was observed in the air relative humidity recorded at 0.5 m (RH1) and 1.5 m (RH2) above the surface. The air close to the soil surface is warmer than it is higher up (at 0.5 m and 1.5 m above the soil surface) from April to August in 2011. The same trend is not observed in the months with lower temperatures (October and November 2011). Wind speeds between 0 and 5.5 m/s were recorded in 2011. The mean monthly wind speed was about 1.0 m/s for the entire monitoring period. Wind speed is important because stronger winds cause more evapotranspiration (Strunk, 2009).

Table 4 - Variation of the soil surface temperatures (Maximum, Minimum and Mean Monthly) recorded every 30min from April to November 2011.

Month (2011)	Maximum temperature soil surface (°C)	Minimum temperature soil surface (°C)	Mean monthly temperature soil surface (°C)
April (A)	33.99	-0.36	14.91
May (M)	44.64	4.89	19.10
June (J)	44.32	6.04	20.05
July (J)	41.12	4.24	17.92
August (A)	41.68	5.09	20.49
September (S)	38.17	2.6	17.21
October (O)	32.77	-1.99	10.93
November (N)	24.95	-3.63	7.24

3.2. Estimation of atmospheric water balance (*B* values)

Figure 3 presents the estimation of *B* values for the investigated region in 2011 based on the recorded rainfall (*P*) and computed potential evaporation values: ET_T (Thornthwaite, 1948) and ET_{R1} (using measured RH1) and ET_{R2} (using measured RH2) estimated by Romanenko (1961). The difference (5-10%) observed in the air relative humidity recorded at 0.5 m (RH1) and 1.5 m (RH2) above the ground surface resulted in variation (over 20 mm in June 2011) in the ET_{R1} and ET_{R2} values calculated by Eq. 2 (Romanenko, 1961). Fluctuations in the calculated ET_T were generally consistent with the measured air temperatures in the region during 2011. According to the ET methods used in this paper, the months of water deficit (*B* negative) were April and

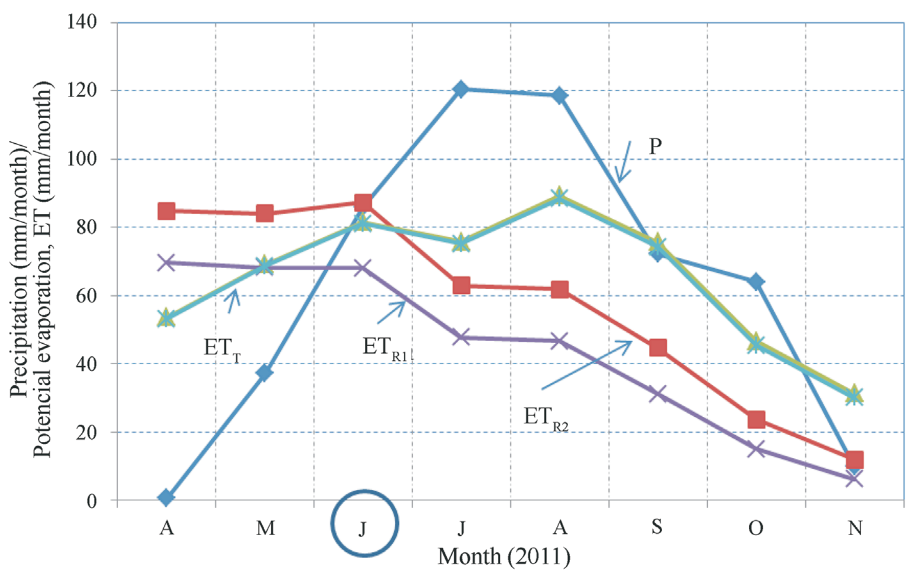

Figure 3 - Comparison among estimated monthly potential evaporation values (ET_{R1}, ET_{R2}, ET_T) and measured precipitation (P) at the site from April (A) to November (N) in 2011.

May. The period of water surplus (*B* positive) was from July to October. In June 2011, B varies from 0 (*i.e.*, ET_{R2}) to +20 mm (i.e, ET_{R1}), and in November 2011, *B* values may be negative or positive depend on the adopted ET method.

The difference observed in the two methods can be attributed to variations of measured air relative humidity during 2011. Thornthwaite (1948) considered only the air temperature as input data while Romanenko (1961) considered the air temperature and relative humidity as input data. The mean monthly solar radiation and wind speed measured values in the region remained essentially unchanged during the evaluation period; therefore, it may be reasonable the assumption of no influence of the solar radiation and wind speed on the evaporation considered by the used methods for the region in 2011. The results, presented in Fig. 3, indicate that ET_T is lower than ET_{R1} and ET_{R2} during the period of water deficit (B negative) and higher than ET_R during the period of water surplus (B positive). Even though, Blight (1997) showed that the Thornthwaite (1948) equation consistently underestimates the measured evapotranspiration; Chen *et al.* (2005) suggested that the Thornthwaites (1948) method overestimates ET where climate is relatively humid, while for arid and semiarid parts of China it produces an underestimation.

3.3. Responses of soil suction, moisture and temperature to meteorological changes

The layer of the slope located at about 1.8 m from the embankment base, approximately at mid-slope, was selected for the investigations and analysis because it is symmetrically instrumented with sensors for measuring suction and water content, located close to allow the estimation of the *in situ* soil water retention curves for the two treated soils.

The *in situ* soil water retention curves (SWRC) obtained from April to July 2011 for the two investigated treated soils, CL + 2% CaO and CH + 4% CaO, are presented in Figs. 4a and 4b, respectively. The relationships between soil suction and degree of saturation for the two soils were obtained considering no volume changes, and the soil porosity value of about 53% for the lime treated CH soil and 43% for the lime treated CL soil. A small variation

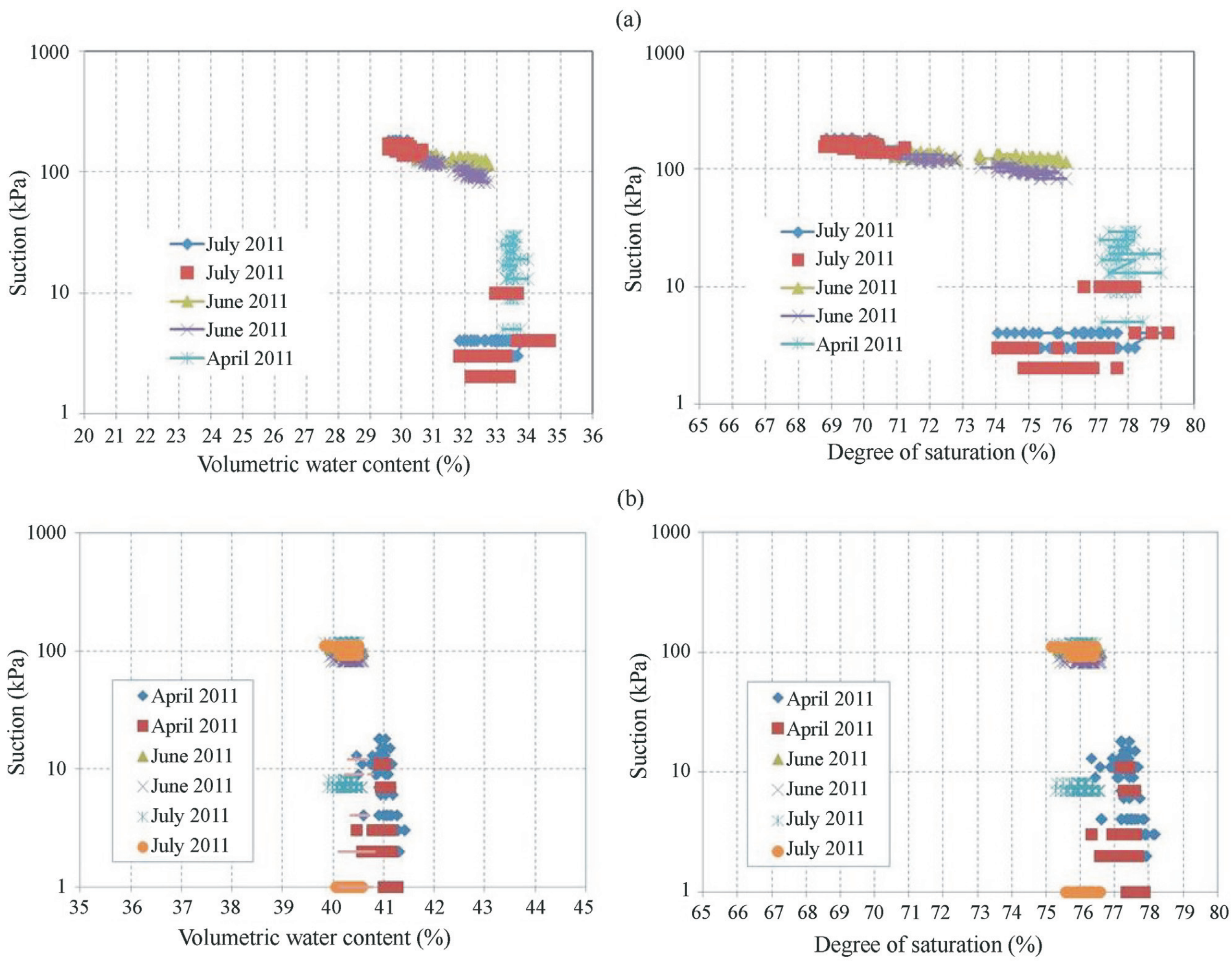

Figure 4 - The *in situ* soil water retention curves obtained from April to July 2011 for: (a) CL + 2% CaO soil and (b) CH + 4% CaO soil.

was observed in the volumetric water content and corresponding soil suctions in the two treated soils during the investigated period.

The laboratory soil water retention curves (SWRC) of the used soils have not yet been measured. It is well known that SWRC is hysteretic, with bounding curves defining the wetting and drying processes. Consequently, it very difficult to estimate the *in situ* relationship between water content and soil suction from laboratory measurements. The lime treated CL shows a more pronounced variation in the degree of saturation from April to July 2011. No appreciable degree of saturation difference (< 2%) was observed in the investigated layer in the CH + 4% CaO section.

Figures 5 and 6 summarize the *in situ* soil suction, volumetric water content and rainfall measurements collected daily from April (month 04) to November (month 11) in 2011. Figures 5a and 6a show the *in situ* soil suction measurements for the two groups of three sensors symmetrically installed at the same layer along the face of each section of the embankment constructed with the lime treated

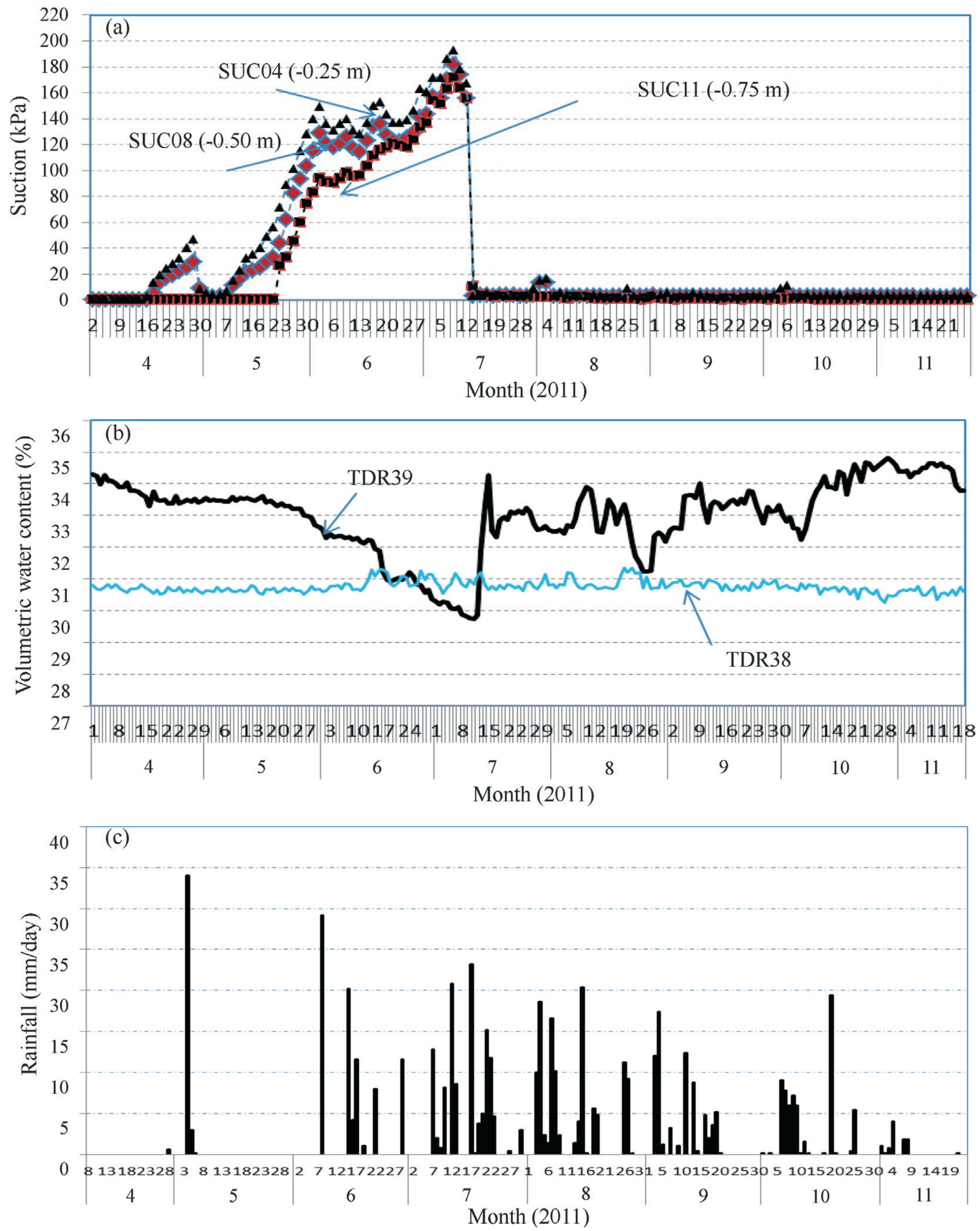

Figure 5 - The daily measured (a) soil suctions, (b) volumetric water contents, and (c) rainfall, in different locations from slope face (mid-slope, CL+ 2% CaO section) from April to November, 2011.

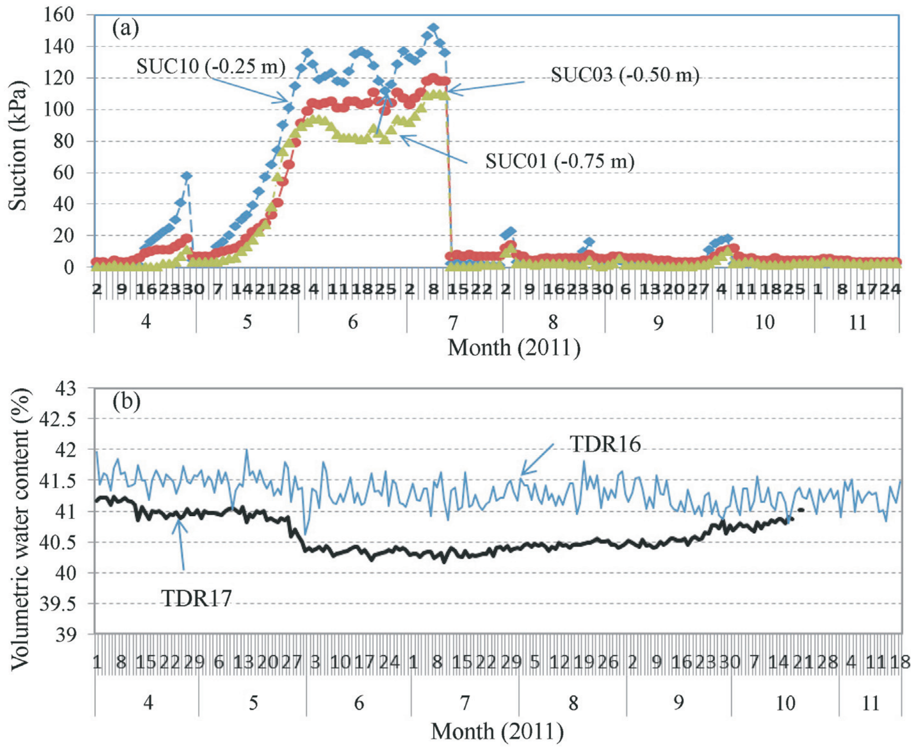

Figure 6 - The daily measured (a) soil suctions, (b) volumetric water contents, in different locations from slope face (mid-slope, CH+ 4% CaO section) from April to November, 2011.

clays, CL +2% CaO and CH + 4% CaO, respectively. As can be seen, suction is usually less than 200 kPa, and the pressure limit can be determined by the soil suction sensor. At each section of the slope the three Watermark soil suction sensors were placed at 0.25 m, 0.5 m, and 0.75 m from the ground surface (mid-slope face) as shown in Fig. 1. The results show similarities in the daily variations trend of suctions in the two treated fine-grained soils. The suction values are high near the ground surface, sensors placed at -0.25 m of the slope face, during the period of water deficit (*i.e.*, from April to June 2011) in the two investigated soils, and the fluctuation of the suction measurements generally decrease with depth.

The suction values observed in the CH + 4% CaO soil are generally lower than those at the correponding points in the CL + 2% CaO soil, mainly due to the difference in the magnitude of the corresponding measured volumetric water content values: 39-43% (lime treated CH) and 29-35% (lime treated CL). The maximum volumetric water content of a given soil volum is the saturated volumetric water content or the soil porosity. Considering the soil porosity value of about 53% for the lime treated CH and 43% for the lime treated CL, the degrees of saturation change from 74% to 81% in the investigated layer in the CH +4% CaO section and from 68 to 81% in the investigated layer in the CL +2% CaO section.

The data presented in Figs. 5a and 6a show that the daily suctions are recovered gradually in response to the period of water deficit from April to June 2011 in the two treated clays. Even at the location of -0.75 m (soil suction sensors SUC11, CL + 2% CaO and SUC01, CH+ 4% CaO) from the mid-slope face the effect of evaporation was observed in the daily suction and moisture measurements in the two treated soils. The soil moisture responses observed in the TDR 39 (located between the soil suction sensors SUC08 and SUC11) in the soil CL + 2% CaO are consistent with the soil suction measurements: the volumetric water content gradually decreased as the water moved down into the soil or evaporated from April to June 2011. The soil moisture responses observed in the TDR 38 (located at a greater depth, about -0.875 m from TDR39 and -1.5 m from the ground surface or the slope face) remained almost constant in the lime treated CL soil (Fig. 5b).

The same soil moisture response was not observed in the lime treated CH soil, in general, very small changes in the soil moisture were observed at the corresponding location. This may be explained by the differences in the hydraulic conductivity and water retention curves of the two treated soils presented in Fig. 4. Blight (1997) reported that the rate of infiltration is affected by the hydraulic conductivity of the soil, its surface gradient and its water content or suction. Taibi *et al.* (2009) present experimental results on two fine-grained soils showing that the relative hydraulic conductivity, k_r, which is defined as the ratio of the effective hydraulic conductivity at a given saturation to the saturated hydraulic conductivity, has a small value (≈ 0.05) while the degree of saturation, S_r, is relatively high (≈ 80%). These results are consistent with the measured k_r values presented in previous studies (Taibi, 1994; Bicalho, 1999) for fine-grained soils.

The field monitoring has also shown, in general, no significant hydrologic response of the soils to some rainy periods of heavy rain (10-50 mm/h) observed during the period of water deficit (*i.e.*, no rainfall infiltration is observed from April to June 2011). The rainfall events showed a significant effect on the soil suction changes (dramatic drop of suction) in the initial period of rainy season (July 2011) after a long period of water deficit in the two treated soils (see Figs. 5a and 6a).

Figure 7 presents a comparison among mean monthly measured soil suction (i.e, soil suction sensors SUC10 and SUC04) and volumetric water content (*i.e.*, TDR 17 and TDR 39) values, at mid-slope (about -0.25 m from slope face) in the two treated soil sections from April to November 2011. Figure 7c show that the mean monthly degrees of saturation change from about 73% to 80% in the investigated layer in the CL + 2% CaO section. No appreciable degree of saturation difference (< 2%) was observed in the investigated layer in the CH + 4% CaO section. The soil porosity of the lime treated CH and CL were 53% and 43%, respectively.

The simplified atmospheric water balance based on mean monthly potential evaporation calculated using stan-

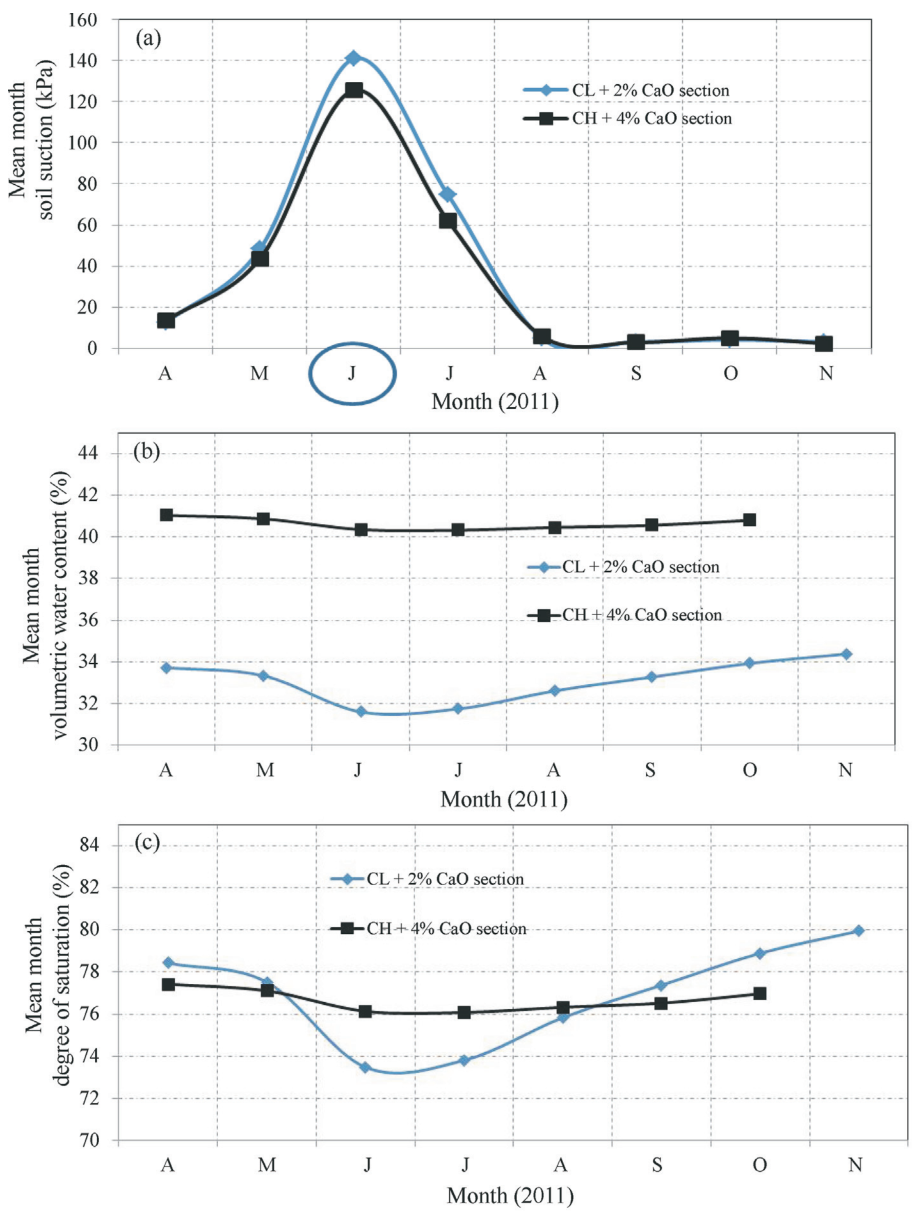

Figure 7 - Comparison among mean monthly measured (a) soil suctions, (b) volumetric water contents, and (c) degrees of saturation at mid-slope in the two treated soil sections from April to November 2011.

dard meteorological observations in the region, presented in Fig. 3, describes well the period of water deficit observed in the responses of the mean monthly suction and moisture measurements (see Fig. 7). There is an qualitative agreement between the period of water deficit observed in the responses of the mean monthly suction and moisture measurements in the treated soils and the atmospheric water balance (B values) based on mean monthly potential evaporation calculated using standard meteorological observations (*i.e.* Thornthwaite, 1948; Romanenko, 1961) in the region. The mean values data (observational and estimated by Romanenko (1961) using the air relative humidity recorded at 1.5 m, RH2, above the ground surface) show a similar defined shift from dry to wet climate (in terms of soil suction) in June (J) 2011.

Figure 8a shows the mean daily air temperatures recorded at soil surface, 0.5 m and 1.5 m above the soil surface and there are no substantial differences between the two observed results (*T*). From the results presented in Fig. 8a, it can be seen that the mean daily temperatures recorded at soil surface (*Ts*) are higher than the temperatures recorded at 0.5 m and 1.5 m above the soil surface (*T*). June (month 06) and August (month 08) were the hottest months in 2011 and November (month 11) was the coldest. The temperature fluctuations at the ground surface are diminishing as the depth of the ground increases in the two treated soils. Deeper soils experience less extreme seasonal

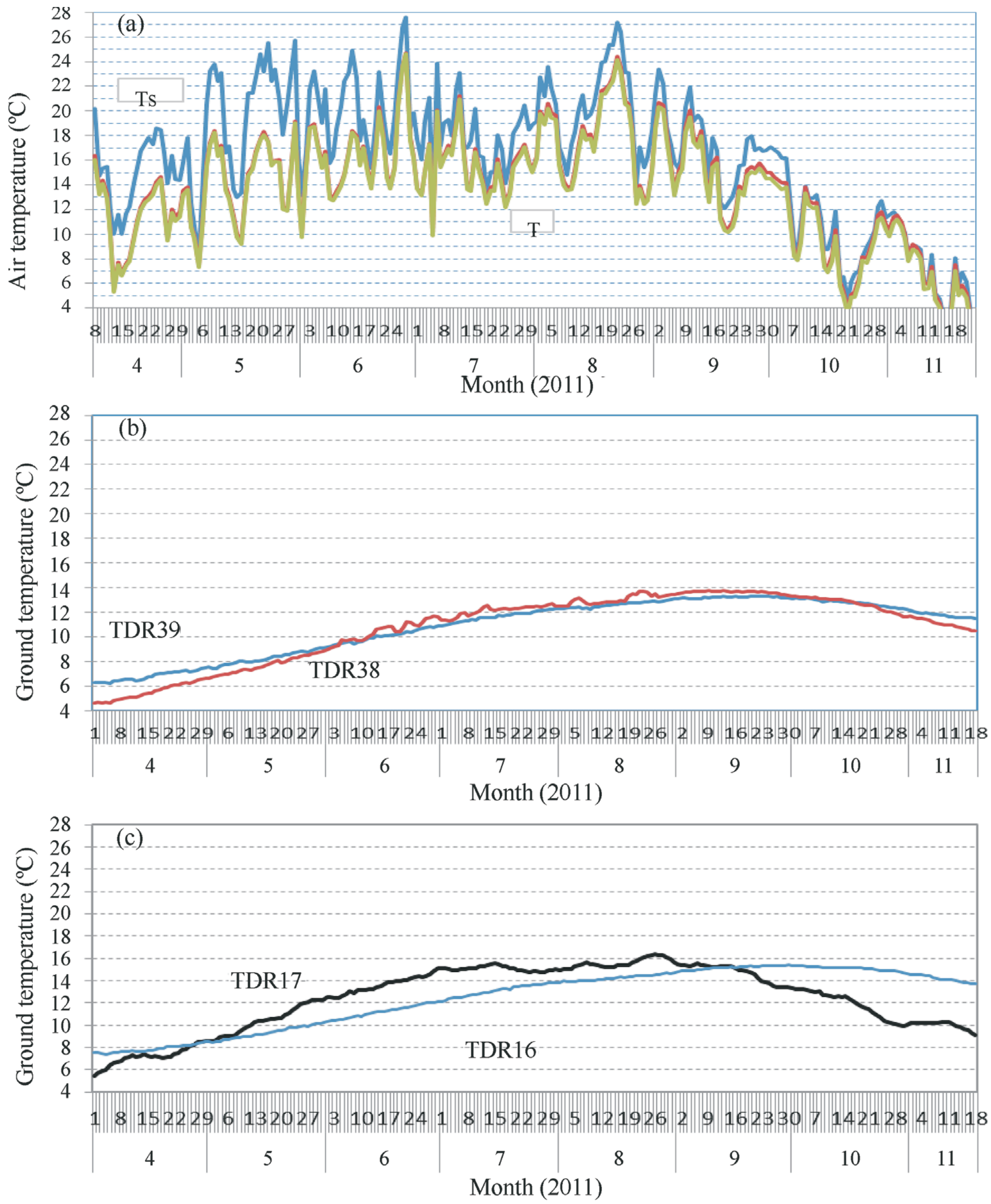

Figure 8 - Mean daily measured (a) air temperatures, and ground temperatures in the (b) CL+ 2% CaO (c) CH+ 4% CaO at mid-slope at diferent locations from April to November, 2011.

variations in the ground temperatures than shallower soils and the amplitude of seasonal soil temperature changes with the depth from soil surface. Liu *et al.* (2005) stated that the period of soil temperature variation increases and the amplitude of temperature fluctuation drops remarkably with the increase in depth.

Alike the observed soil moisture responses (Fig. 5b), the soil temperatures observed in the sensors TDR 38 and TDR39 are almost the same in the lime treated CL soil (Fig. 8b). The sensor TDR 38 is located at a greater depth, about -0.875 m from TDR39 and -1.5 m from the ground surface or the mid-slope face (see Fig. 1). It can be seen that a similar trend is observed in the treated CH soil (Fig. 8c). Therefore the zone in which the interchange of water between the atmosphere and the soil occurs is different from the one in which the interchange of heat between the atmosphere and the soil takes place. Heat transfer capability tends to increase as soil texture decrease and the degree of saturation increase (Van Rooyen & Winterkorn, 1957; Mitchell, 1991; Leong *et al.*, 1998).

One should be aware that the soil moisture sensors can behave differently with soil types, different soil depths and different parts of the embankment. Weather and soil physical conditions may be additional factors which directly or indirectly influence the sensitivity of the sensors. In this paper, the locations of the instrumentation for both treated fine-grained soils are similar. For the particular site of Hericourt, France, the data show similarities in the daily variations trend of suctions in the two treated soils.

The used soil moisture and soil suction sensors worked well on monitoring the soil suction and moisture responses to the meteorological changes in the two fine-grained soils. The data have also shown a consistent correlation between the increase in the soil suction and the relative decrease in the soil moisture. Even though a small variation was observed in the volumetric water content and corresponding soil suctions in the two treated soils (*i.e.*, a very small piece of the in situ soil water retention curves) over a period of eight months.

4. Conclusions

Some of on-going field monitoring of an experimental embankment constructed with two different clays, a silty clay and an expansive clay, treated with lime and/or cement in northeast of France, have been presented and evaluated herein. Field monitoring showed that weather effects are limited to a shallow depth. The results suggest similarities in the suction daily variations in the two treated fine-grained soils, and that the daily suctions are recovered gradually in response to soil evaporation during the period of water deficit. Even at the location of -0.75 m from the slope face the effect of evaporation was observed in the daily suction measurements.

No significant hydrologic response of the soils to rainfall was observed during the period of water deficit. The rainfall events showed a significant effect on the soil suction changes (dramatic drop) at the initial period of rainy season (July 2011) after long and warm dry period (or higher soil suction values).

The used sensors Watermark soil suction and Quasi-TDR based TRIME PICO 64 worked well on monitoring the soil suction and moisture responses to the meteorological changes in the two fine-grained soils in the instrumented embankment. The soil moisture responses observed in the TDR measurements are consistent with the soil suction measurements: the volumetric water content gradually decreased as the water moved down into the soil or evaporated from April to June 2011 for the investigated site in France.

Generally, the atmospheric water balance (B values) based on mean monthly potential evaporation calculated using standard meteorological observations (*i.e.* Thornthwaite, 1948; Romanenko, 1961) in the region describes well the period of water deficit observed in the responses of the mean monthly suction and moisture measurements in the treated soils. The uncertainties regard to the potential evaporation value, which depends on the model structure and input data, resulted in different values of B. The difference (5-10%) observed in the air relative humidity recorded at 0.5 m (RH1) and 1.5 m (RH2) above the ground surface resulted in variation of about 25% (over 20 mm in June 2011) in the potential evapotranspiration values ET_{R1} and ET_{R2} estimated by Romanenko (1961). The mean values data observational (*i.e.*, soil suction and moisture measurements) and predicted by Romanenko (1961) (using the air relative humidity recorded at 1.5 m, RH2, above the ground surface) show a similar defined shift from dry to wet climate (in terms of soil suction and moisture).

Acknowledgments

The first author is grateful for sponsorship by the Brazilian government agency CNPq (N. 202014/2011-8). This work has been performed within the French Projet TerDOUEST ANR-07-PCGU-006-10. The helpful comments and corrections by the reviewers are also appreciated.

References

Bell, F. G. (1996). Lime stabilization of clay minerals and soils. Engineering Geology, 42:4, p. 223-237.

Blight, G. E. (1997). Interactions between the atmosphere and the earth. Géotechnique, 47: 4, p. 715-767.

Blight, G. E. (2013). Unsaturated Soil Mechanics in Geotechnical Practice. CRC Press, Taylor & Francis Group, London, 597 p.

Bicalho, K. V. (1999). Modeling Water Flow in an Unsaturated Compacted Soil. PhD. Thesis, Department of Civil Engineering, University of Colorado, Boulder, 235 p.

Bicalho, K. V.; Znidarcic, D. & Ko, H. Y. (2000). Air Entrapment Effects on Hydraulic Properties. Geotechnical Special Publication, 99:1 , p. 517-528.

Brand, E.W. (1981). Some Thoughts on Rain-induced Slope Failures. Proceedings of the International Conference on Soil Mechanics and Foundation Engineering, Stockholm, Swed., v. 3, pp. 373-376.

Chen D. ; Gao, G. ; Xu, C-Y ; Guo, J. & Ren, G. (2005). Comparison of the Thornthwaite method and pan data with the standard Penman-Monteith estimates of reference evapotranspiration in China. Climate Research, 28:1, p. 123–132.

Croft J. B. (1967). The influence of soil mineralogical composition on cement stabilization. Géotechnique, 17:2, p. 119–135.

Cui, Y.J. ; Lu, Y.F. ; Delage, P. & Riffard, M. (2005). Field simulation of in-situ water content and temperature changes due to ground-atmospheric conditions. Géotechnique, 55:7, p. 557-567.

Cui, Y.J.; Gao, Y. B. & Ferber, V. (2010). Simulating the water content and temperature changes in an experimental embankment using meteorological data. Engineering Geology, 141:3, p. 456–471.

Fetter, C.W. (1994). Applied Hydrogeology, 3rd ed. Macmillan College Publishing, Inc., New York, 616 p.

Froumentin, M. (2012). TerDOUEST, Projet ANR-07-PCGU-006-10, Rapport de construction de l’ouvrage experimental RD438 Héricourt (70), Ministère de l'Ecologie, du Développement durable, des Transports et du Logement.

Gens, A. (2010). Soil–environment interactions in geotechnical engineering. Géotechnique, 60:1, p. 3-74.

Hemmati, S.; Gatmiri, B.; Cui, Y.J. & Vincent, M. (2012). Thermo-hydro-mechanical modelling of soil settlements induced by soil-vegetation-atmosphere interactions. Engineering Geology, 161:6, p. 139-140.

Huang, C.C.; Ju, Y.J.; Hwu, L.K. & Lee, J.L. (2009). Internal soil moisture and piezometric responses to rainfall-induced shallow slope failures. Journal of Hydrology, 370:1, p. 39–51.

Irrometer. (2005). Watermark Soil Moisture Measurement: Installation and Operation Manual.

Leong, W. H.; Tarnawskib, V. R. & Aittoma, A. (1998). Effect of soil type and moisture content on ground heat pump performance. Int J. Refrig., 21:8, p. 595–606.

Le Runigo, B. (2008). Durabilité d’un Limon Traité à la Chaux et Soumis à Différentes Sollicitations Hydrauliques: étude des Comportements Physico-chimique, Hydraulique, Microstructural et Mécanique. PhD. Thesis, Department of Civil Engineering, Ecole Centrale de Nantes, Nantes, 276 p.

Lim, T.T.; Rahardjo, H.; Chang, M.F. & Fredlund, D.G (1996). Effect of rainfall on matric suctions in a residual soil slope. Canadian Geotechnical Journal, 33:4, p. 618-628.

Liu B.C.; Liu W. & Peng, S. W. (2005). Study of heat and moisture transfer in soil with a dry surface layer. International Journal of Heat and Mass Transfer, 48:2, p. 4579–4589.

Lund, O.L. & Ramsey, W.J. (1959). Experimental lime-stabilisation in Nebraska. Highway Res. Board Bull., 231:1, p. 24-59.

Mitchell, J.K. (1991). Conduction phenomena: From theory to geotechnical practice. Géotechnique, 41:3, p. 299-340.

Okyay, U.S. & Dias, D. (2010). Use of lime and cement treated soils as pile supported load transfer platform, Engineering Geology, 114:4, p. 34-44

Rahardjo, H.; Li, X.W.; Toll, D.G. & Leong, E.C., (2001). The effect of antecedent rainfall on slope stability. Journal of Geotechnical and Geological Engineering, 19:3, p. 371–399.

Rahardjo, H.; Lee, T.T.; Leong, E.C. & Rezaur, R.B. (2005). Response of a residual soil slope to rainfall. Canadian Geotechnical Journal, 42:5, p. 340–351.

Romanenko, V.A. (1961). Computation of the Autumn Soil Moisture using a Universal Relationship for a Large Area. Proceedings Ukrainian Hydrometeorological Research Institute, Kiev, v. 1, pp. 1-3.

Shock, C. C.; Barnum, J.M. & Seddigh, M. (1998). Calibration of Watermark Soil Moisture Sensors for Irrigation Management, Proc. of the International Irrigation Show, San Diego, v.1, pp. 139-146.

Spaans, E.J.A. & Baker, J.M. (1992). Calibration of Watermark soil moisture sensors for soil matric potential and temperature. Plant and Soil, 143:2, p. 213-217.

Springman, S.M.; Jommi, C. & Teysserie, P. (2003). Instabilities on moraine slopes induced by loss of suction:a case history. Géotechnique, 53:1, p. 3–10.

Strunk, R. L. (2009). An Evaluation of the Performance of prototype instrumented soil covers at the Regina Municipal Landfill. M.Sc. Dissertation, Department of Civil Engineering. University of Saskatchewan. Canada. 240 p.

Taibi, S. (1994). Comportement mécanique et hydraulique des sols soumis à une pression interstitielle négative – Etude expérimentale et modélisation. PhD. Thesis, Department of Civil Engineering, Ecole centrale de Paris, 374 p.

Taibi, S.; Bicalho, K. V.; Sayad-Gaidi, C. & Fleureau, J-M. (2009). Measurements of unsaturated hydraulic conductivity functions of two fine-grained materials. Soils and Foundations, 49:2, p. 176-181.

Thornthwaite, C.W. (1948). An approach toward a rational classification of climate. Geographical Review, 38:1, p. 55-94.

Topp, G.C.; Davis, J.L. & Annan, A.P. (1980). Electromagnetic determination of soil water content: Measurement in coaxial transmission lines. Water Resources Res, 16:2, p. 574-582.

Toll, D. G. ; Lourenço, S.D.N. ; Mendes, J. ; Gallipoli, D. ; Evans, F.D. ; Augarde, C.E. ; Cui, Y.J. ; Tang, A.M. ; Rojas, J.C. ; Pagano, L. ; Mancuso, C.; Zingariello, C. & Tarantino, A. (2011). Soil suction monitoring for landslides and slopes, Quarterly Journal of Engineering Geology & Hydrogeology, 44:2 , p. 23-33.

Van Rooyen, M. & Winterkorn, H.F. (1957). Structural and Textural Influences on Thermal Conductivity of Soils. Highway Research Board Proceedings. v.39, pp.576-621.

Wilson, G.W.; Fredlund, D.G. & Barbour, S.L. (1997). The effect of soil suction on evaporative fluxes from soil surfaces. Canadian Geotechnical Journal, 34:1, p. 145–155.

Wolle, C.M. & Hachich, W. (1989). Rain-induced Landslides in South-eastern Brazil. In: Proceedings of 12th international conference soil mechanics and foundation engineering, v. 3, pp.1639–1644.

Xu, C.-Y. & Singh, V. P. (2001). Evaluation and generalization of temperature-based methods for calculating evaporation. Hydrol. Process., 15:2, p. 305–319.

Static Load Tests in an Instrumented Rock Socket Barrette Pile

M. Musarra, F. Massad

Abstract. The foundation for the new Petrobras headquarters building in Salvador, Bahia, northwest of Brazil, had barrette pile rock socketed units chosen as the best engineering solution, due to shallow top rock, given schedule and cost. Even though the soil strata was stiff to very stiff silt, the required design load was not able to be based on soil side resistance only, resulting in a rock socket design. A 300 kPa ultimate shear stress was assumed by the designers and static load tests were performed to verify this parameter. This paper evaluates the results obtained from the test without discussing the designer assumption. Rock socket shear stress verification was made possible by placing an expanded polystyrene block below the pile steel cage, eliminating any possible bottom resistance. Beyond the usual top instrumentation, electric retrievable extensometers were installed along the shaft to afford depth load transfer evaluation. This paper presents the results of the load tests as well as an application of analytical and semi-empirical methods available in the literature to prove their usefulness and effectiveness, revealing and confirming many aspects of field behavior.
Keywords: rock socket, static load tests, barrette pile, instrumentation.

1. Introduction

Based on geological profile and subsurface investigations, a high load foundation was designed for the new Petrobras headquarters building in Salvador, Bahia, by means of rock socketed barrette piles. The working load was set by the designer assuming 300 kPa of shear stress in the rock embedment, without any soil and tip contribution. This assumption complies with common design procedures, in which soil side and rock tip resistances are not considered to evaluate the safety factors. Also, those resistances could be currently considered in a less conservative approach. To verify the design assumptions two static load tests were performed in an instrumented pile through dial gauges and electric extensometers, described in detail hereafter.

The city of Salvador (in the Bahia State, Brazil) is located in the Salvador Terrace Belt, which is sectioned into two parts by the Iguatemi Fault. Most of the rock is granulite, occurring gneisses towards eastern-north from fault. The altitude at the jobsite area is 25 m above sea level, on average, and it is located where the top of the bedrock (see Fig. 1) rises sharply in a crossing lane, reaching up to 22 m above sea level. This geological profile reveals soft to sound granulite rocks (Barbosa *et. al*., 2005).

2. Materials and Methods

2.1. Site characterization

The site investigation involved 11 drilled borings in in which SPT blow counts were measured in soil strata and retrieval of rock cores samples were carried out, wherein *RQD* (rock quality designation) and recovery were determined. The locations of bore holes and pile test are shown in Fig. 2.

The closest borehole to test pile was SM-03, which was taken as a reference in evaluating load transfer along depth. The overburden was characterized by clayey silt with fine and medium sand, and even gravel, overlying sandy silt (residual soil). The layers are shown in Fig. 3, as well as the bedrock depth. The water table was found at a depth of 10.7 m.

Rock samples from depth spots were tested to provide unconfined compressive strength (q_u). The q_u values of all samples (see Fig. 4) had an average of 47 MPa. A range of 35-90 MPa was taken to comply with the *RDQ* determined in the SM-03 rock samples, with more than 50% located in socket depth.

2.2. Pile data

The pile had a rectangular section, 3.15 m x 0.80 m, 7.90 m perimeter, and was located next to the main building (see Fig. 2 for location). The excavation was made using a truck-mounted crane and clamshell bucket for overburden and hydromill to advance in the bedrock (see Fig. 5) using a bentonite mud for trench stabilization. The pile had a 9.76 m length in the soil and 1.54 m length in rock. Below the pile bottom an EPS (Expanded Polystyrene Styrofoam) block was positioned through a steel cage, with dimensions of 2.95 m x 0.68 m x 0.90 m (length, thickness, height). A

M. Musarra, M.S., Escolade Engenharia, Universidade de São Paulo, Layne Christensen Company - 6811 Ash Street, Frisco, TX 75034, United States. e-mail: marcello.musarra@layne.com, mussarra@usp.br.
F. Massad, Senior Professor, Escolade Engenharia, Universidade de São Paulo, Av. Prof. Luciano Gualberto, travessa 3, 380 05508-010, São Paulo, SP, Brazil. e-mail: faissal@usp.br.
Submitted on December 21, 2014; Final Acceptance on June 3, 2015; Discussion open until December 31, 2015.

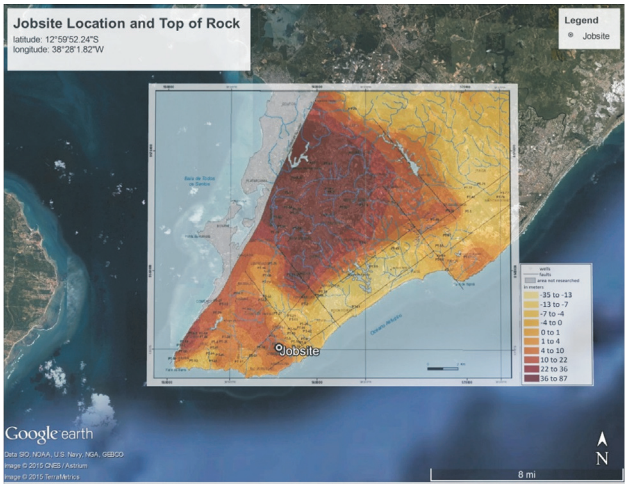

Figure 1 - Jobsite location and top of rock from sea level (after Barbosa *et. al.*, 2005).

chamfer was necessary to dovetail the shape of the rock surface due to the hydromill wheels geometry.

Even though the design assumption was clear, meant not overcoming 300 kPa for rock socket shear stress, it was decided to investigate further and be less conservative for test worthiness. Therefore, to maintain the 12 MN ultimate load for a rock socket 1.54 m long, instead of 5 m, a rock-shaft shear stress of 986 kPa was required.

Taking into account concrete resistance (f_{ck}) of 25 MPa, given by 6 axial compressive tests, the pile Young's Modulus (E) was estimated as 23.8 GPa, according to the Brazilian Standard ABNT (2002), *i.e.*:

$$E = 0.85 \cdot 5{,}600 \cdot \sqrt{f_{ck}} \tag{1}$$

2.3. Pile instrumentation

Four sensors or electric retrievable Geokon extensometers, Model A9, were placed inside a 50.8 mm (2") metallic pipe, casted in place inside the pile, with a top cap. They were fixed into the pipe walls with nitrogen gas pressure through expandable anchors. The sensors were interconnected by metallic galvanized rods; their positions are shown in Fig. 3. This type of instrumentation provides changes of length (shortening) between each sensor, allowing thus determining the strain. An incorrect fixation of sensor 3 occurred, which may have caused some sensor slip inside the pipe. Therefore, imperfections on segments 2-3 and 3-4 were solved by adding these lengths and eliminating sensor 3 referential readings. Lengths from 1 to 4 were added and became segment 1-4, corresponding to the soil length, approximately. This total measured shortening was correct, according to the Fugro In Situ, responsible for the installation of the sensors (Debas, 2014). The instrumentation position layout is displayed on Fig. 6.

The top displacement was measured by four dial gauges, with hundredths of mm precision. After the slow maintained load, another dial gauge was added to obtain a better average value.

3. The Static Pile Load Tests

The reaction system consisted of 8 rock socket tieback anchors, each connected to a hydraulic jack. The fixed length was designed using the Bustamante/Habib

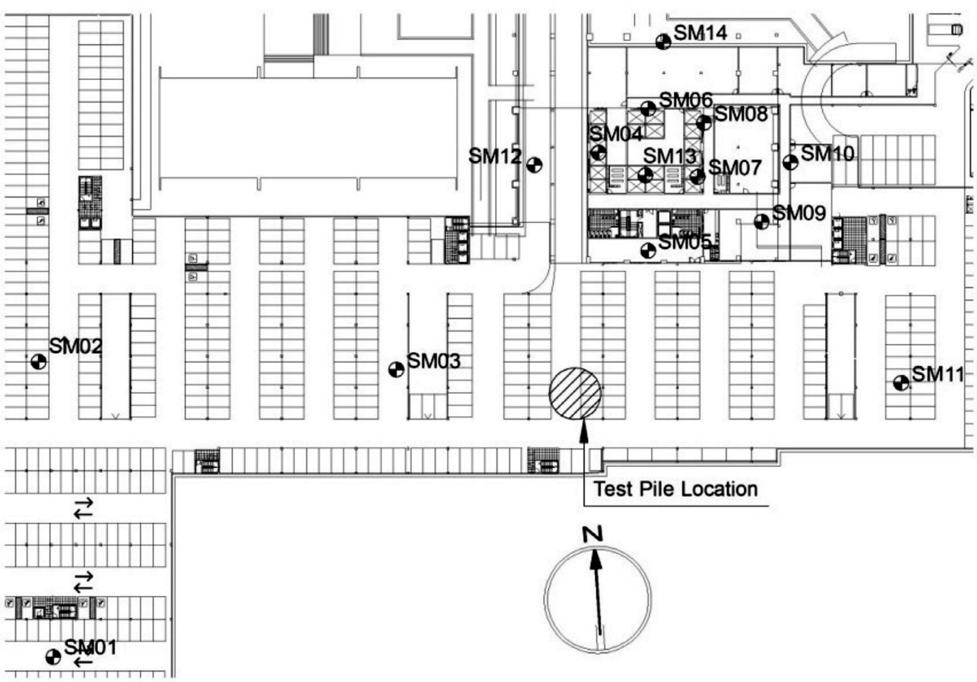

Figure 2 - Geotechnical investigation and pile test location.

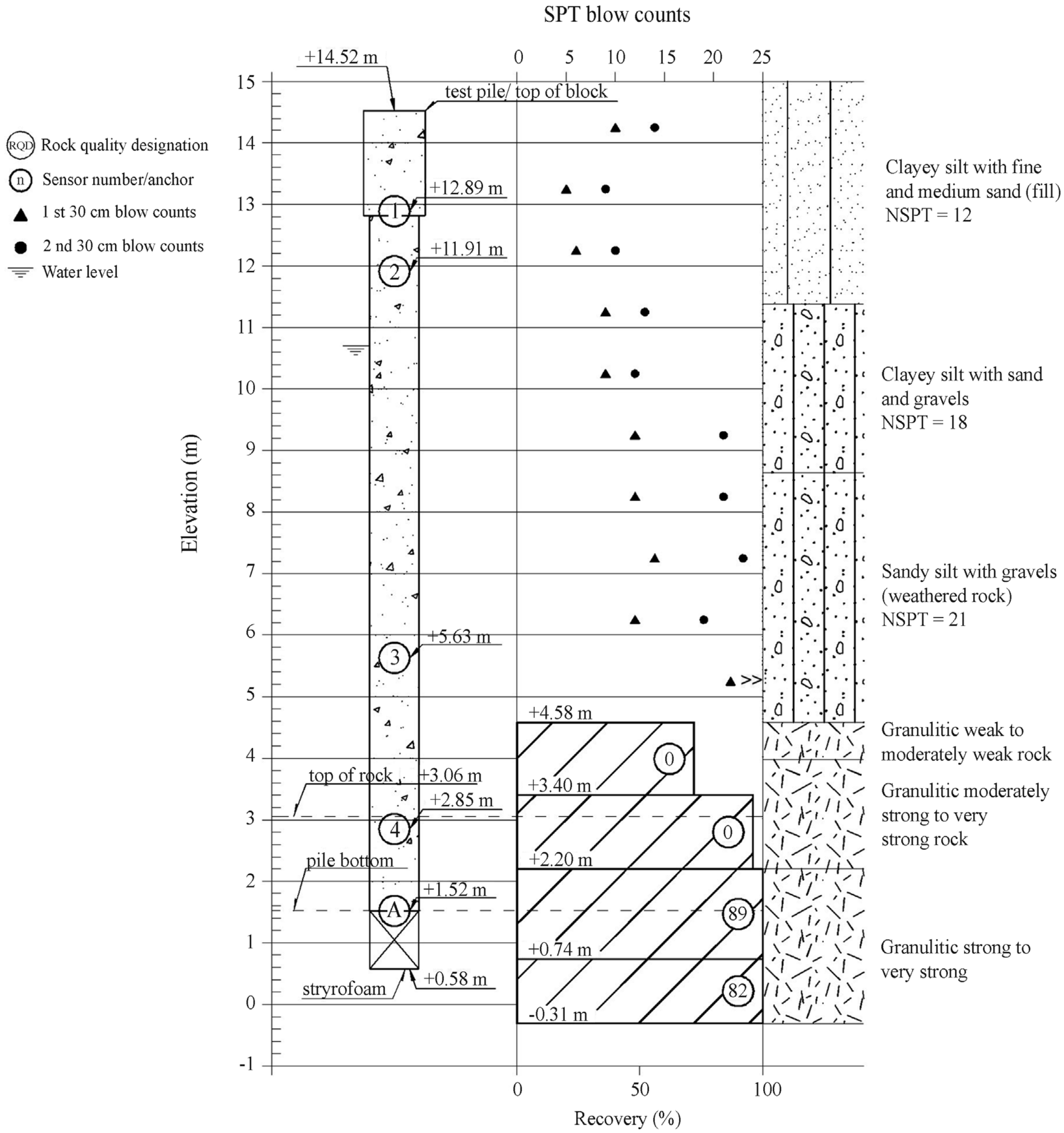

Figure 3 - Test pile cross section along with data from SM 03 borehole.

method (1989) *apud* Hachich *et al.* (1998). Eight CP 190 RB type tendons were used, 15.2 mm in diameter each, with a 1.72 MN ultimate load, through a 9 m anchor bulb length. Free length was 12 m and all anchors were inclined 15° from vertical axis. The setup is shown in Fig. 7.

The nearest horizontal distance between the anchor-bulb axis and vertical axis of the pile was 12 m x sin(15°) = 3.11 m, thus, 1.74 times the equivalent pile diameter, *i.e.*, 1.79 m. The minimum value according to Brazilian standards is 1.5 m, and thus acceptable. The anchor pre-stresses were performed with the hydraulic jacks, connected to four pumps. Each hydraulic jack/pump/jack set was calibrated by IPT (Instituto de Pesquisas Tecnológicas – São Paulo - Brazil).

The first static test was performed with slow maintained loading, according to Brazilian standards ABNT (2010) and ABNT (2006). Ten increments of 1.20 MN were applied and the readings of the dial gauges were taken at 2, 4, 8, 15, 30, 60, 120 minutes and so on until stabilization of the displacements. No failure has occurred. The maximum load (11.82 MN) was maintained for 12 h. The unloading proceeded in 5 stages, with a 2.40 MN decrease. Each load was maintained for 15 min.

Since there was no failure, a second test was done to attain either failure or reaction system limit, whichever could come first. The second static test was performed in the same pile, subsequently, with quick loading according to the same Brazilian standards. The instrumentation sensors were not reset.

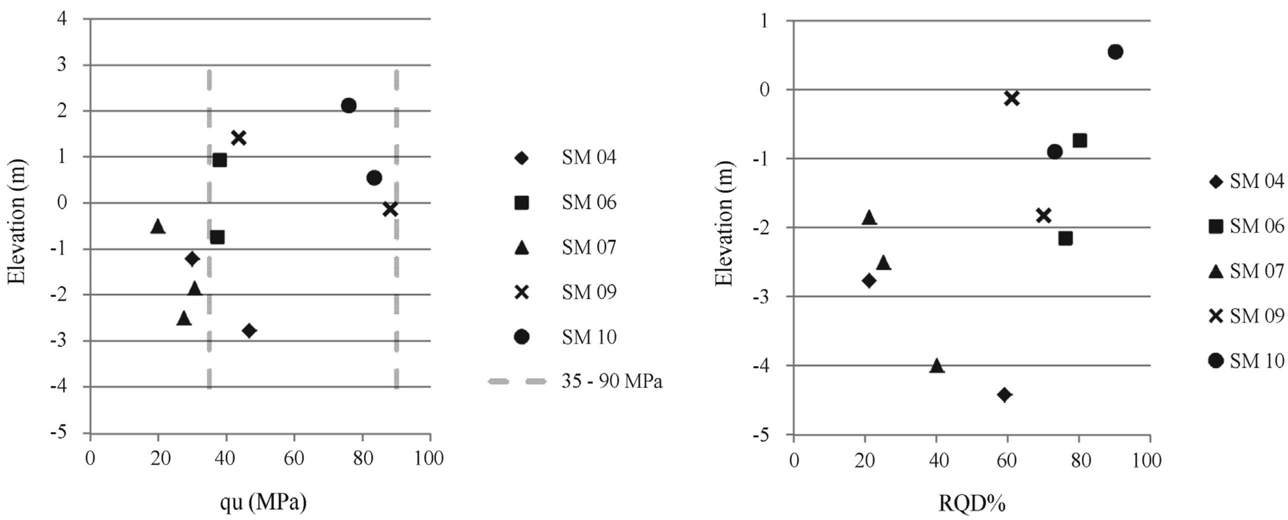

Figure 4 - Results of q_u and RQD vs. elevation.

The 1.20 MN increments were applied up to 12 MN and, afterwards, 0.6 MN increments up to the maximum reaction system (15 MN). Again, no failure occurred and increments were maintained for 10 minutes, independently of displacement stabilization.

4. Results and Interpretations

4.1. Load-displacement curves at the pile top

From top instrumentation results, load *x* displacement (P_o *x* y_o) curves were drawn for slow and quick tests, as illustrated in Figs. 8 (a) and (b). The maximum top displacement measured from the slow test was 2.81 mm, whereas 2.13 mm for quick test.

These values represented only 0.16% and 0.12%, respectively of the equivalent pile diameter. Furthermore, the maximum displacement measured in the slow test was 32% higher than in the quick test, indicating probable displacements of the rock mass fractures at the end of the slow test and prior to the reload. This phenomenon was studied in detail by Williams (1980), who performed laboratory tests on

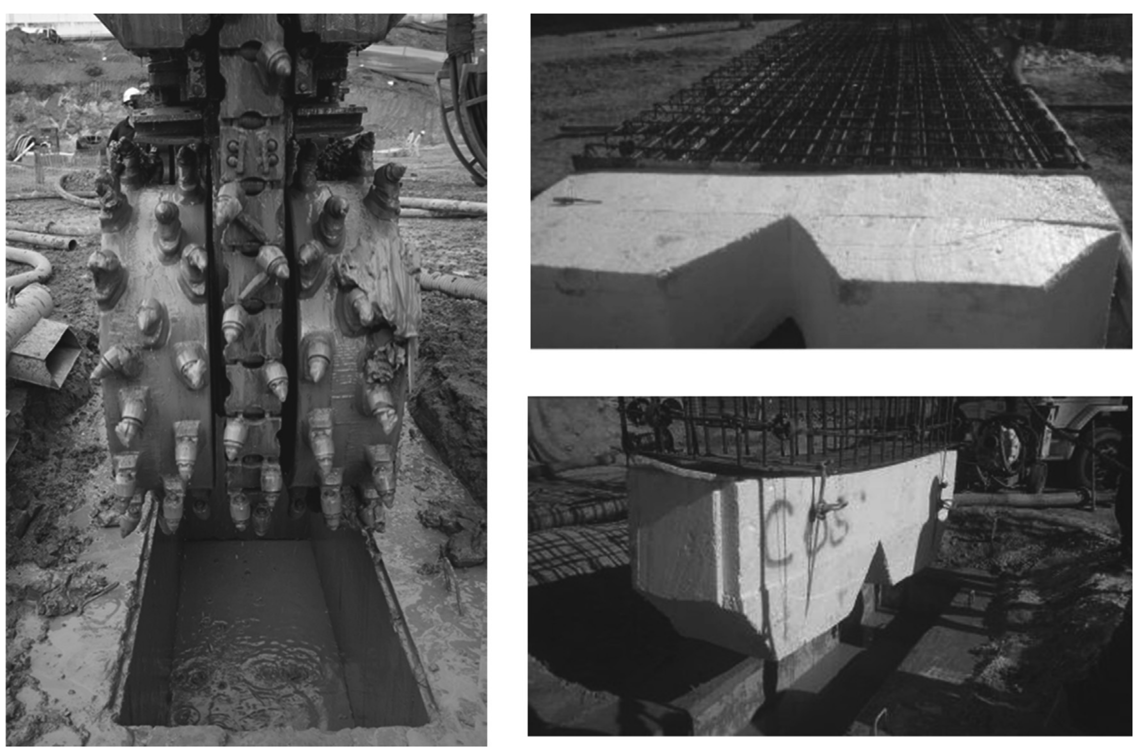

Figure 5 - Details of the hydromill trench cutter and EPS block below the steel cage.

concrete-rock joints, approaching it as rock-rock joints. The tests provided information regarding the relationship between shear stress, displacement and normal stress, in consequence, stiffness. As long as the normal stress developed on a concrete-rock joint is high, the slip finds more resistance to occur, increasing the skin friction. This normal stress development comes from either the Poisson effect or/and joint dilatation (as it needs to expand to slip). More detail of this phenomenon can be found in Carter & Kulhawy (1988) and Musarra (2014).

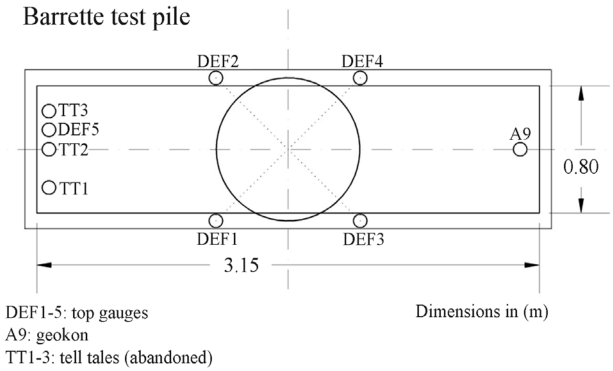

Figure 6 - Barrette test instrumentation layout.

4.2. Pile shortening and tip displacement. Determination of *E.S*

With the data given by the instrumentation, it was possible to obtain the shortening of the pile (Δe) along the soil and rock lengths (1-4 and 4-a segments, respectively), and the displacement of the tip (y_{tip}). Both plots, pile shortening (Δe) and tip displacements (y_{tip}) versus top load (P_o), are shown in Fig. 9.

Figure 7 - Overview of the setup for the static load tests in rock socketed barrette pile.

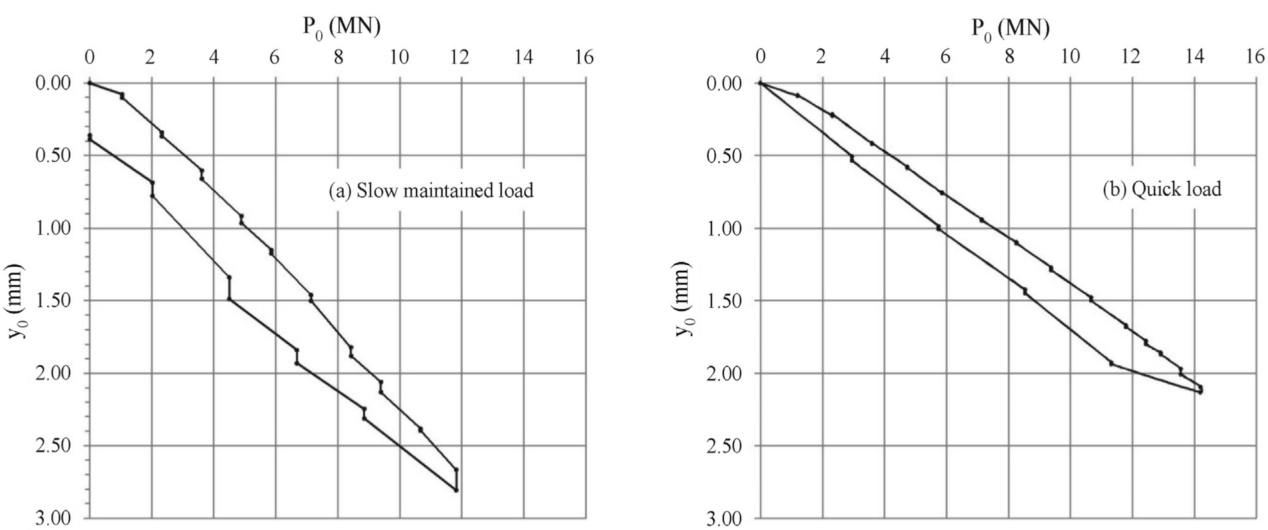

Figure 8 - Top load x displacement curves for slow load (a) and quick load (b).

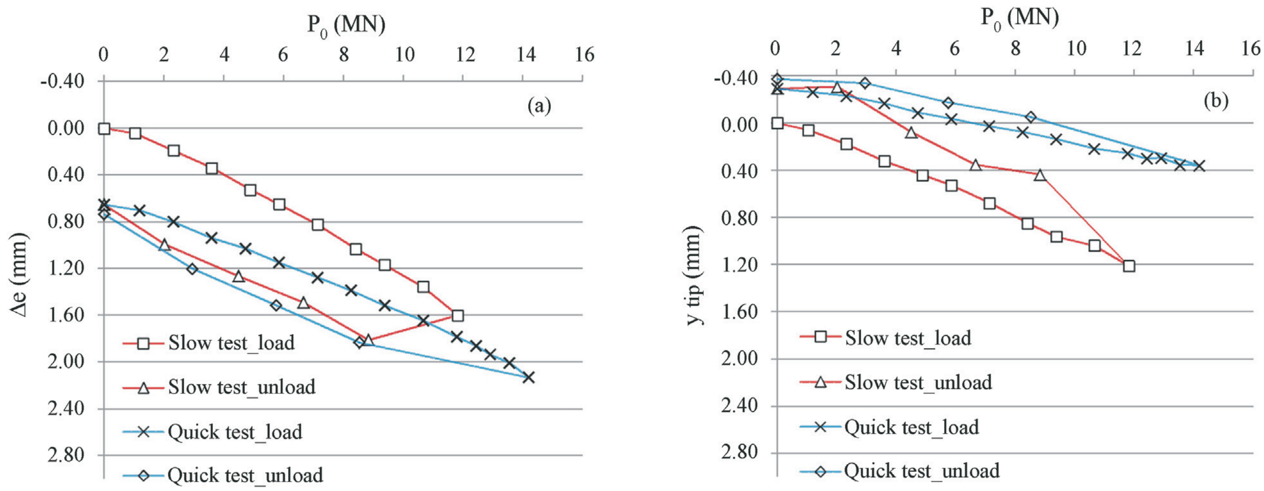

Figure 9 - Shortenings of segment 1-4 and fictitious tip displacements for the slow loading test.

Two behaviors could be pointed out. First, the shape of the shortening curves for the slow and quick loads are quite different, even though the maximum values are almost the same (rounding 1.60 mm), which could suggest distinct pile behavior taking place by influence of the joint concrete-rock. Second, after unloading was performed in the slow test, a negative tip displacement occurred, indicating that a pile shortening was trapped due to the appearance of a residual load, detailed afterward herein.

The analysis of the top load x strain curves in an instrumented pile can give useful information regarding the resistances of the 1-4 and 4-a segments. In this case, when the subsequent measured pair points in a segment seems to align straight, it is known that the ultimate resistance was reached in that segment and the product *E.S* can be calculated as shown on Figs. 10 (a) and (b). As the cross sectional area (*S*) of the pile is known its elastic modulus (*E*) can be estimated. Strain values were calculated by dividing shortenings by segment lengths.

In fact, reporting to Fig. 10 (a), for a top load $P_o = 10.7$ MN and microstrain of rougly 120 (*i.e.*, a strain of ~120.10^{-6}), the total side friction reached its maximum value A_{lr}^{m} above mid height of segment 1-4. This means that the following relation holds (Massad, 2011):

$$P_o = A_{lr}^{m} + E \cdot S \cdot \mu\varepsilon \quad \text{for} \quad \varepsilon \geq 120.10^{-6} \tag{2}$$

In other words, for $\varepsilon \geq 120.10^{-6}$ the linear relationship between P_o and microstrain has an inclination equals to *E.S*. The same reasoning may be applied to the quick load, Fig. 10 (b). This inclination refers only to the last two points, highlighted in Figs. 10 (a) and 10 (b), even though some additional pair points (with higher loads and displacements) would be needed to confirm the value of *E.S*.

From the product *E.S* found in slow and quick tests, 53 and 58 GN, respectively, elastic modulus values of 21 GPa and 23 GPa were calculated. The difference of almost 10% could be explained by the "Rüsch effect" (Rüsch, 1960), *i.e.*, loading velocity and creep effect. These figures are in close agreement with the results obtained in the tests over the concrete samples, as described before, and with the Tangent Modulus Method (Fellenius, 1989) evaluation, as presented in Figs. 11 (a) and (b). These plots relate the tangent modulus with the deformation of the segments 1-4 (along soil length) and 4-a (along socket length). As can be seen, the curves tend asymptotically to the same figures presented above. Furthermore, Fig. 11 (b) (quick test) displays that the shaft-soil system would have more resistance to develop due to the distance between the 23 GPa line and the asymptote. This confirm that higher loads and displacements, as stated above, could lead to mobilized loads closer to the ultimate soil skin friction.

4.3. Load distribution along the shaft and the estimation of the unit shear stresses

The load distribution along the shaft was calculated through the elasticity theory considering: a) the deformations of segments 1-4 and 4-a obtained from the extensometers; and b) a cross sectional area (*S*) equals to 2.52 m^2. Figures 12 and 13 show the results for both slow and quick static load tests. From these figures it follows that the ultimate shaft resistance (unit shear stress) was reached along the soil, but not on the rock embedment. The presence of residual loads at the end of the slow test and in the beginning of the quick load test (Fig. 13) can also be seen.

To evaluate the residual load generated at the end of the static loading, a pile model was created, represented in Fig. 14, establishing the top of rock socket as a "fictitious" tip, with a resistance (q_p) estimated by converting the socket mobilized side friction (f_s) as follows:

$$f_s\,(\text{rock}) = q_p \cdot \frac{S}{p \cdot L} \tag{3}$$

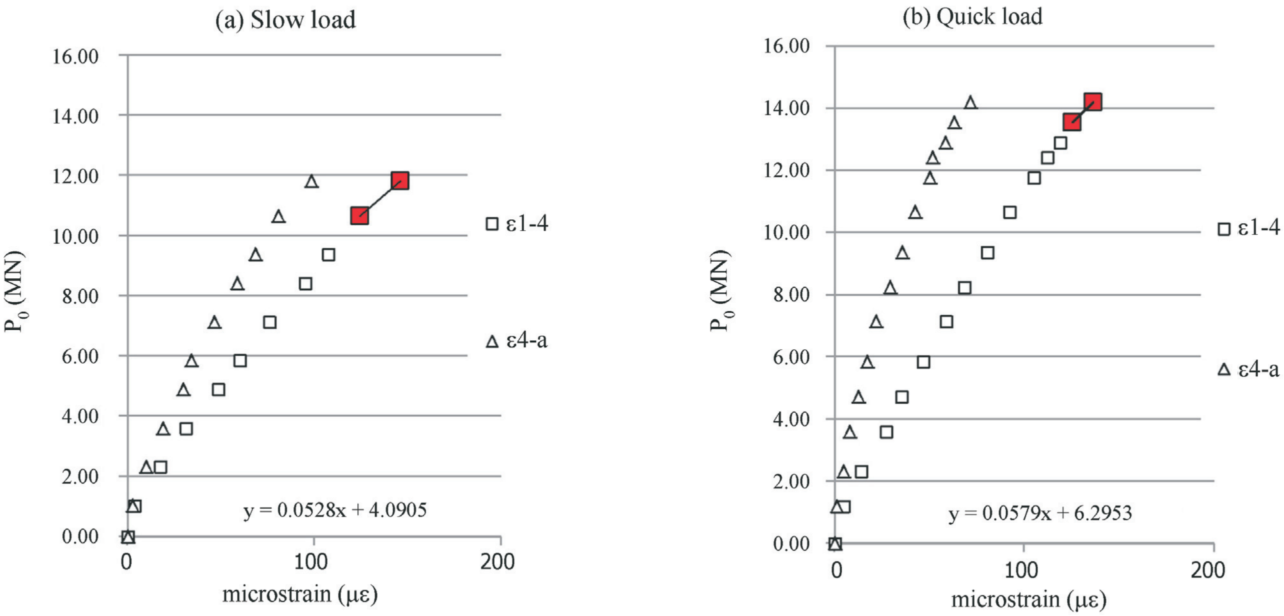

Figure 10 - Estimation of pile stiffness (*E.S*) by instrumentation from slow (a) and quick (b) load tests.

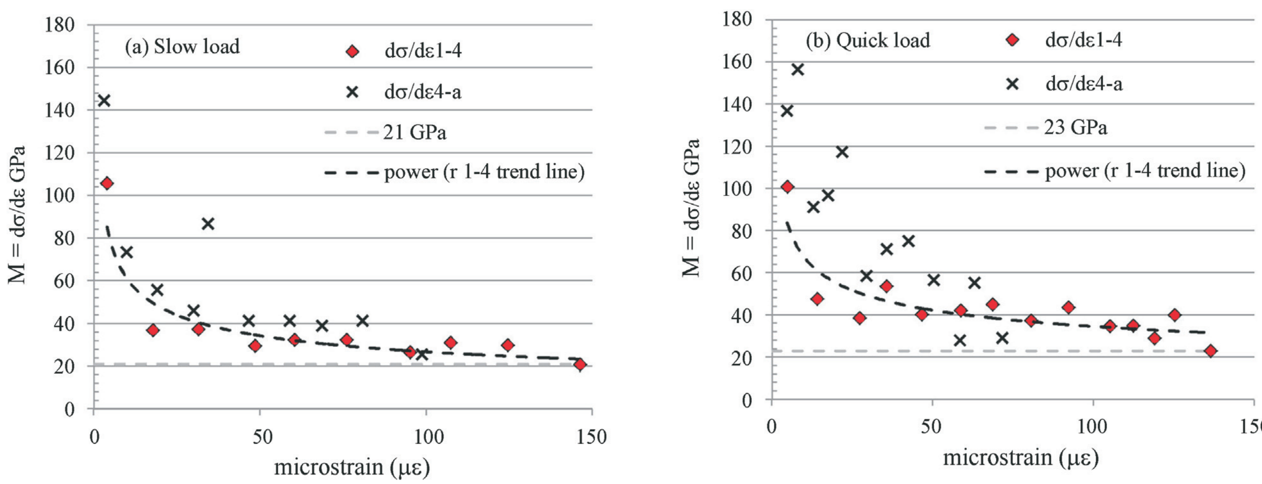

Figure 11 - Tangent modulus of the concrete as a function of strain for slow (a) and quick (b) tests.

where S is the pile cross sectional area, p its perimeter and L the length of rock socket (the embedment height).

Graphs displaying these data are shown in Figs. 15 (a) (slow test) and 15 (c) (quick test) that relate the unit shear stress or skin friction (f_s) in the soil interface, as a function of the displacement at the pile mid-height (y_o - $\Delta e_{1\text{-}4}/2$). Similarly, Figs. 15 (b) (slow test) and 15 (d) (quick test) relate the “fictitious tip” reaction (q_p) with its displacement (y_{tip}).

For the slow load test, it can be seen that the unit shear stress reached its ultimate value of 53 kPa in the soil interface (f_{su}), while for the quick load test this value was at least 41 kPa. On the other hand, the maximum q_p values of Figs. 15 (b) and 15 (d) are, in reality, the unit shear stress (f_s) in the rock interface (embedment). Using Eq. 3 the figures of 637 kPa (slow test) and 910 kPa (quick test) were found for f_s in the rock interface, with no failure. These figures are up to 3 times 300 kPa, assumed in the design and, according to the quick test, close to the new required value of 986 kPa, disregarding tip and soil resistances. Table 1 summarizes these results, as total ultimate A_{lr} (soil) or mobilized A_l (rock) resistances and load transferred to the rock socket embedment as a percentage of the total applied load (P_{omax}). It may also be concluded that the soil contribution to the shaft resistance amounted 100% - 65% = 35% in the slow test and little more than 100% - 75% = 25% in the quick test.

It is possible to validate the values of f_{su} on soil interface, shown in Table 1, using empirical methods based on

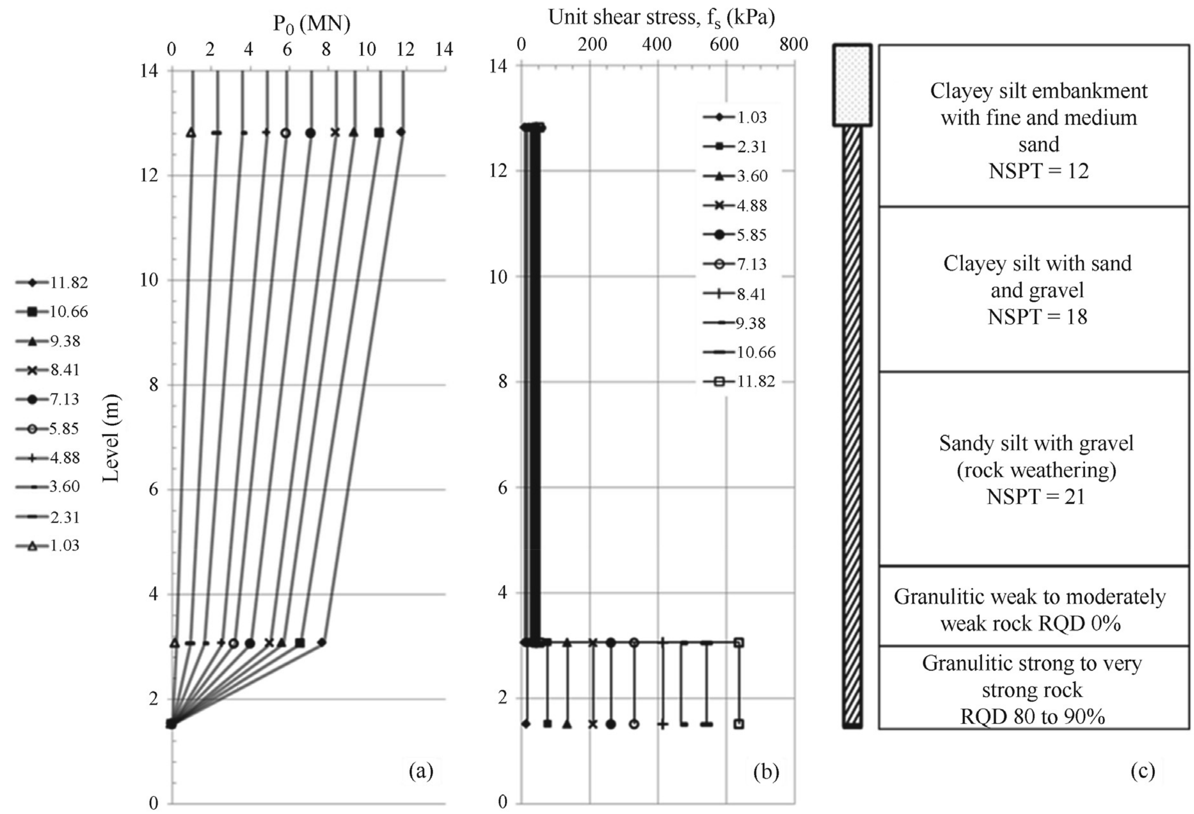

Figure 12 - Load distribution along the shaft for slow load test.

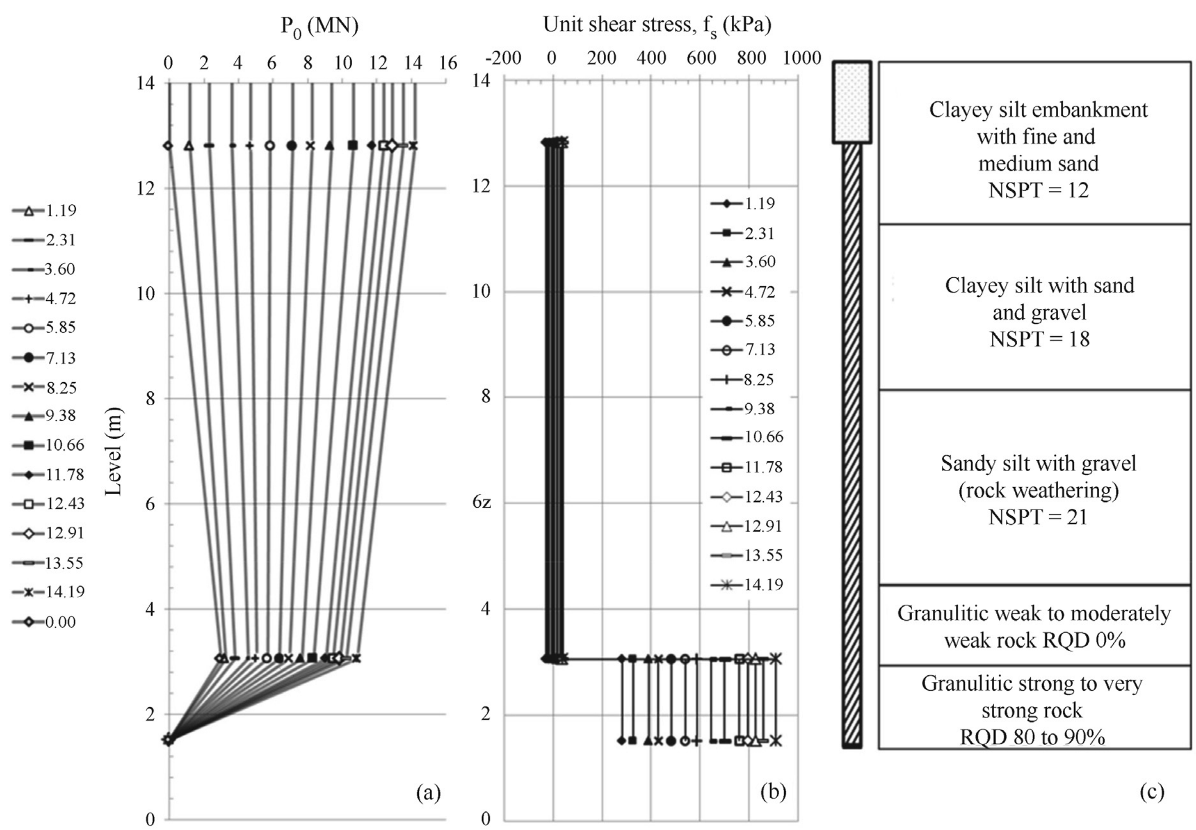

Figure 13 - Load distribution along the shaft for the quick load.

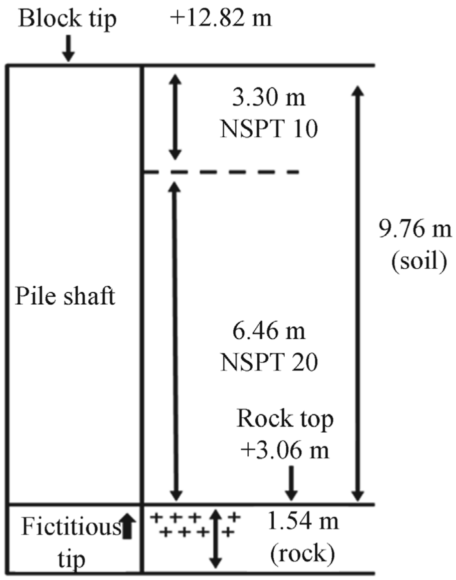

Figure 14 - Fictitious tip model.

SPT (N) blow counts given by boring SM-03 (Fig. 3), as follows:

a) Aoki-Velloso's Method (Aoki & Velloso, 1975)

- Parameters: sandy clayey silt, $K = 450$ kPa, $\alpha = 2.8\%$, average $N = 17$ and $F_2 = 3.5$

$$f_{su}\,(\text{soil}) = \alpha \cdot N \cdot \frac{K}{F_2} = 61\,\text{kPa} \tag{4-a}$$

b) Décourt-Quaresmas Method (Décourt & Quaresma, 1978) and Décourt (1998)

- Parameters: average $N = 17$, β equal 0.60

$$f_{su}\,(\text{soil}) = \beta \cdot 10 \cdot \left(\frac{N}{3} + 1\right) = 40\,\text{kPa} \tag{4-b}$$

Once again, is noticeable the presence of a residual load before starting to load the pile again (before quick test), as well as in the completed unloaded condition (Figs. 15c and 15d).

As far as the f_{su} on the rock interface, the following relationship was applied:

$$\frac{f_{su}}{p_a}(\text{rock}) = C \cdot \left(\frac{q_u}{p_a}\right)^n \tag{5}$$

where p_a is the atmospheric pressure and C varies between 0.6 to 1.2 (see Musarra, 2014).

Without being extremely conservative, a C average of 1.0, which coincidentally corresponds to the proposition of Prakoso (2002), was adopted. Equation 5 and the q_u range provided by Fig. 4 lead to f_{su} (rock) varying from 1,900 kPa to 3,000 kPa, with an average of 2,200 kPa. These round numbers are greater than the f_s (rock) as shown in Table 1, *i.e.*, the rock in the embedment did not collapse, as mentioned before.

4.4. Load x displacement calculated by Massad's Method: validation of the analysis

a) Massads Mathematical Method

A method to predict single pile performance under vertical loading, proposed by Massad (1995 and 2001), was employed to validate the results obtained so far by interpreting the instrumentation (sensors of Geokon extensometer type) along the shaft. The validation was carried out, as shown hereafter, working with the pile top displacement measured by four dial gauges, therefore in an independent way and free from the incorrect fixation of sensor 3, as previously mentioned.

Herein, one can find a brief description of method; more detailed information can be found in the given references. The method includes many aspects of load transfer phenomena, like the pile compressibility, progressive failure and the residual stresses due to driving or subsequent loadings. The solutions are analytical, in closed form, and were derived using as load transfer functions the modified Cambefort's Laws (Massad, 1995 and Cambefort, 1964), comprising the current knowledge about the shaft and tip displacements, needed to mobilize the full resistances. These modified laws are represented in Figs. 16 and 17. They may be applied to bored, jacked or driven piles; first or subsequent loading-unloading cycles. The soil is supposed to be homogeneous with depth, along the pile shaft. A coefficient that measures the relative stiffness of the pile-soil (shaft) system was introduced and defined as follows:

$$k = \frac{A_{lr}}{K_r y_l} \tag{6}$$

with:

$$K_r = \frac{ES}{h} \tag{7}$$

Table 1 - Summary of results.

Loading test	P_{omax} (kN)	f_{su} (soil) (kPa)	f_s (rock) (kPa)	q_p (**) (kPa)	A_{lr} (soil) (kN)	A_l (rock) (kN)	A_l (rock)/P_{omax}
Slow	11837	53 (*)	637	3075	4087 (*)	7750	65%
Quick	14231	> 41	910	4400	> 3160	11070	< 75%

Notes: (*) Ultimate values (**) Fictitious tip (See appended list of symbols).

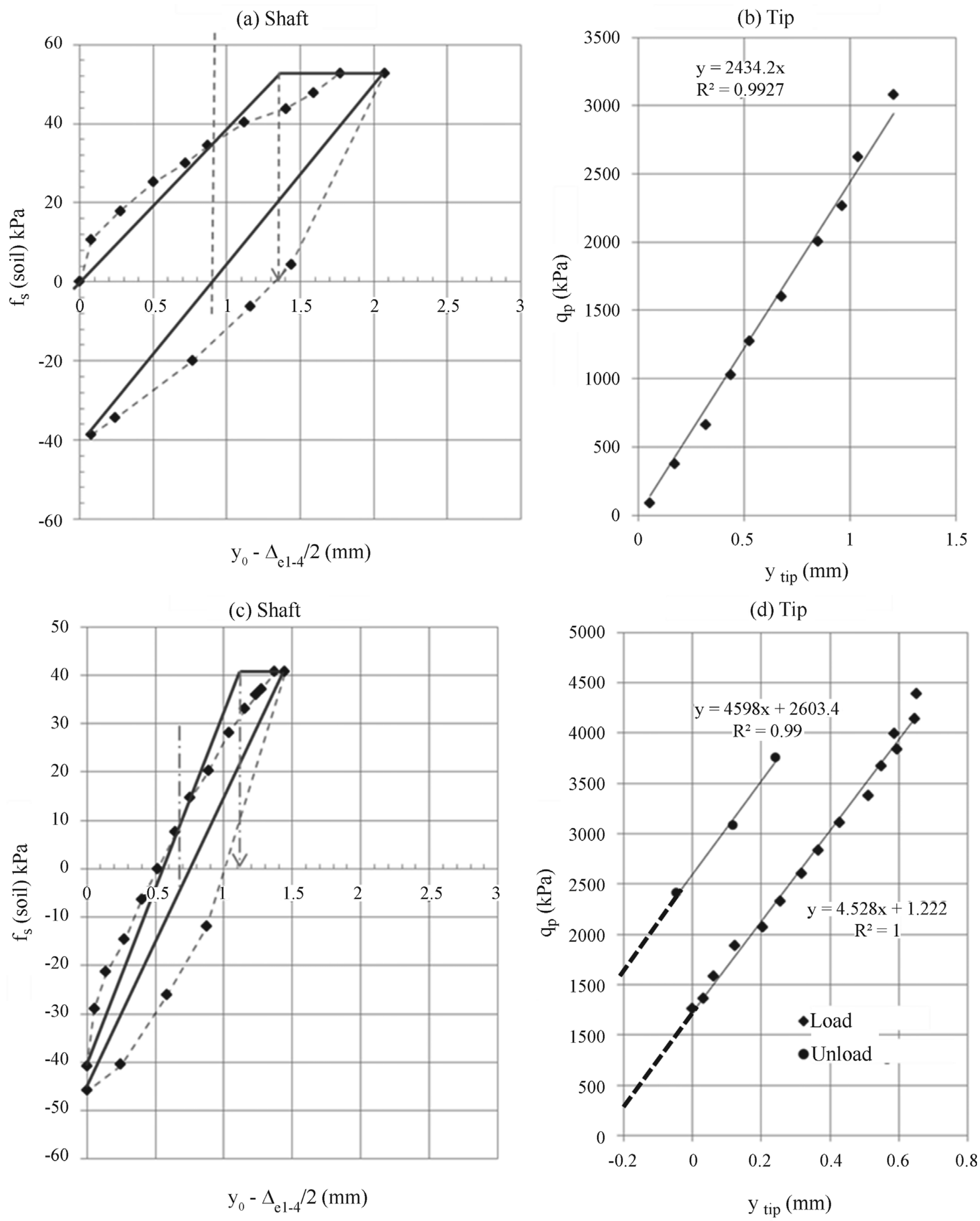

Figure 15 - *fs* and *qp* as a function of displacements: slow test (a, b) and quick (c, d) test.

where A_{lr} is the ultimate shaft load; y_1, the pile displacement, of the order of a few millimeters, required to mobilize full shaft resistance (see Fig. 16); D and h are the diameter and height of the pile; B is a Cambefort parameter; K_r is the pile stiffness; E, the modulus of elasticity of the pile material and S its cross sectional area.

The model gave a further insight on pile behavior and led to a new pile classification, with respect to the k values: “short” or rigid ($k \leq 2$); intermediate ($2 \leq k \leq 8$); and “long” or compressible ($k \geq 8$).

All Figs. 16, 17, 18 and 19 can be found in Massad (1995 and 2001).

The residual stresses can be dealt with a magnifier factor (μ):

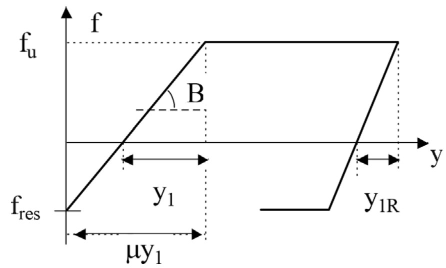

Figure 16 - Modified 1st Cambefort's Law.

$$\mu = 1 + \frac{P_h}{A_{lr}} \tag{8}$$

where P_h is the residual toe load, which is in equilibrium with the residual negative shaft resistance, supposed to be constant with depth. For a first loading of a bored pile, $P_h = 0$, then $\mu = 1$. Otherwise, as $P_h \leq A_{lr}$, it follows that $\mu \leq 2$. In general, this factor, when greater than 1, is upper bounded by the smaller value between 2 and Q_{pr}/A_{lr}, where $Q_{pr} = R_p.S$ is the toe load at failure (see also Fig. 17). Note that the maximum and the residual unit shaft resistances (f_u and f_{res}) are supposed to be constant along the pile shaft. One advantage of using μ is that it allows taking the residual loads as shaft loads in the model.

Reporting to Fig. 18, the load (P_o)-settlement (y_o) curve at pile top may be expressed by the following equations (see Massad, 1995):

- range 0-3 (pseudo elastic)

$$P_o = \mu \cdot A_{lr} \cdot \frac{\beta'_3}{z} \cdot \frac{y_o}{\mu y_l} \tag{9}$$

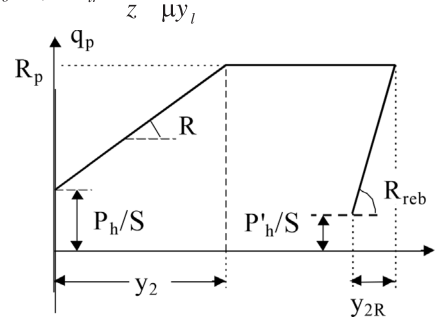

Figure 17 - Modified 2nd Cambefort's Law.

- range 3-4 (progressive mobilization of shaft resistance, from top to bottom)

$$P_o = \mu \cdot A_{lr} \cdot \frac{h - h'}{h} + \frac{\mu \cdot A_{lr}}{z} \cdot \beta' \tag{10-a}$$

$$\frac{y_o}{\mu \cdot y_l} = \left[1 - \frac{(\beta')^2}{2}\right] + \frac{k}{2} \cdot \left(\frac{P_o}{\mu \cdot A_{lr}}\right) \tag{10-b}$$

- range 4-5 (free development of tip resistance)

$$\frac{P_{o\max} - P_o - \mu \cdot A_{lr}}{y_{o\max} - y_o - \dfrac{\mu \cdot A_{lr}}{2K_r}} = \frac{1}{\dfrac{1}{RS} + \dfrac{1}{K_r}} \tag{11}$$

The coefficient β' of Eqs. 10-a and 10-b depends on the characteristics of the soil-pile system and is given by:

$$\beta' = \frac{\tanh\left(\dfrac{h'}{h \cdot z}\right) + \lambda}{1 + \lambda \cdot \tanh\left(\dfrac{h'}{h \cdot z}\right)} \tag{12}$$

with $z = \sqrt{k}$ and $\lambda = \dfrac{RS/K_r}{z}$

where λ is the relative stiffness of the pile-soil (shaft and toe) system (Massad, 1995) and h' indicates the progressive mobilization of shaft resistance with depth. Reporting to Figs. 18 and 19, $h' = 0$ and $h' = h$ correspond to points 3 and 4, respectively. In point 3 $\beta' = \beta'_3$.

Equations 9, 10 and 11 also apply to the unloading ranges 6-7, 7-8, and 8-9 (Fig. 18): it is sufficient to use the appropriate Cambefort's parameters for rebound, as shown in Figs. 16 and 17; moreover, if the loading stage ends further than point 4 (full mobilization of shaft friction), $\mu = 2$ at $P_o = P_{omax}$ (Massad, 1995).

b) Comparison between the measured and the calculated *Po* x *yo* curves

Table 2 summarizes the pile characteristics. The full lines presented in Fig. 15 stand for the modified Cambeforts Laws, whose parameters are shown in Table 3.

To apply the Massads Method, the intermediate parameters were determined using Eqs. 6, 7, 8 and 12, as pre-

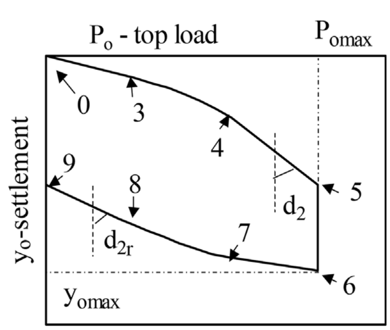

Figure 18 - Theoretical Load-settlement curve.

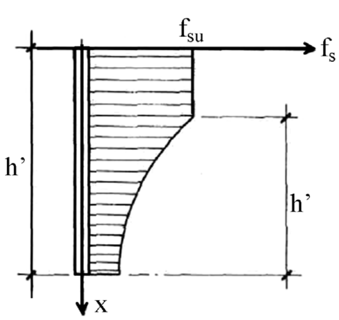

Figure 19 - f_s mobilization, range 3-4.

sented in Table 4. As $k < 2$ and $\lambda > 1.5$, the pile behaved as a rigid pile with a great influence of the "fictitious tip". Furthermore, the values of μ were high, reaching the upper limit of 2 at the end of unloading in the quick test, because $f_{res} \cong -f_{su}$ in the soil strata, confirming the results shown in Fig. 15 (c).

To draw the P_o x y_o theoretical curves, Tables 5 to 8 were prepared for the slow and the quick tests, using Eqs. 9, 10-a and 10-b. Looking at Figs. 15 (a) and 15 (c), it is possible to see that the pseudo elastic range of the First Cambefort Law does not pass through the origin. Actually, there is an intercept of roughly 10 kPa, which corresponds to an initial shaft load of 10 kPa x 9.76 x 7.90 = 800 kN. Therefore, the values previously computed P_o were adjusted with the addition of the number 800 kN.

Figures 20 and 21 show the results obtained. It can be seen that there is agreement between both curves, drawn independently, *i.e.*, the measured (with dial gauges) and the calculated (based on the plots of Fig. 15 that were established using data from the electric retrievable extensometers). These results validate the analysis done so far with the electric retrievable extensometers.

5. Analysis of the Stiffness of the Rock Embedment

Carter & Kulhawy (1988) presented an analytical closed-form solution for pile stiffness, *i.e.*, the relation between the load and the displacement at the top of piles embedded in rock. The authors developed equations to evaluate cases of complete (tip and side resistances) or partial

Table 2 - Pile test characteristics.

Loading test	Dimensions (m)	Perimeter (m)	S (m^2)	h (m)	E (GPa)	K_r (kN/mm)
Slow	3.10 x 0.80	7.90	2.52	9.76	21	5422
Quick					23	5939

Table 3 - Cambefort's parameters for the pile test.

Loading test	Shaft resistance (1st Cambefort Law)				Fictitious tip reaction (2nd Cambefort Law)		
	f_{res} (kPa)	f_u (kPa)	y_1 (mm)	y_{1R} (mm)	P_{lt}/S (kPa)	R (kPa/mm)	R_{reb} (kPa/mm)
Slow	0	53	1.35	1.15	0	2434	4528
Quick	-46	> 41	0.55	0.69	3035	4528	4598

Table 4 - Intermediate results.

Loading test	A_{lr} (kN)	Loading				Unloading (rebound)			
		k	λ	β'_3	μ	k	λ	β'_3	μ
Slow	53x9.76x7.9 = 4086	0.56	1.51	1.1	1.0	0.66	2.60	1.19	1.77
Quick	> 41x9.76x7.9 = 3161	0.97	1.95	1.09	1.77	0.77	2.22	1.14	2.00

Table 5 - P_o x y_o values from Massad's Model - slow loading test.

P_o (kN)	y_o (mm)	h' (m)	$z.h'/h$	$tgh(z.h'/h)$	β'	P_o (adjusted) (kN)
0	0	-	-	-	-	800
5995	1.35	9.8	0.75	0.63	1.10	6795
7448	1.71	7.0	0.54	0.49	1.15	8248
8612	2.03	5.0	0.38	0.37	1.21	9412
9577	2.33	3.5	0.27	0.26	1.27	10377
10657	2.67	2.0	0.15	0.15	1.35	11457
11132	2.83	1.4	0.11	0.11	1.40	11932
12358	3.25	0.0	0.00	0.00	1.51	13158

Table 6 - P_o x y_o values from Massad's Model - slow unloading test.

P_o (kN)	y_o (mm)	$P_{omax} - P_o$ (kN)	$y_{omax} - y_o$ (mm)	h' (m)	*z.h'/h*	*tgh(z.h'/h)*	β'
11932	2.83	0	-	-	-	-	-
4862	2.16	7070	1.35	-	-	-	2.60
3325	1.48	8606	1.71	6.0	0.50	0.46	1.39
1476	0.81	10456	2.16	4.0	0.33	0.32	1.59
58	0.56	11874	2.52	2.8	0.23	0.23	1.77

Table 7 - P_o x y_o values from Massad's Model - quick loading test.

P_o (kN)	y_o (mm)	h' (m)	*z.h'/h*	*tgh(z.h'/h)*	β'	P_o (adjusted) (kN)
0	-	-	-	-	-	800
6893	1.08	9.8	0.98	0.75	1.09	7693
8848	1.42	7.3	0.74	0.63	1.16	9648
11002	1.86	5.0	0.50	0.47	1.27	11802
12660	2.23	3.5	0.35	0.34	1.38	13460
14242	2.61	2.3	0.23	0.23	1.51	15042
18472	3.66	0.0	0.00	0.00	1.95	19272

Table 8 - P_o x y_o values from Massad's Model - quick unloading test.

P_o (kN)	y_o (mm)	$P_{omax} - P_o$ (kN)	$y_{omax} - y_o$ (mm)	h' (m)	*z.h'/h*	*tgh(z.h'/h)*	β'
15042	2.61	-	0	-	-	-	-
9095	1.61	1.00	5947	-	-	-	1.14
4639	0.82	1.78	10403	7.3	0.66	0.58	1.23
1997	0.26	2.34	13045	4.9	0.44	0.41	1.37
146	-0.16	2.77	14896	3.5	0.31	0.30	1.51

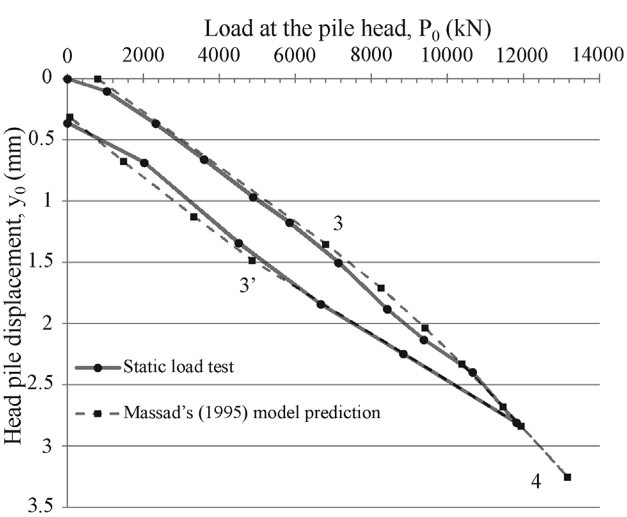

Figure 20 - Validation of instrumentation analysis - slow test.

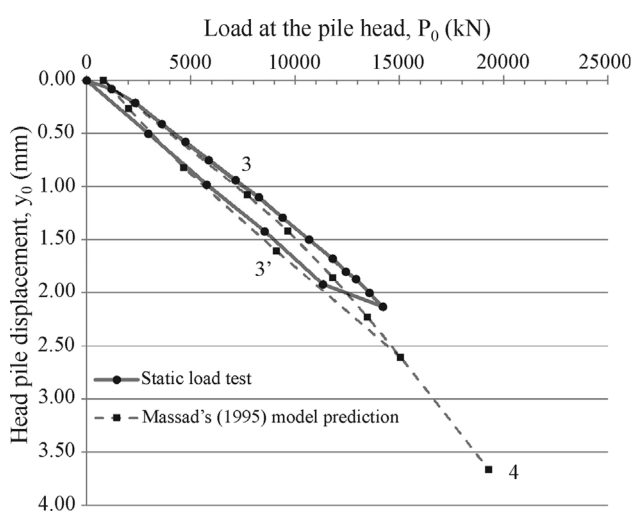

Figure 21 - Validation of instrumentation analysis - quick test.

embedment (side only), with development based on the prior work of Randolph & Wroth (1978).

For the latter case, concerning the barrette rock socket pile test, these authors came up with the following expression for the pile stiffness in the elastic range of the load-displacement relation:

$$RS = \frac{\pi \cdot E_r \cdot L}{(1+\nu_r)\zeta} \tag{13}$$

where E_r and ν_r are the Elasticity Modulus an the Poissons ratio of the rock mass and:

$$\zeta = \ln\left(5 \cdot (1-\nu_r) \cdot \frac{L}{D}\right) \tag{14}$$

It is worth noting that the term inside the brackets of this equation is the ratio between the influence radius of the pile to the pile radius.

The values of Cambeforts parameter R of Fig. 17, related to the embedment of the barrette pile test, can be obtained from the data of Figs. 15 (b) and 15 (d). They are presented in Table 9 showing also the estimated E_r values, using Eqs. 13 and 14.

The difference between the E_r values in slow and quick tests could be explained by the volume variation of rock mass, with the closing of the joints (fractures), as mentioned above. The E_r of the slow test is about 53% of the E_r of the quick test. This may be validated by the correlations presented in the literature that for RQD in the range of 80 to 90%, as displayed by the SM3-03 boring (see Fig. 3), this relation averages 50%.

Furthermore, Rowe & Armitage (1987) proposed the following equation to estimate E_r (in MPa) based only on q_u (in MPa), *i.e.*, the unconfined compressive strength:

$$E_r = 215 \cdot \sqrt{q_u} \tag{15}$$

The data from Fig. 4 lead to E_r varying in the range of 1,250 MPa to 2,040 MPa, with an average of 1,500 MPa. These numbers validate the E_r of the slow test (see Table 9).

6. Conclusions

The static load tests presented in this paper are believed to be some of the first performed in an instrumented rock socketed barrette pile in Brazil. The tests were carried out successfully; both in regard to measurements made in the top of the pile as well as by instrumentation along its shaft, where side mobilized resistances were calculated.

Table 9 - Modulus of Elasticity of the rock mass.

Loading test	R (kPa/mm)	$R.S$ (kN/mm)	E_r (MPa)
Slow	2434 (load)	6134	1879
Quick	4528 (load)	11411	3496
	4598 (unload)	11587	3550

The probable fixation error in one sensor did not affect the overall interpretation of the data. The results also displayed a different rock mass behavior in quick loading, followed by prior slow loading, probably due to residual loads and the irreversible closure of fractures. In this context, the rock mass elastic modulus increased from 1,900 MPa (slow test) to 3,500 MPa (quick test), in round numbers.

The unit shear stress in rock socket increased up to 900 kPa, three times the value assumed in the first design (300 kPa), but much smaller than the estimated value at failure of 2,200 kPa, based on average uniaxial compressive strength of the rock. These results were used for design parameters review and, therefore, shorter socket lengths have been adopted than assumed initially. The soil resistance contribution was 35% in the slow test and little more than 25% in the quick test. These figures were, nevertheless, in accordance with estimations of the ultimate unit shear stress of the soil strata by the Aoki-Velloso and Décourt-Quaresma methods.

Finally, the use of analytical methods available in the literature proved to be useful and effective, confirming in many aspects the instrumentation results from the electric retrievable extensometers, validated by the measured load-settlement curves, given by the dial gauges.

Acknowledgments

The authors acknowledges the support given by EPUSP (Polytechnic School, University of São Paulo) and would like to thank the companies Costa Fortuna Engineering and Fugro In Situ for their assistance and for releasing the data for this work.

References

ABNT (2002). Concrete Structures Design – Procedures - NBR 6118. Brazilian Association of Technical Standards, Brazil, 154 p (In Portuguese).

ABNT (2006). Piles-Static Load Test-Performance Method - NBR 12131. Brazilian Association of Technical Standards, Brazil, 8 p (In Portuguese).

ABNT (2010). Foundation Design and Performance - NBR 6122. Brazilian Association of Technical Standards, Brazil, 91 p (In Portuguese).

Aoki, N. & Velloso, D. (1975). An approximate method to estimate the bearing of piles. Proc. 5th Pan-American Conf. of Soil Mechanics and Foundation Engineering, Buenos Aires, vol. 1, pp. 367-376.

Barbosa, J.S.; Correa-Gomes, L.C.; Dominguez, J.M.L.; Cruz, S.A.S. & Souza, J.S. (2005). Petrography and Lithogeochemistry of rocks in west, high Salvador-BA. Revista Brasileira de Geociências, 35:4, p. 9-22.

Cambefort, M. (1964). Essai sur le comportement en terrain homogène des pieux isolés et des groupes des piex. Annales de l'Institut du Batiment et des Travaux Public no. 204.

Carter, J. & Kulhawy, F. (1988). Analysis and design of drilled shaft foundations socketed into rock. Report EL-5918. Electric Power Research Institute, Palo Alto.

Debas, L.F. (2014). Personal communication.

Décourt, L. & Quaresma, A. (1978). Ultimate pile resistance from SPT values. In: VI Congresso Brasileiro de Mecânica dos Solos e Engenharia de Fundações, ABMS, Rio de Janeiro, vol. 6, pp. 45-53 (In Portuguese).

Décourt, L. (1998). Deep foundation design and analysis - Piles. Hachich *et al.* (eds) Foundations: Theory and Practice. Pini, São Paulo, p. 265-301 (In Portuguese).

Fellenius, B.H. (1989). Tangent modulus of piles determined from strain data. In: Foundation Engineering: Current Principles and Practices. Proceedings of the 1989 Foundation Engineering Congress, Evanston, vol. 101, pp. 25-29.

Hachich, W.; Falconi, F.F.; Saes, J.L.; Frota, R.G.Q.; Carvalho, C.C. & Niyama, S. (1998). Hachich *et al.* (eds). Foundations, Theory and Practice. Pini, São Paulo, 753 p (In Portuguese).

Massad, F. (1995). The analysis of piles considering soil stiffness and residual stresses. In: X Congreso Panamericano de Mecánica de Suelos e Ingeniería de Cimentaciones, Guadalajara, México, pp. 1200-1210.

Massad, F. (2001). On the use of the elastic rebound to predict pile capacity. 15th International Conference on Soil Mechanics and Geotechnical Engineering, Istambul. Ed. Balkema, London, vol. 2, pp. 959-963.

Massad, F. (2011). Unexpected behavior of long steel H piles in Santos City, Brazil In: 14th Pan-American Conference on Soil Mechanics and Geotechnical Engineering, Toronto. Available at http://geoserver.ing.puc.cl/info/conferences/PanAm2011.

Musarra, M. (2014). Behavior Analysis of Rock Socketed Barrette Pile. Master of Science Dissertation. Polythecnic School, University of São Paulo, São Paulo, 254 p. (In Portuguese)

Prakoso, W. (2002). Reliability-Based Design of Foundations on Rock Masses for Transmission Line and Similar Structures. PhD Thesis, Cornell University, Ithaca, 781 p.

Randolph, M.F. & Wroth, C.P. (1978). Analysis of deformation of vertically loaded piles. Journal of the Geotechnical Engineering Division, v. 104:12, p. 1465-1488.

Rowe, R.K. & Armitage, H.H. (1987). Theoretical solutions for axial deformation of drilled shafts in rock. Canadian Geotechnical Journal, v. 24:1, p. 114-125.

Rusch, H. (1960). Researches toward a general flexural theory for structural concrete. ACI Journal of the American Concrete Institute, v. 57:7, p. 1-28.

Williams, A.F. (1980). Principles of side resistance development in rock socketed piles. In: Australia-New Zealand Conference on Geomechanics, Wellington, New Zealand v. 6:1 (G), p. 87-94.

List of Symbols

A_l: Shaft load
A_{lr}: Ultimate shaft load
c: Leonard's & Lovell coefficient
C_2: Elastic shortening of the pile
C_3: Elastic displacement of the tip of the pile or the toe quake
D: Equivalent diameter of the barrette pile
E: Modulus of Elasticity of the concrete
E_r: Modulus of Elasticity of the rock mass
f_{ck}: Characteristic stress resistance of concrete
f_{res}: Residual negative shaft resistance
f_s: Unit shear stress or skin friction
f_{su}: Ultimate unit shear stress
h: Pile heigth
h': Heigth associated to the progressive mobilization of f_{su}
k: Relative stiffness of the pile-soil (shaft) system
K_r: Pile stiffness (E.S/h)
L: Length of rock socket
N: Average value of SPT
NSPT: Blow counts from SPT test
p: Nominal perimeter of the cross section of the pile
P_h: Residual load at the pile tip
P_o: Pile top load
P_{omax}: Maximum value of P_o
q_p: Reaction stress at the fictitious tip
Q_{pr}: Toe load at failure
q_u: Uniaxial compressive strength of rock
R: Parameter of the Second Law of Cambefort
RQD: Rock quality designation
S: Nominal cross sectional area of the pile
SM: Core barrel and SPT blow counts sounding
SPT: Standard Penetration Test
y_1: Shaft quake
y_2: Tip quake
y_o: Pile top displacement
y_{tip}: Displacement of the fictitious tip of the pile
Δe: Elastic shortening of the pile (the same as C_2)
μ: Shaft friction magnifier factor due to residual loads
$\mu\varepsilon$: Microstrain
λ: Relative stiffness of the pile-soil (shaft and toe) system
ν_r: Poisson ratio of the rock mass

Technical Notes

Experimental Research on the Impact of Confining Pressure on the Permeability Characteristics of Non-Darcy Flow in Post-failure Rocks

H. Xu, Y. Zhao, W. Bu

Abstract. Researches on the impact of the confining pressure on the permeability characteristics of non-Darcy flow in rocks during the post-failure behaviour plays a significant role in the instability of the non-Darcy flow systems. The permeability characteristics of non-Darcy flow under different confining pressures is studied using a patented device combined with the MTS815.02. The experimental data indicates that the permeability rate of the non-Darcy flow decreases with the increasing in the confining pressure and this relationship can be fitted by an exponential function, while the absolute value of the β factor of non-Darcy flow increases with the increasing in the confining pressure and the relationship can be fitted by a logarithmic function.

Keywords: rock mechanics, post-failure behaviour, non-Darcy flow, confining pressure, permeability, laboratory research.

1. Introduction

The rock matrix can be considered as a porous media showing low permeability under low stress levels and reasonable agreement with the linear relationship of seepage which is also called Darcy law. It was firstly observed on the experiment on the movement of water in pipes (Darcy, 1858). Then, the capillary tube model (Scheidegger, 1953), the network model (or fractured model) (Fatt, 1956; Snow, 1965; Parsons, 1966), the hydraulic radius model (Willie *et al.*, 1952; Carman, 1956), the flow resistance model (Rumer, 1969) and the equation of Navier-Stokes (Whitaker, 1966) were used to obtain the Darcy law in theory. Common permeability tests on rock matrix can get this linear relationship of seepage and are operated on the more intact and denser rocks, while study on the permeability of post-failure rocks has not attracted enough attention so far. In fact, using Darcy law to describe rock permeability in general brings to errors with random permeability rate, no matter that the rocks are in pre-peak stage or post-failure stage (Cheng *et al.*, 2004). According to the practices in mining engineering and the theory of mining pressure and strata control, the stress in surrounding rocks usually exceeds its ultimate strength and the plastic zones are also formed in surrounding rocks. There are many fractures in surrounding rocks. It is called that the surrounding rocks of coal mining are in the state of post-failure. So, the permeability coefficient of surrounding rocks is higher than the permeability coefficient of intact and denser rocks by several orders of magnitude. In addition, the hydraulic pressure in aquifer is higher, sometimes being more than 5 MPa or even more. The water inrush usually occurs in a short time according to the actual disasters in mining engineering. The sudden change in seepage is the primary cause of water inrush disaster, while the linear relationship of seepage can't explain the sudden change in seepage. Thus, it can be concluded that the seepage in surrounding rocks has a nonlinear relationship, which is called non-Darcy flow. In recent years, Professor Xie Xing Miao puts forward the key water-resisting strata theory (Miao *et al.*, 2007; Miao *et al.*, 2008) and seepages instability model (Miao *et al.*, 2004), and establishes rock seepage under mining theory and points out that the destabilization of non-Darcy system in post-failure rocks is the key to water inrush and coal-gas outburst dynamic disasters (Miao *et al.*, 2003), and that has a close relationship with the permeability rate and the β factor of non-Darcy flow. Meanwhile, the coal mining engineering is different from the common underground rock engineering, in which the boundary of mining surrounding rocks is time-varying boundary condition and the confining pressure of post-failure rocks is changing continuously (Ma *et al.*, 2006; Sun *et al.*, 2003). Therefore, it is of great importance to the destabilization of non-Darcy system to carry out some researches on the influence of confining pressure on the permeability characteristics of non-Darcy flow during the post-failure behaviour.

This paper uses a patented device which is combined with the Electro-hydraulic Servo-controlled Rock Mechanics Testing System (which is called MTS815.02) as a new testing system. The experimental scheme and testing system for non-Darcy flow in post-failure rocks are designed. The permeability characteristics of non-Darcy flow in sand shale, limestone and sandstone during the post-

Hui Xu, PhD, Postgraduate, School of Mechanics & Civil Engineering, China University of Mining & Technology, Xuzhou, China. e-mail: xu_hui521@126.com.
Yu Cheng Zhao, Tutor for Doctor, Professor, School of Mechanics & Civil Engineering, China University of Mining & Technology, Xuzhou, China. e-mail: zhaoyc1972@163.com.
Wan Kui Bu, PhD, Associate Professor, Resources and Environment Department, Heze University, Heze, China. e-mail: bwk239@126.com.
Submitted on November 21, 2012; Final Acceptance on June 3, 2015; Discussion open until December 31, 2015.

failure behaviour are obtained with different confining pressure. According to the experimental data, the relationship between the permeability characteristics of non-Darcy flow and confining pressure are analysed and presented for sand shale, limestone and sandstone during the post-failure behaviour. In this paper, the permeability characteristics of non-Darcy flow mainly include two parameters: (1) the permeability rate of non-Darcy flow; (2) the β factor of non-Darcy flow.

2. Experimental Principle and Methodology

The permeability experiments of unconsolidated porous media show that the relationship between pressure gradient ∇p (Pa/m) and seepage velocity $\vec{V}$ (m/s) can be described using the Forchheimer Equation considering the inertia and turbulence effects. Eq. 1 shows the relationship between pressure gradient ∇p and seepage velocity $\vec{V}$ (Forchheimer, 1901; Kong, 1999; Wang *et al.*, 2006):

$$\nabla p = -\frac{\mu}{k}\vec{V} - \rho\beta V\vec{V} \tag{1}$$

In this equation, p is the pressure (Pa), μ is the dynamic viscosity (Pa.s), k is the non-Darcy flow permeability (m^2), ρ is the fluid density (kg/m^3) and β is the β factor of non-Darcy flow (m^{-1}).

The momentum equation of the one-dimensional non-Darcy flow based on Forchheimer relation is showed in Eq. 2.

$$\rho c_a \frac{\partial V}{\partial t} = -\frac{\partial p}{\partial x} - \frac{\mu}{k}V - \rho\beta V^2 + F \tag{2}$$

where C_a is related to the acceleration coefficient of fluid, F is related to the body forces (N) and t is the time (s).

When the time is above to some critical value, the seepage achieves a stable condition and the pressure distribution along the axial rock is a linear function, as shown in Eq. 3 (the fluid compressibility is not considered).

$$\rho p = \left[\frac{\mu}{k}(\rho V) + \beta(\rho V)^2\right](h - x) \tag{3}$$

where h is the height of rock specimen (m), and x is the distance to the bottom of rock specimen (m).

Thus, the pressure gradient can be approximately described by the ratio of pressure difference Δp at the ends of rock specimen and the height of rock specimen h, which is recorded as δp in Eq. 4.

$$\delta p = \frac{\Delta p}{h} = \frac{\mu}{k}V + \rho\beta V^2 \tag{4}$$

In this equation, the permeability rate of non-Darcy flow k and the β factor of non-Darcy flow are used to describe the permeability characteristics. Thus, the pressure (or pressure gradient) and seepage velocity (or mass flow rate) signals are collected to determine the non-Darcy flow permeability characteristics. There are more than ten methods for testing permeability characteristics of rock specimen in laboratory (Miao *et al.*, 2004), but these methods can be roughly divided into two types: stable method and transient method. The stable method tests the stable seepage velocity by keeping the pressure gradient unchanged and gets the permeability characteristics by the fitting curve of pressure gradient and seepage velocity. However, the transient method tests a series of pressure gradient within a certain period of time and calculates the pressure gradient changing rate. Thus, the transient method gets the permeability characteristics by the fitting curve of pressure gradient and pressure gradient changing rate. There are three disadvantages for the transient method: (1) it is difficult to seal the rock specimen; (2) the testing can't keep going on when the pore pressure is greater than the confining pressure; (3) the testing also can't keep going on when the axial strain of rock specimen equals to zero (Wang *et al.*, 2006). Therefore, the stable method is taken to test the permeability characteristics of non-Darcy flow in this paper.

The proposed assemblage (one MTS815.02 coupled with a developed patented device) were used to obtain the relationship between the pressure gradient and the seepage velocity (δp-V). Here, the seepage velocity V is controlled by the velocity of supercharger's piston V_p in MTS815.02. Equation 5 shows the relationship between the seepage velocity V and the velocity of supercharger's piston V_p:

$$V = \frac{d_p^2}{d^2}V_p \tag{5}$$

In this equation, d_p *is* the diameter of the supercharger's piston (m) and d the diameter of the rock specimen (m).

Considering a group of seepage velocity $V_1, V_2, ..., V_n$ and a group of corresponding stable pressure gradients δp_1, δp_2, ..., δp_n, the parameters μ/k and $\rho\beta$ can be obtained by fitting the pressure gradient and the seepage velocity using the second-order polynomial:

$$\frac{\mu}{k} = \frac{\sum_{i=1}^{n}\left.\frac{\partial p}{\partial x}\right|_i V_i(i)\sum_{k=1}^{n}V_k^4(k) - \sum_{i=1}^{n}\left.\frac{\partial p}{\partial x}\right|_i V_i^2(i)\sum_{k=1}^{n}V_k^3(k)}{\sum_{i=1}^{n}V_i^2(i)\sum_{k=1}^{n}V_k^4(k) - \sum_{i=1}^{n}V_i^3(i)\sum_{k=1}^{n}V_k^3(k)} \tag{6}$$

$$\rho\beta = \frac{\sum_{i=1}^{n}\left.\frac{\partial p}{\partial x}\right|_i V_i^2(i)\sum_{k=1}^{n}V_k^2(k) - \sum_{i=1}^{n}\left.\frac{\partial p}{\partial x}\right|_i V_i(i)\sum_{k=1}^{n}V_k^3(k)}{\sum_{i=1}^{n}V_i^2(i)\sum_{k=1}^{n}V_k^4(k) - \sum_{i=1}^{n}V_i^3(i)\sum_{k=1}^{n}V_k^3(k)} \tag{7}$$

Thus, the permeability rate k and the β factor of non-Darcy flow can be obtained by using Eq. 5 to Eq. 7.

For explaining how the permeability rate k and the β factor of non-Darcy flow are obtained, the experimental data of rock specimen during the post-failure behaviour, taken from the reference (Miao *et al.*, 2004) as an example, are listed in Table 1. During these testing, the dynamic viscosity of fluid μ is 1.01 x 10^{-3} (Pa.s), the fluid density ρ is 1.0 x 10^{3} (kg/m^3) and the diameter of the supercharger's piston d_p is 5.5 x 10^{-2} (m). The permeability rate k and the β factor of non-Darcy flow are calculated by combining the equations from Eq. 5 to Eq. 7, which are listed in Table 2.

3. Experimental System and Scheme

3.1 Experimental system

The experimental system includes a patented device made in China (shown in Fig.1) and MTS815.02 (shown in Fig.2) working together. Heat shrinkable plastic film is used to seal the cylindrical surface of rock specimen. Porous plate (No.4) and felt pad (No.5) are used at the upper end of the rock specimen. The porous plate is designed to make the fluid flow evenly and the felt pad is used to avoid the MTS815.02 System being polluted by the fluid. The rock specimen and the cylinder bore (No.7) are separated by epoxy resin preventing the radial flow. The cylinder bottom of patented device and the pedestal of MTS815.02 are connected by the one-way valve, which including spool (No.11), valve casing (No.12), spring (No.10), baffle (No.13) and bolt (No.9). Standardized sealing ring with "O" type is used to enclose the axial gaps between the cover plate (No.2) and the spherical indenter of axial load system in MTS815.02, the cover plate and the cylinder bore, the cylinder bore and valve casing, and the cylinder bottom of patented device and the pedestal of MTS815.02.

The fluid flows from the pore pressure system in MTS815.02 and goes through globe valves S12 and S14 into the rock specimen, and outflows through porous plates, felt pad and globe valves S1 and S15 in order.

3.2. Experimental scheme

The rock specimen is pressed in post-failure at a given strain value with uniaxial compression in

Table 2 - The permeability characteristics of rock specimen during the post-failure behaviour.

Number of rock specimen	Permeability rate k (m^2)	β factor of non-Darcy flow (m^{-1})
1	7.47 x 10^{-15}	1.72 x 10^{15}
2	9.99 x 10^{-15}	1.56 x 10^{15}
3	5.20 x 10^{-15}	1.23 x 10^{15}
4	8.62 x 10^{-15}	1.01 x 10^{15}

Table 1 - The experimental data of rock specimen during the post-failure behaviour.

Number of rock specimen	Diameter of rock specimen (m)	Height of rock specimen (m)	The velocity of supercharger's piston (m/s)	Pressure gradient (Pa)
1	5.36 x 10^{-2}	9.21 x 10^{-2}	0.03 x 10^{-3}	0.215 x 10^{6}
			0.05 x 10^{-3}	0.755 x 10^{6}
			0.10 x 10^{-3}	3.11 x 10^{6}
			0.15 x 10^{-3}	6.42 x 10^{6}
			0.20 x 10^{-3}	9.38 x 10^{6}
2	5.34 x 10^{-2}	9.82 x 10^{-2}	0.03 x 10^{-3}	0.455 x 10^{6}
			0.05 x 10^{-3}	0.841 x 10^{6}
			0.10 x 10^{-3}	2.44 x 10^{6}
			0.15 x 10^{-3}	6.01 x 10^{6}
			0.20 x 10^{-3}	8.76 x 10^{6}
3	5.36 x 10^{-2}	9.91 x 10^{-2}	0.03 x 10^{-3}	0.531 x 10^{6}
			0.05 x 10^{-3}	1.23 x 10^{6}
			0.10 x 10^{-3}	3.64 x 10^{6}
			0.15 x 10^{-3}	5.98 x 10^{6}
			0.20 x 10^{-3}	9.45 x 10^{6}
4	5.38 x 10^{-2}	9.86 x 10^{-2}	0.03 x 10^{-3}	0.151 x 10^{6}
			0.05 x 10^{-3}	0.689 x 10^{6}
			0.10 x 10^{-3}	2.43 x 10^{6}
			0.15 x 10^{-3}	4.45 x 10^{6}
			0.20 x 10^{-3}	6.61 x 10^{6}

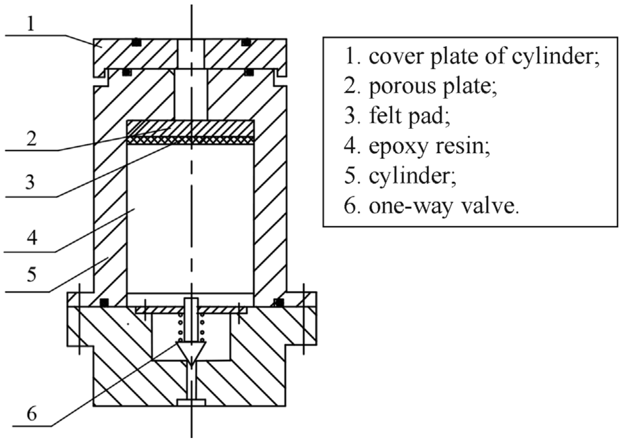

Figure 1 - Patented device in the experimental system.

MTS815.02. Because the axial strain of rock specimen is very small, such as, the maximum axial strain is 0.03 during the testing, the height of rock specimen after unloading can be approximately equal to the height before unloading. In order to prevent the rock pieces emerge from the womb after fracturing, a plastic film is used to seal the cylinder surface and the influence of the plastic film on the rock specimen deformation is tiny.

The assembly is used for steady-state permeability measurement. The confining pressure is fixed at $P_c = 4$ MPa firstly, and then the seepage velocity or pressure are controlled by the pore pressure system. TestStar IIm Controller, including a network distributor, two computers and testing software, is used to collect and process the experimental data. After that, the confining pressure P_c is changed to 6 MPa, 8 MPa, 10 MPa, 14 MPa respectively and then the above-mentioned process should be repeated.

Table 3 - The physical properties of rock samples.

Rock	Density/(gcm^3)	Porosity/(%)	Water absorption/(%)
Sand shale	2.33	1.02	2.33
Limestone	2.62	2.21	0.83
Sandstone	2.51	5.35	5.15

Experimental Results and Analysis

The specimens used in the tests were prepared in sand shale, limestone and sandstone from the Shanxi Province of China. The Physical properties of rock samples are listed in Table 3. The permeability tests were performed under different confining pressure. The fluid was water with density ρ equalling to 1,000 kg/m^3 and dynamic viscosity μ equalling to 1.01 x 10^{-3} Pa.s. The non-Darcy permeability characteristics of the rock specimens (non-Darcy permeability rate k, β factor of non-Darcy flow) could be computed using the data obtained from the tests. The relationship between the confining pressure P_c and the non-Darcy permeability rate k and the relationship between the confining pressure P_c and the β factor of the non-Darcy flow for the three rock types studied are showed in Figure 3a-c.

According to Fig. 3 based on the experimental data, the permeability (k) of the non-Darcy flow for the sand shale, the limestone and the sandstone in post-failure, decrease with the increasing in the confining pressure P_c. The correlation coefficient (Table 4) shows a good fitting with an exponential function. In fact, the confining pressure has restrictive effect on the fracture deformation of transverse tensile, and the increasing of the confining pressure makes the axial fractures to be closed in the specimen. With the

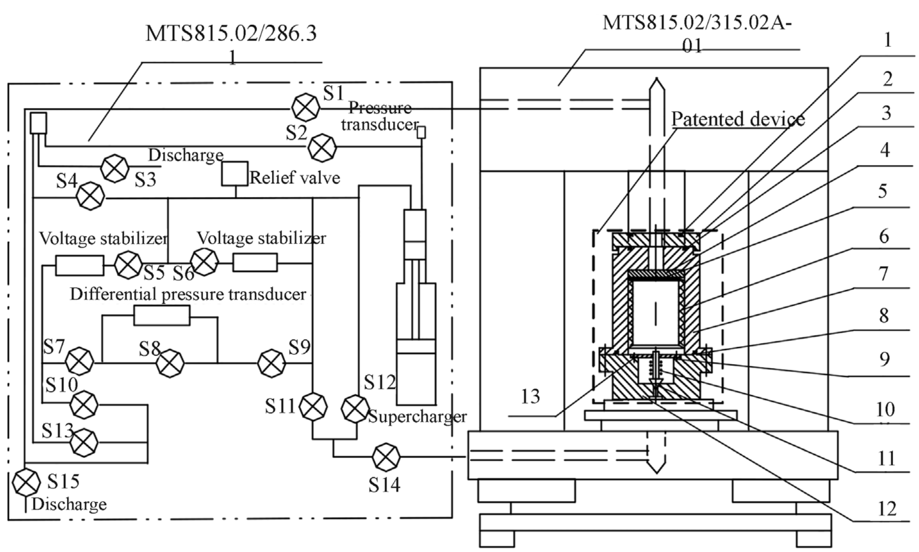

1. nut; 2. cover plate of cylinder; 3. bolt; 4. porous plate; 5. felt pad; 6. epoxy resin; 7. cylinder; 8. nut; 9. bolt; 10. spring; 11. spool; 12. valve casing; 13. baffle.

Figure 2 - Coupled assembly used in the experiment (MTS815.02 with a developed patented device).

Table 4 - Fitting function between non-Darcy permeability k and confining pressure P_c.

Rock	Fitting function	Correlation coefficient
Sand shale in post-failure	$k = 8.66 \times 10^{-19} e^{-0.165Pc}$	0.9586
Limestone in Post-failure	$k = 1.42 \times 10^{-17} e^{-0.126Pc}$	0.9309
Sandstone in Post-failure	$k = 3.84 \times 10^{-17} e^{-0.253Pc}$	0.9472

axial fractures closing, the roughness of the fracture walls and the rock bridges change, affecting the aperture, the tortuosity of the flow channels and the resistance effect on the fluid flow, which also leads to the permeability decreasing. In addition, the permeability of the non-Darcy flow in post-failure rocks is higher than that in intact and denser rocks by one or two orders of magnitude, which can explain the sudden change in seepage in surrounding rocks when the coal seam is excavated.

The absolute values of the β factor of non-Darcy flow for the sand shale, the limestone and the sandstone in post-failure increase with the increasing in the confining pressure as shown in Fig.4a-c. The relationship between the value of the β factor of the non-Darcy flow and the confining pressure P_c can be well fitted by a logarithmic function as shown in Table 5.

4. Conclusion

The rock matrix seepage, especially in post-failure state, which is a main factor for the water inrush disasters in geotechnical engineering (Galybin, 1997; Wu *et al.*, 2004; Nomikos *et al.*, 2011), shows the characteristics of

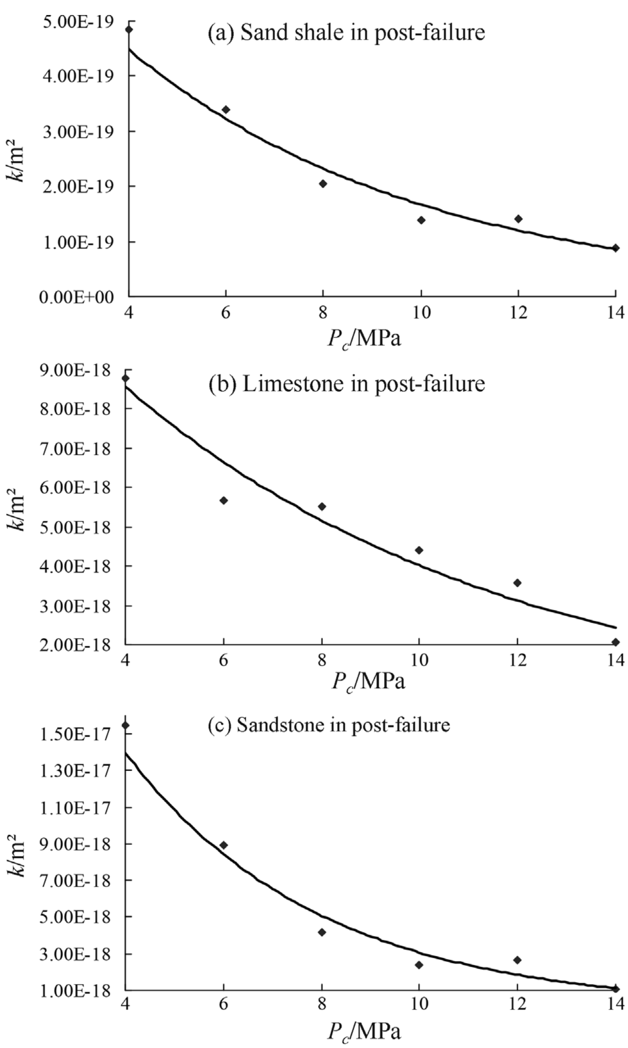

Figure 3 - Relationship between the non-Darcy permeability (k) and the confining pressure (P_c) for the three rock types.

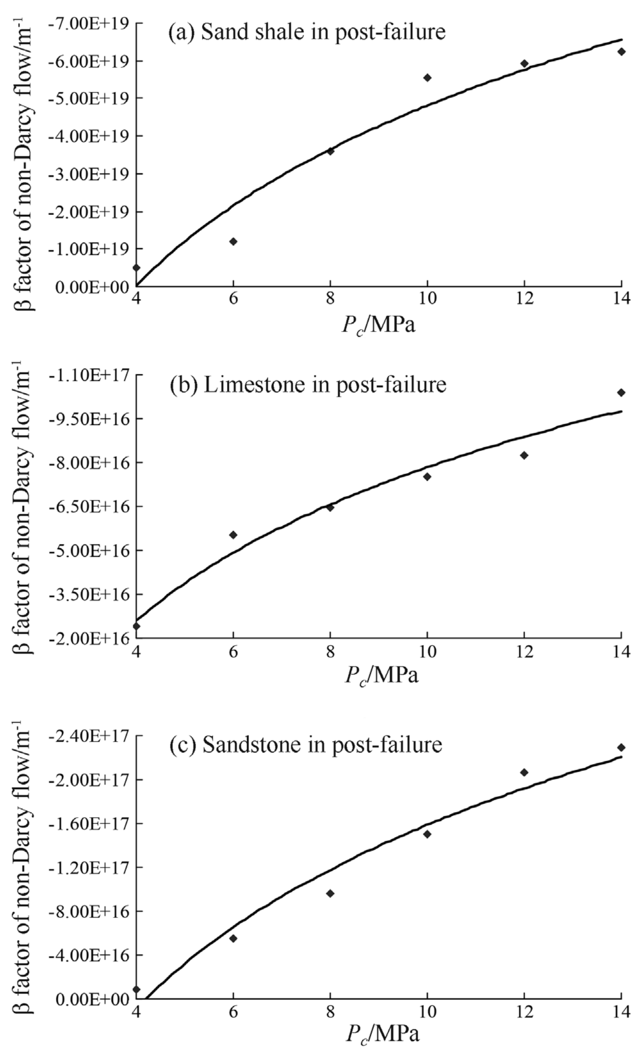

Figure 4 - Relationship between the β factor of the non-Darcy flow and the confining pressure (P_c) for the three rock types.

Table 5 - Fitting functions between the value of β factor of non-Darcy flow and confining pressure P_c.

Rock	Fitting function	Correlation coefficient
Sand shale in post-failure	$\beta = -(5.22\ln(P_c)+7.20) \times 10^{19}$	0.9432
Limestone in Post-failure	$\beta = -(5.71\ \ln(P_c)+5.32) \times 10^{16}$	0.9647
Sandstone in Post-failure	$\beta = -(1.83\ \ln(P_c)+2.62) \times 10^{17}$	0.9663

non-Darcy flow. In this paper the combined assemblage of a patented device with MTS815.02 were used to study the non-Darcy flow permeability in three rock types considering different confining pressures. The experimental data show that the permeability rate of the non-Darcy flow decreases with the increasing of the confining pressure and the best fit is achieved through an exponential function. Also, the absolute value of the β factor of the non-Darcy flow increases with the increasing of the confining pressure and the best fit is achieved through a logarithmic function. The experimental data show that the permeability of the non-Darcy flow in post-failure rocks is higher than that in intact and denser rocks by one or two orders of magnitude. So, it can be concluded that the non-Darcy flow in post-failure rocks is one of the main factors for the water inrush disasters in rock engineering. Thus, these experimental data and related expressions in this paper will provide an important basis for the seepage destabilization in the layered rocks.

Acknowledgments

Financial support for this work, provided by the National Basic Research Program of China (973 Program) (No.2007CB209400), the Key Project of National Nature Science Foundation of China (No.50834004), the China Postdoctoral Science Foundation (No.20110491486) and the Research Foundation of Heze University(No.XY14KJ01) are gratefully acknowledged.

References

Carman, P.C. (1956). Flow of Gases Through Porous Media. Butterworths Scientific Publications, London, 182 p.

Cheng, Y.K.; Chen, Z.Q.; Miao, X.X. & Mao, X.B. (2004). Testing study on permeability of non-Darcy flow in post-peak sandstone. Chinese Journal of Rock Mechanics and Engineering, 23(12):2005-2009 (in Chinese).

Darcy, H.P.G. (1858). Experimental research on the movement of water in pipes. Mémoires Présentés à l'Académie des Sciences de l'Institut de France, 14:141 (in French).

Fatt, I. (1956). The network model of porous media. Trans Am Inst Mem Metall Pet Eng, 207:144-181.

Forchheimer, P.Z. (1901). Wasserbewegungdurch Boden. Zeitschrift des Vereins Deutscher Ingenieure, 45:1782-1788.

Galybin, A.N. (1997). A model of mining-induced fault sliding. International Journal of Rock Mechanics and Mining Sciences. 34(3-4):91-103.

Kong, X.Y. (1999). Advanced Percolation Mechanics. University of Science and Technology of China Press, Hefei, pp. 55-63 (in Chinese).

Ma, Z.G.; Huang, W.; Guo, G.L. & Chen, Z.Q. (2006). Analysis on failure of covering rock in ehuobulake mine by using mechanics of systems with variable boundaries. Journal of Liaoning Technical University, 25(4):515-517 (in Chinese).

Miao, X.X.; Chen, R.H. & Bai, H.B. (2007). Fundamental concepts and mechanical analysis of water-resisting key strata in water-preserved mining. Journal of China Coal Society, 32(6):561-564 (in Chinese).

Miao, X.X.; Chen, Z.Q.; Mao, X.B. & Chen, R.H. (2003). The bifurcation of non-Darcy flow in post-failure rock. Acta Mechanica Sinica, 35(6):660-667 (in Chinese).

Miao, X.X.; Liu, W.Q. & Chen, Z.Q. (2004). Dynamics of Systems of Seepage Flow in Surrounding Rock Affected by Mining. Science Press, Beijing, pp 33-49 (in Chinese).

Miao, X.X.; Pu, H. & Bai, H.B. (2008). Principle of water-resisting key strata and its application in water-preserved mining. Journal of China University of Mining & Technology, 37(1):1-4 (in Chinese).

Nomikos P.P. & Sofianos A.I. (2011) An analytical probability distribution for the factor of safety in underground rock mechanics. International Journal of Rock Mechanics and Mining Sciences, 48(4):597-605.

Parsons, R.W. (1966). Permeability of idealized fractured rock. Society of Petroleum Engineers Journal, 6(2):126-136.

Rumer, R.R. (1969). Resistance to flow through porous media, Flow through Porous Media, Academic Press, New York, pp. 91-108.

Scheidegger, A.E. (1953). Theoretical models of porous matter. Producers Monthly, 17(10):17-23.

Snow, D.T. (1965). A Parallel Plate Model of Fractured Permeable Media. Ph.D. Thesis, Department of Civil Engineering, University of California, Berkeley, 331 p.

Sun, M.G.; Tang, P. & Chen, Z.Q. (2003). Expectation on dynamic system with variable boundary. Journal of Changde Teachers University (Natural Science Edition), 15(2):12-15 (in Chinese).

Wang, X.S. & Chen, Z.Q. (2006). Hydrodynamic analysis of transient method in rock seepage tests. Chinese Journal of Rock Mechanics and Engineering, 25(S1):3098-3103 (in Chinese).

Whitaker, S. (1966). The equations of motion in porous media. Chemical Engineering Science, 21(3):291-300.

Wu, Q.; Wang, M. & Wu, X. (2004). Investigations of groundwater bursting into coal mine seam floors from fault zones. International Journal of Rock Mechanics and Mining Sciences, 41:557-571.

Wyllie, M.R. & Spangler, M.B. (1952). Application of electrical resistivity measurements to problem of fluid flow in porous media. Bulletin of the American Association of Petroleum Geologists, 36(2):359-403.

SOILS and ROCKS
An International Journal of Geotechnical and Geoenvironmental Engineering

Publication of
ABMS - Brazilian Association for Soil Mechanics and Geotechnical Engineering
SPG - Portuguese Geotechnical Society
Volume 38, N. 2, May-August 2015

Author index

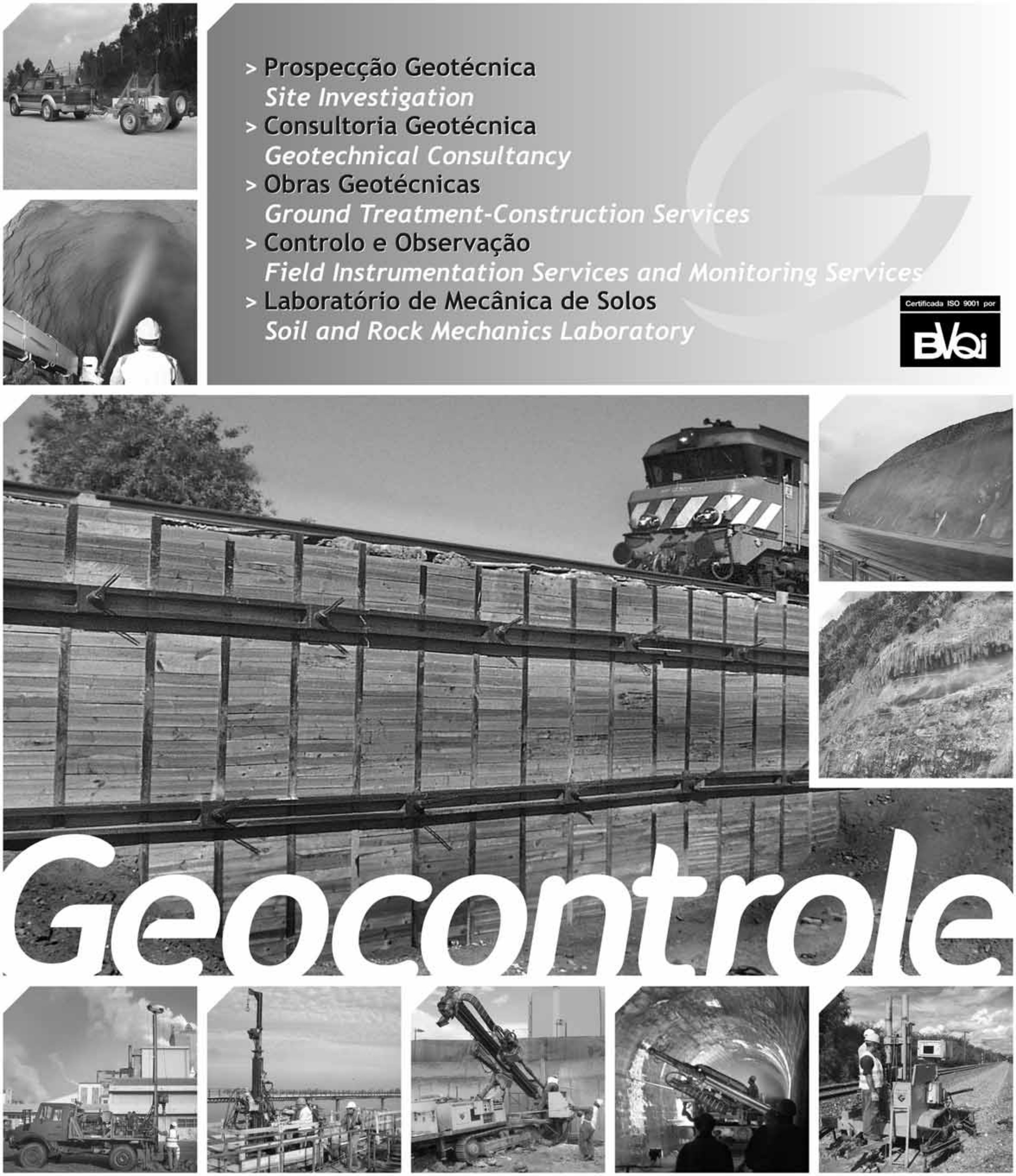
> Prospecção Geotécnica
Site Investigation
> Consultoria Geotécnica
Geotechnical Consultancy
> Obras Geotécnicas
Ground Treatment-Construction Services
> Controlo e Observação
Field Instrumentation Services and Monitoring Services
> Laboratório de Mecânica de Solos
Soil and Rock Mechanics Laboratory
Certificada ISO 9001 por
BVQi
Geocontrole

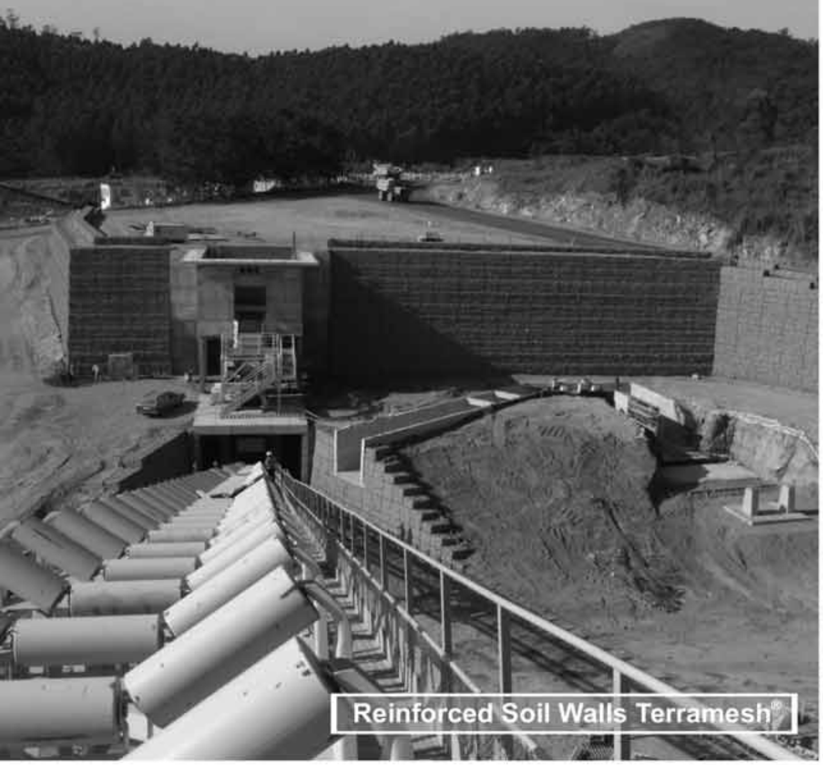

Reinforced Soil Walls Terramesh®

Gabions Retaining Walls

Waterproofing of Reservoirs, Lakes and Channels

Dynamic rockfall barriers

Instructions for Submission of Manuscripts

Category of the Papers

Soils and Rocks is the international scientific journal edited by the Brazilian Association for Soil Mechanics and Geotechnical Engineering (ABMS) and the Portuguese Geotechnical Society (SPG). The aim of the journal is to publish (in English) original research and technical works on all geotechnical branches.

According to its content the accepted paper is classified in one of the following categories: Article paper, Technical Note, Case Study or Discussion. An article paper is an extensive and conclusive dissertation about a geotechnical topic. A paper is considered as a technical note if it gives a short description of ongoing studies, comprising partial results and/or particular aspects of the investigation. A case study is a report of unusual problems found during the design, construction or the performance of geotechnical projects. A case study is also considered as the report of an unusual solution given to an ordinary problem. The discussions about published papers, case studies and technical notes are made in the Discussions Section.

When submitting a manuscript for review, the authors should indicate the category of the manuscript, and is also understood that they:

a) assume full responsibility for the contents and accuracy of the information in the paper;

b) assure that the paper has not been previously published, and is not being submitted to any other periodical for publication.

Manuscript Instructions

Manuscripts must be written in English. The text is to be typed in a word processor (preferably MS Word), **single column**, using ISO A4 page size, left, right, top, and bottom margins of 25 mm, Times New Roman 12 font, and line spacing of 1.5. All lines and pages should be numbered. The text should be written in the third person.

The first page of the manuscript must include the title of the paper followed by the names of the authors with the abbreviation of the most relevant academic title. The affiliation, address and e-mail must appear below each author´s name. An abstract of 200 words follows after the author´s names. A list with up to six keywords at the end of the abstract is required.

Although variations on the sequence and title of each section are possible, it is suggested that the text contains the following sections: Introduction, Material and Methods, Results, Discussions, Conclusions, Acknowledgements, References and List of Symbols. A brief description of each section is given next.

Introduction: This section should indicate the state of the art of the problem under evaluation, a description of the problem and the methods undertaken. The objective of the work should be clearly presented at the end of the section.

Materials and Methods: This section should include all information needed to the reproduction of the presented work by other researchers.

Results: In this section the data of the investigation should be presented in a clear and concise way. Figures and tables should not repeat the same information.

Discussion: The analyses of the results should be described in this section.

Conclusions: The content of this section should be based on the data and on the discussions presented.

Acknowledgenments: If necessary, concise acknowledgements should be presented in this section.

References: References to other published sources must be made in the text by the last name(s) of the author(s), followed by the year of publication, similarly to one of the two possibilities below:

…while Silva and Pereira (1987) observed that resistance depended on soil density… or *It was observed that resistance depended on soil density (Silva and Pereira, 1987).*

In the case of three or more authors, the reduced format must be used, *e.g.*: Silva *et al.* (1982) or (Silva *et al.*, 1982). Two or more citations belonging to the same author(s) and published in the same year are to be distinguished with small letters, *e.g.*: (Silva, 1975a, b, c.). Standards must be cited in the text by the initials of the entity and the year of publication, *e.g.*: ABNT (1996), ASTM (2003).

Full references shall be listed alphabetically at the end of the text by the first author´s last name. Several references belonging to the same author shall be cited chronologically. Some examples are listed next:

Papers: Bishop, A.W. & Blight, G.E. (1963). Some aspects of effective stress in saturated and unsaturated soils. Geotechnique, 13(2):177-197.

Books: Lambe, T.W & Whitman, R.V. (1979). Soil Mechanics, SI Version. John Wiley & Sons, New York, 553 p.

Book with editors: Sharma, H.D.; Dukes, M.T. & Olsen, D.M. (1990). Field measurements of dynamic moduli and Poisson's ratios of refuse and underlying soils at a landfill site. Landva, A. & Knowles, G.D. (eds), Geotechnics of Waste Fills - Theory and Practice, American Society for Testing and Materials - STP 1070, Philadelphia, pp. 57-70.

Proceedings (printed matter or CD-ROM): Jamiolkowski, M.; Ladd, C.C.; Germaine, J.T. & Lancellotta, R. (1985). New developments in field and laboratory testing of soils. Proc. 11th Int. Conf. on Soil Mech. and Found. Engn., ISSMFE, San Francisco, v. 1, pp. 57-153. (specify if CD ROM).

Thesis and dissertations: Lee, K.L. (1965). Triaxial Compressive Strength of Saturated Sands Under Seismic Loading Conditions. PhD Dissertation, Department of Civil Engineering, University of California, Berkeley, 521 p.

Standards: ASTM (2003). Standard Test Method for Particle Size Analysis of Soils - D 422-63. ASTM International, West Conshohocken, Pennsylvania, USA, 8 p.

Internet references: Soils and Rocks available at http://www.abms.com.br and downloaded on August 6th 2003.

On line first publications must also bring the digital object identifier (DOI) at the end.

Figures shall be either computer generated or drawn with India ink on tracing paper. Computer generated figures must be accompanied by the corresponding digital file (.tif, .jpg, .pcx, etc.). All figures (graphs, line drawings, photographs, etc.) shall be numbered consecutively and have a caption consisting of the figure number and a brief title or description of the figure. This number should be used when referring to the figure in text. Photographs should be black and white, sharp, high contrasted and printed on glossy paper.

Tables shall be numbered consecutively in Arabic and have a caption consisting of the table number and a brief title. This number should be used when referring to the table in the text. Units should be indicated in the first line of the table, below the title of each column. Acronyms should be avoided. When applicable, the units should come right below the corresponding column heading. Additional comments can be placed as footnotes.

Equations shall appear isolated in a single line of the text. Numbers identifying equations must be flushed with the right margin. International System (SI) units must be used. The definitions of the symbols used in the equations must appear in the List of Symbols. It is recommended that the symbols used are in accordance with Lexicon in 8 Languages, ISSMFE (1981) and the ISRM List of Symbols.

The text of the submitted manuscript (including figures, tables and references) intended to be published as an article paper or a case history should not contain more than 30 pages, formatted according to the instructions mentioned above. Technical notes and discussions should have no more than 15 and 8 pages, respectively. Longer manuscripts may be exceptionally accepted if the authors provide proper explanation for the need of the required extra space in a cover letter.

Discussion

Discussions must be written in English. The first page of a discussion should contain:

The title of the paper under discussion;

Name of the author(s) of the discussion, followed by their position, affiliation, address and e-mail. The author(s) of the discussion should refer to himself (herself/themselves) as the reader(s) and to the author(s) of the paper as the author(s).

Figures, tables and equations should be numbered following the same sequence of the original paper. All instructions previously mentioned for the preparation of article papers, case studies and technical notes also apply to the preparation of discussions.

Editorial Review

Each paper will be evaluated by reviewers selected by the editors according to the subject of the paper. The authors will be informed about the results of the review process. If the paper is accepted, the authors will be required to submit a version of the revised manuscript with the suggested modifications. If the manuscript is rejected for publication, the authors will be informed about the reasons for rejection. In any situation comprising modification of the original text, classification of the manuscript in a category different from that proposed by the authors, or rejection, the authors can reply presenting their reasons for disagreeing with the reviewer comments.

Submission

The author(s) must upload a digital file of the manuscript to the Soils and Rocks website.

Follow Up

The online management system will provide a password to the corresponding author, which will enable him/her to follow the reviewing process of the submitted manuscript at the Soils and Rocks website.

Volume 38, N. 2, May-August 2015

Table of Contents